TR-N-MCM-008

NORTHEAST UTILITIES
SERVICE COMPANY
Millstone Nuclear Unit no. 2

evaluation OF irradiated capsule W-97

REACTOR VESSEL MATERIALS IRRADIATION SURVEILLANCE PROGRAM

APRIL 1982

POWER SYSTEMS
COMBUSTION ENGINEERING, INC.

8401200168 840104
PDR ADOCK 05000336
P PDR

NORTHEAST UTILITIES
SERVICE COMPANY
MILLSTONE NUCLEAR
UNIT NO. 2

POST-IRRADIATION EVALUATION OF REACTOR VESSEL SURVEILLANCE CAPSULE W-97

April 1982

Prepared by: S. T. Byrne Date: 4-1-82
S. T. Byrne, Cognizant Engineer

Approved by: John J. Koziol Date: 4.16.82
J. J. Koziol, Program Manager

Approved by: R. C. Jacques Date: 4-19-82
R. C. Jacques, Millstone Unit #2
Project Manager

Combustion Engineering, Inc.
Nuclear Power Systems
Windsor, Connecticut

TABLE OF CONTENTS

List of Tables

List of Tables (cont'd)

List of Figures

List of Figures (Cont'd)

List of Figures (Cont'd.)

I. SUMMARY

The first surveillance wall capsule (W-97) was removed from the Millstone Unit 2 reactor vessel in August 1980 after 3.0 effective full power years of reactor operation. The surveillance test specimens and monitors were evaluated at C-E's Windsor, Connecticut laboratory facility.

Post-irradiation evaluation of the temperature monitors indicated that the irradiation temperature was between 536 F and 558 F. Analysis of the neutron threshold detectors provided a capsule fluence of 3.78×10^{18} n/cm^2 (E>1 MeV), which corresponded to a maximum fluence at the inside surface of the reactor vessel of 2.78×10^{18} n/cm^2.

Radiation induced changes in the tension and impact properties were determined for the base metal, weld metal and heat-affected zone surveillance materials. Transition temperature shifts ranged from 76°F for the weld metal to 96°F for the base metal plate. The upper shelf impact energy after irradiation was in excess of 75 ft-lb for each of the surveillance materials, ranging from 79 ft-lb for the base metal to 98 ft-lb for the weld metal. The base metal exhibited the greatest toughness property change even though the residual copper content of the weld (0.30 w/o) was higher than for the plate (0.14 w/o). This difference in copper content was confirmed by chemical analysis of the irradiated base and weld metal Charpy specimens. The analysis also confirmed that the chemistry of the irradiated materials was consistent with the chemistry originally reported for the surveillance materials.

The base metal, weld metal and HAZ exhibited similar changes in tensile properties after irradiation. The yield strength and ultimate strength increased approximately 11%, while total elongation and reduction in area decreased 3% to 5% after irradiation.

The NDTT shift prediction method from the Millstone Unit 2 Technical Specifications was found to be conservative by a factor of 25% for the base metal and 58% for the weld metal based on the W-97 surveillance capsule measurements. In contrast, shifts predicted using Regulatory Guide 1.99 were 140% higher than measured for the weld metal and 35% less than measured for the base metal. The greater radiation resistance of the weld is attributed to the low nickel content (.06%). Based upon experimental data, the weld metal shift will continue to be less than that of the plate, despite the difference in copper content. Therefore, a more accurate shift prediction method was developed based on the measured shift for the controlling base metal and the slope of the Regulatory Guide expression. The predicted end-of-life (32EFPY) adjusted RTNDT at the quarter thickness location in the reactor vessel is 199°F using the revised method for the controlling plate. The predicted end-of-life adjusted RTNDT for the weld is 98°F at 1/4t using a similar projection method.

The predicted decrease in upper shelf energy at end-of-life based on the method given in Regulatory Guide 1.99 is 38% at the one-quarter thickness location in the vessel. Using this conservative prediction, the upper shelf energy of the plates will remain above 65 ft-lb during the design life of the vessel, and the weld shelf energy will remain above 80 ft-lb. These projected values are well in excess of the 50 ft-lb value currently considered to be a reasonable lower limit for continued safe operation.

Recommended changes to the surveillance capsule withdrawal schedule were provided to meet the requirements of 10CFR50, Appendix H. If the proposed schedule is implemented, the next capsule will be withdrawn after 7 effective full power years of operation. Additional surveillance data would then be available before the current operating limits would require updating.

II. Introduction

The purpose of the Millstone Unit 2 surveillance program is to monitor the radiation induced changes in the mechanical properties

of ferritic materials in the reactor vessel beltline during the operating lifetime of the reactor vessel. The surveillance program includes the determination of the preirradiation (baseline) strength and toughness properties and periodic determinations of the property changes following neutron irradiation. These property changes are used to verify and update the operating limits (heat-up and cool down pressure/temperature limit curves) for the primary system.

The Millstone Unit 2 Surveillance program[1] is based upon ASTM E185-70, "Recommended Practice for Surveillance Tests for Nuclear Reactor Vessels." The pre-irradiation (baseline) evaluation results from the Millstone Unit 2 reactor vessel surveillance materials are described in C-E report 18767-TR-MCD-009.[2] The following report describes the results obtained from evaluation of irradiated materials from capsule W-97 which was removed from the reactor in August 1980.

III Surveillance Program Description

The Millstone Unit 2 reactor pressure vessel was designed and fabricated by Combustion Engineering, Inc. The reactor vessel beltline, as defined by 10CFR50, Appendix H, consists of the six plates used to form the lower and intermediate shell courses in the vessel, the included longitudinal seam welds and the lower to intermediate shell girth seam weld. The plates were manufactured from SA533 Grade B Class 1 quenched and tempered plate. The heat treatment consisted of austenization at 1600 $\pm$ 50F for four hours, water quenching and tempering at 1225 $\pm$ 25F for four hours. The ASME Code qualification test plates were stress relieved at 1150 $\pm$ 25F for forty hours, and furnace cooled to 600F. The longitudinal and girth seam welds were fabricated using E8018-C3 manual arc electrodes and Mil B-4 submerged arc weld wire with Linde 124 and Linde 0091 flux. The post weld heat treatment consisted of a forty hour 1150 $\pm$ 25F stress relief heat treatment followed by furnace cooling to 600F. The beltline

materials are identified in Tables III-1 and III-2. The chemical analysis of the six beltline plates is given in Table III-3. The materials included in the surveillance program were obtained from the actual reactor vessel beltline materials. The base metal surveillance material, a section from plate C-506-1, was selected from the six beltline plates on the basis of the highest initial drop weight NDTT. The heat treatment of the surveillance plate duplicated that of the reactor vessel ASME Code qualification test plates. The surveillance weld material was fabricated by welding together sections of plates C-506-2 and C-506-3 using the same weld procedure and wire-flux combination used for the intermediate to lower shell girth seam weld. Mil B-4 submerged arc filler wire and Linde 0091 flux was used. The post-weld heat treatment consisted of a forty hour stress relief at 1125 $\pm$ 25F followed by furnace cooling to 600F. The surveillance heat-affected zone material was fabricated by welding together sections of plates C-506-1 and C-506-3 in the same manner as the surveillance weld material with the same postweld heat treatment. The chemical analysis of the surveillance plate and weld[2] is given in Table III-4.

TABLE III-1

REACTOR VESSEL

BELTLINE PLATES

Location	Piece Number	Code Number	Heat Number	Supplier
Intermediate Shell	215-02A	C-505-1	C-5843-1	Lukens
Intermediate Shell	215-02B	C-505-2	C-5843-2	Lukens
Intermediate Shell	215-02C	C-505-3	C-5843-3	Lukens
Lower Shell	215-03A	C-506-1	C-5667-1	Lukens
Lower Shell	215-03C	C-506-2	C-5667-2	Lukens
Lower Shell	215-03B	C-506-3	A-5518-1	Lukens

TABLE III-2

REACTOR VESSEL BELTLINE WELDS

Location	Weld Seam No.	Wire Heat No.	Flux Type	Flux Batch
Intermediate Shell Longitudinal Seam	2-203A	A-8746	Linde 124	3878
Intermediate Shell Longitudinal Seam	2-203B	A-8746	Linde 124	3878
Intermediate Shell Longitudinal Seam	2-203C	A-8746	Linde 124	3878
		M/A LOBI*	-	-
Lower Shell Longitudinal Seam	3-203A	A-8746	Linde 124	3878
		M/A BOIA *	-	-
		M/A BOLA *	-	-
Lower Shell Longitudinal Seam	3-203B	A-8746	Linde 124	3878
		M/A CAFJ *	-	-
		M/A DBIJ *	-	-
		M/A EODJ *	-	-
Lower Shell Longitudinal Seam	3-203C	A-8746	Linde 124	3878
		M/A BOIA *	-	-
		M/A BOLA *	-	-
Intermediate to Lower Girth Seam	9-203	10137	Linde 0091	3999
		M/A BOLA *	-	-
		90136	Linde 0091	3998
		M/A LAGJ *	-	-
		M/A JACJ *	-	-

* Manual shielded metal arc electrode (all others automatic submerged arc wire).

TABLE III-3

REACTOR VESSEL BELTLINE

PLATES CHEMICAL ANALYSIS

Element	C-505-1	C-505-2	C-505-3	C-506-1	C-506-2	C-506-3
Si	.18	.18	.18	.12	.20	.21
S	.015	.015	.018	.014	.018	.012
P	.006	.008	.007	.006	.007	.005
Mn	1.27	1.25	1.26	1.30	1.30	1.32
C	.26	.21	.21	.21	.21	.27
Cr	.10	.10	.10	.10	.10	.19
Ni	.64	.64	.65	.61	.61	.70
Mo	.60	.60	.62	.63	.63	.62
V	.003	.003	.004	.005	.005	.004
Cb	<.01	<.01	<.01	<.01	<.01	<.01
B	.0004	.0005	.006	.004	.0006	.0003
Co	.009	.009	.010	.011	.011	.012
Cu	.13	.13	.13	.14	.14	.13
Al	.024	.030	.029	.020	.028	.020
W	<.01	<.01	<.01	<.01	<.01	<.01
Ti	<.01	<.01	<.01	<.01	<.01	<.01
As	.012	.014	.014	.011	.012	.012
Sn	.006	.006	.006	.009	.010	.007
Zr	.002	.002	.002	.002	.002	.002
N_2	.009	.008	.008	.009	.008	.009

TABLE III-4

SURVEILLANCE PLATE AND WELD METAL CHEMICAL ANALYSIS

Element	Weight Percent Plate C-506-1[a]	1/4 T - ID Weld C-506-2/C-506-3[b]	1/4 T - OD Weld C-506-2/C-506-3[c]
Si	.12	.17	.15
S	.014	.013	.013
P	.006	.015	.016
Mn	1.26	1.13	1.13
C	.21	.12	.12
Cr	.10	.04	.05
Ni	.61	.06	.06
Mo	.62	.54	.53
V	.004	.006	.007
Cb	<.01	<.01	<.01
B	.0006	.0003	.0003
Co	.011	.009	.009
Cu	.14	.30	.21
Al	.020	<.001	<.001
W	<.01	.01	<.01
Ti	<.01	<.01	<.01
As	.011	.011	.012
Sn	.009	.004	.003
Zr	.002	.002	.002
N_2	.009	.008	.009

a - Heat C-5667-1

b - Mil B-4 wire heat 90136, Linde 0091 flux lot 3998

c - Mil B-4 wire heat 10137, Linde 0091 flux lot 3999

Drop weight, Charpy impact and tension test specimens were machined from the surveillance materials as described in reference 1. In addition to the surveillance material specimens, Charpy impact specimens were machined from a section of plate 01 from the Heavy Section Steel Technology (HSST) program to serve as standard reference material (SRM).

The surveillance and SRM test specimens were enclosed in six capsules for irradiation in the Millstone Unit 2 reactor vessel. The surveillance capsule assembly is shown in Figure III-1. Each assembly consists of four compartments containing Charpy impact specimens (Figure III-2) and three compartments (Figure III-3) containing tension specimens and monitors (flux and temperature). Each capsule is positioned in a holder tube attached to the reactor vessel cladding to irradiate the specimens in an environment which duplicates as closely as possible that experienced by the reactor vessel. Capsule locations are shown in Figure III-4. The axial portion of each capsule is bisected by the midplane of the core. The circumferential locations were selected to coincide with the peak flux regions of the reactor vessel.

The existing Technical Specification withdrawal schedule for the surveillance capsules is given in Table III-5.

The type and quantity of test specimens contained in the W-97 capsule are given Table III-6.

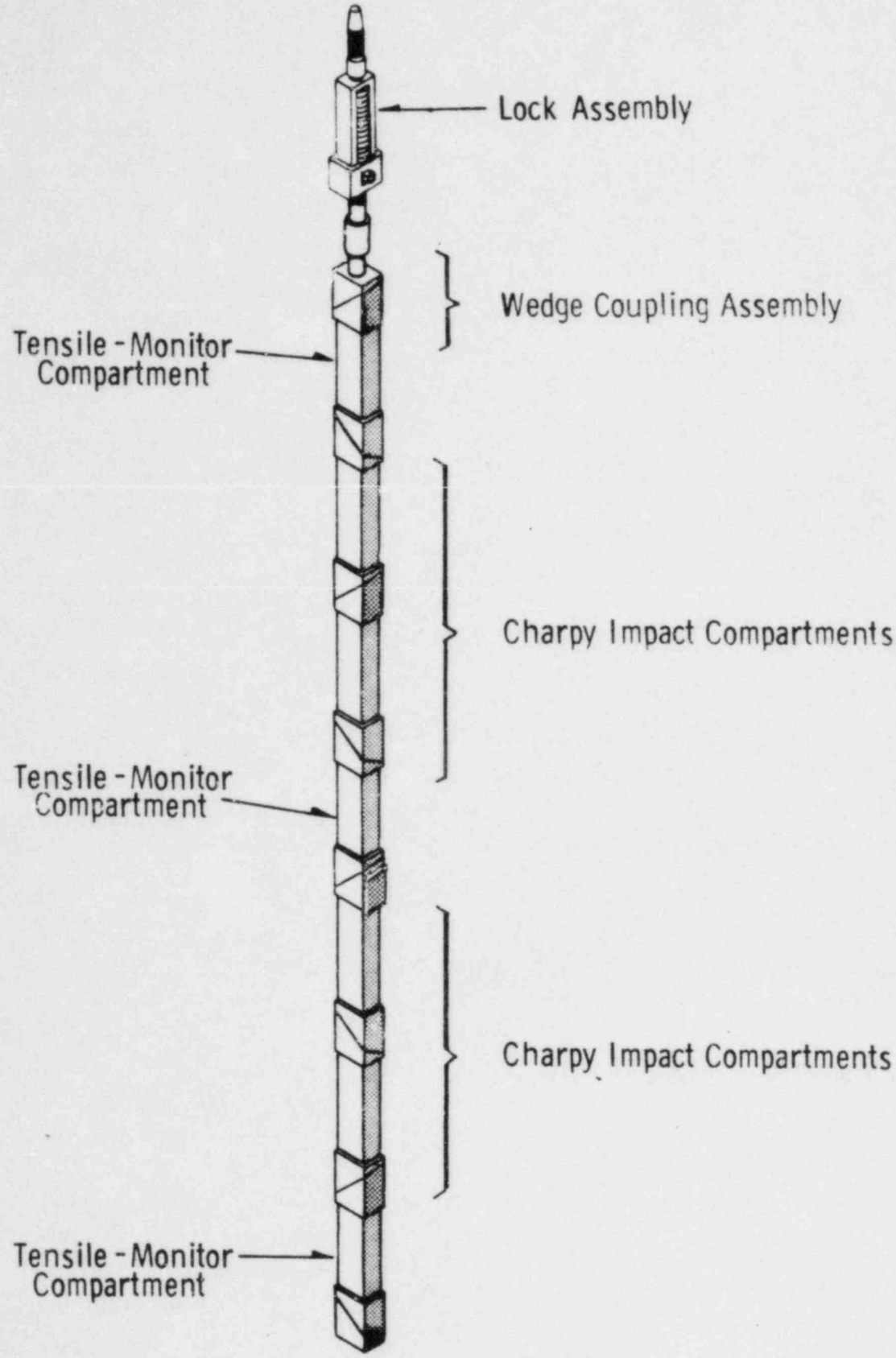

NORTHEAST UTILITIES Millstone Nuclear Power Station Unit No. 2	Typical Surveillance Capsule Assembly	Figure III-1

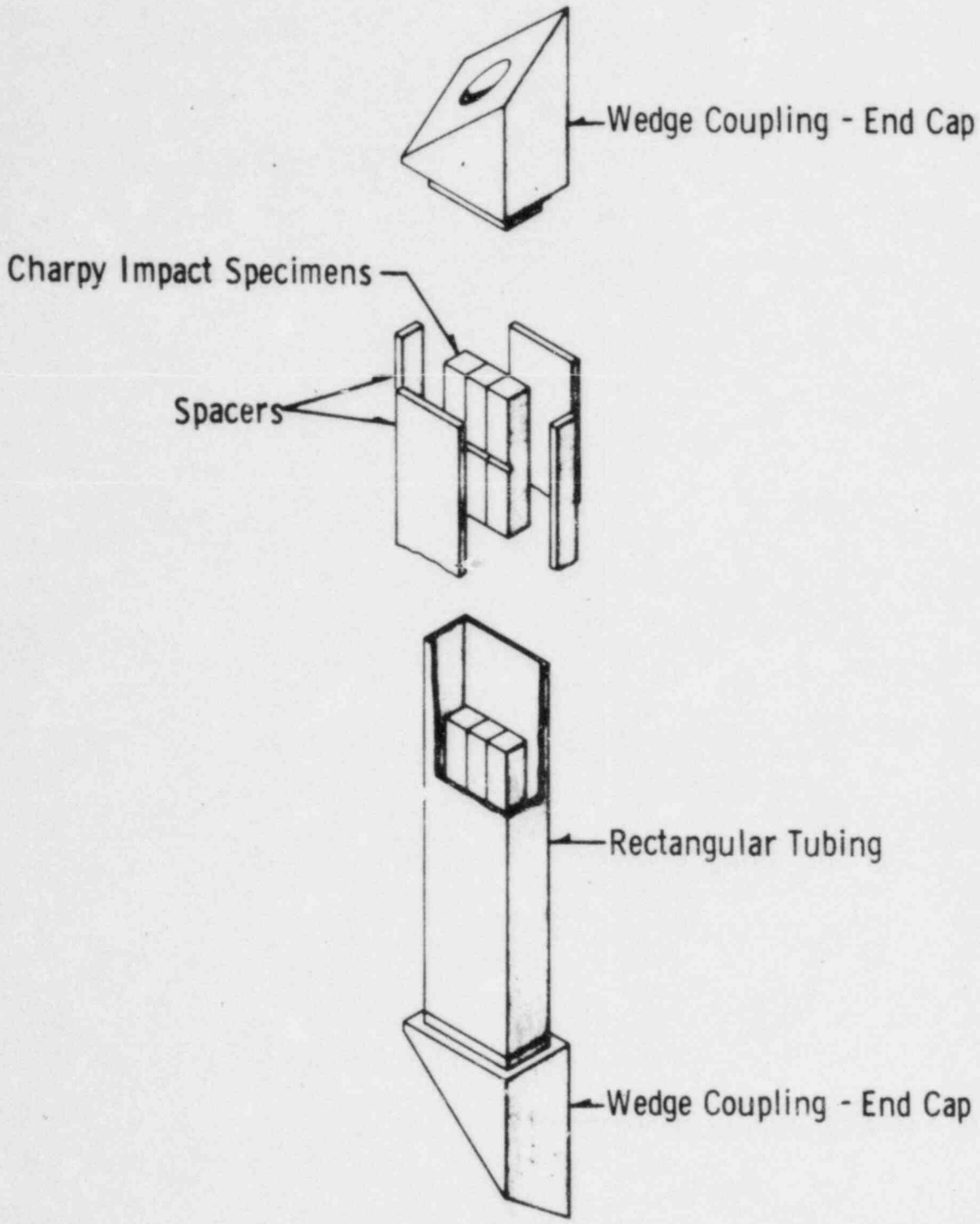

NORTHEAST UTILITIES Millstone Nuclear Power Station Unit No. 2	Typical Charpy Impact Compartment Assembly	Figure III-2

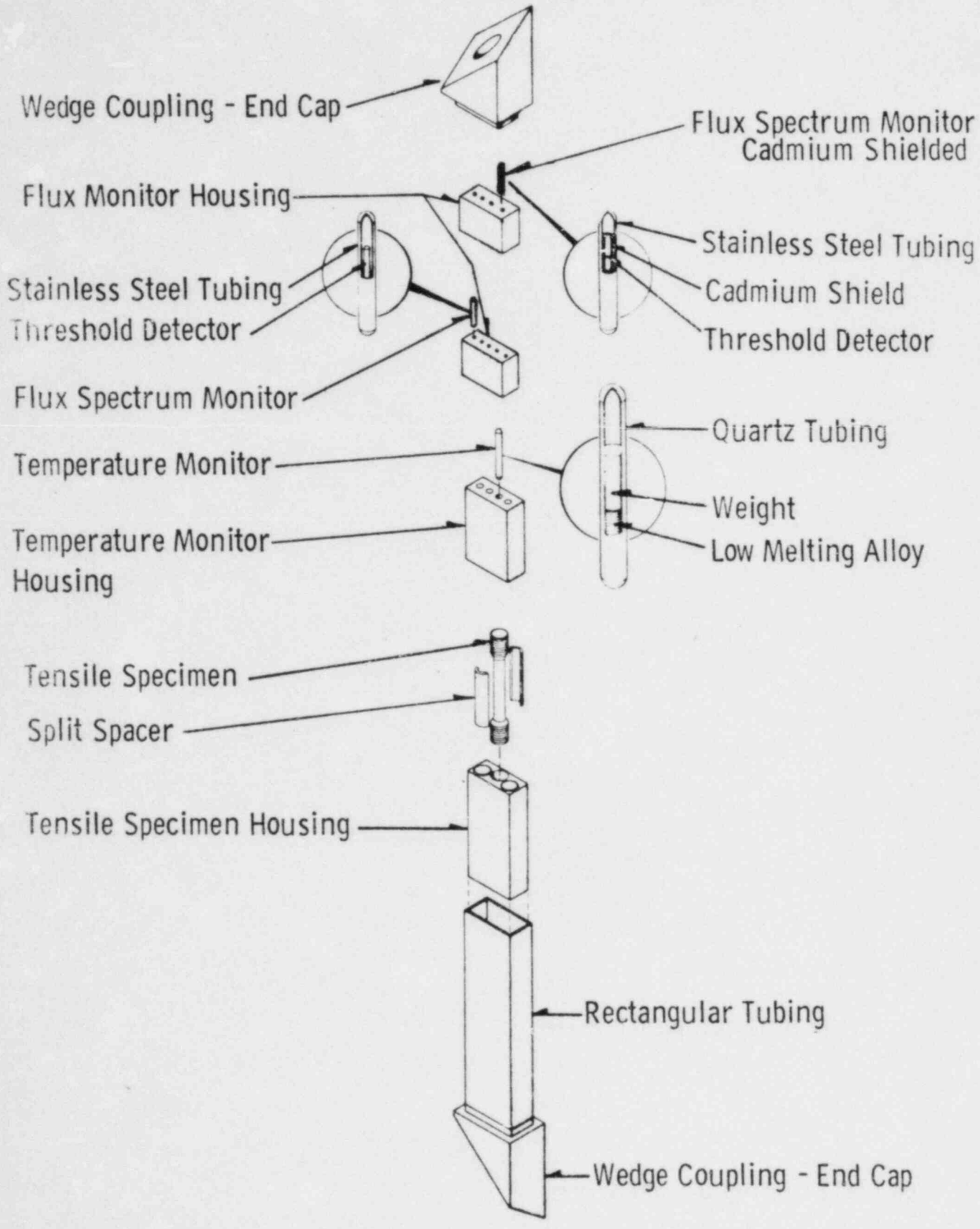

NORTHEAST UTILITIES Millstone Nuclear Power Station Unit No. 2	Typical Tensile-Monitor Compartment Assembly	Figure III-3

NORTHEAST UTILITIES
Millstone
Nuclear Power Station
Unit No. 2

Locations of Surveillance Capsule Assemblies

Figure III-4

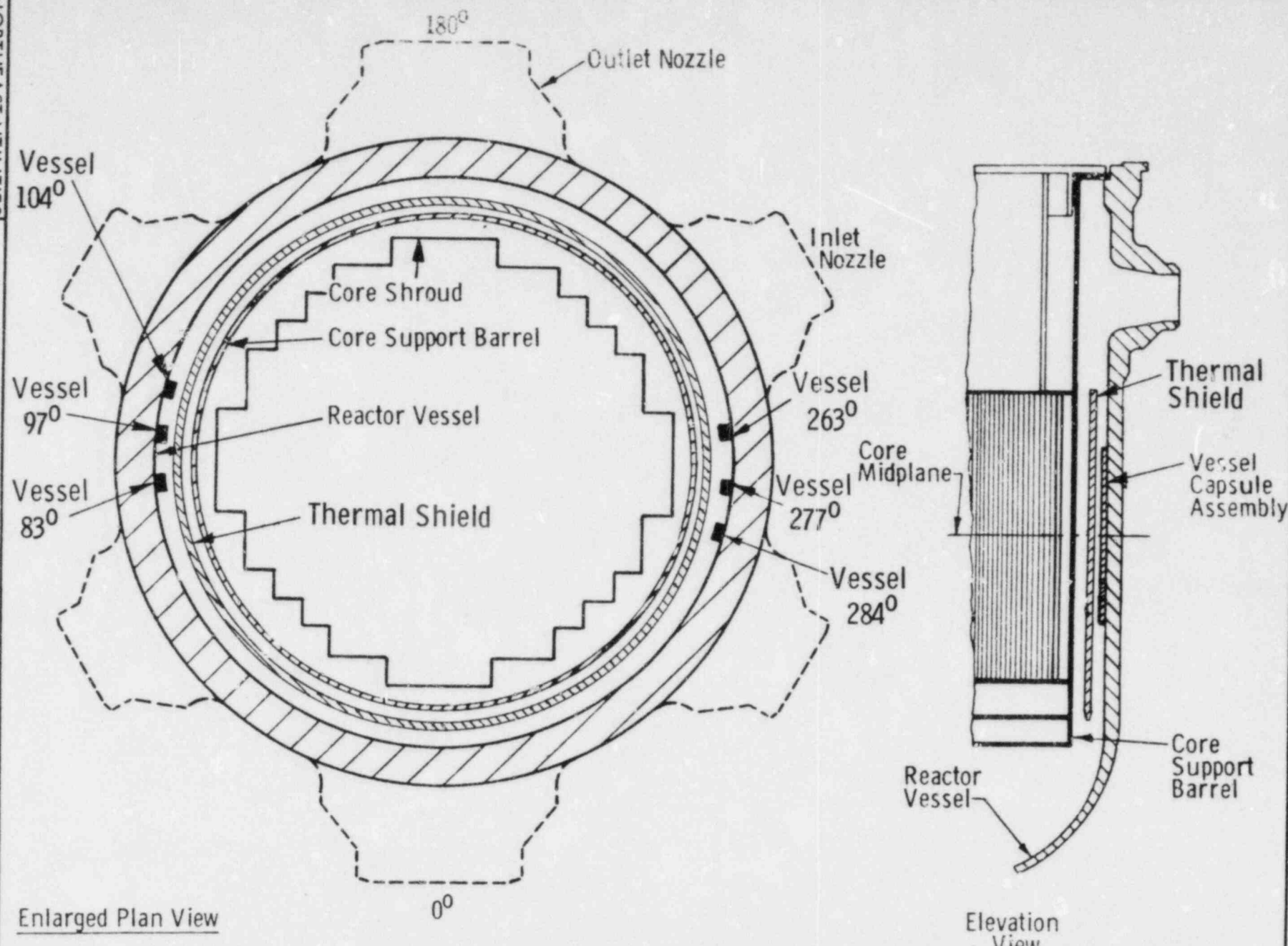

TABLE III-5

EXISTING TECHNICAL SPECIFICATION SCHEDULE FOR
MILLSTONE UNIT 2 REACTOR VESSEL
SURVEILLANCE CAPSULE REMOVAL

Removal Sequence	Azimuthal Location	Approximate Removal Time (Years)	Target Fluence (n/cm^2)
1	97°	8	3.2×10^{18}
2	104°	16	5.7×10^{18}
3	284°	23	8.3×10^{18}
4	263°	30	1.2×10^{19}
5	277°	35	1.4×10^{19}
6	83°	40	1.7×10^{19}

TABLE III-6

TYPE AND QUANTITY OF

SPECIMENS IN W-97 CAPSULE

Material	Charpy Impact	Tension
Base Metal (Transverse)	12	-
Base Metal (longitudinal)	12	3
Weld Metal	12	3
Heat-Affected Zone	12	3
Total	48	9

IV. CAPSULE WITHDRAWAL AND DISASSEMBLY

The Millstone Unit 2 reactor vessel was shut down for refueling at 0800 hours on August 17, 1980. The W-97 surveillance capsule was subsequently inspected using an under-water video system. The capsule was found to be securely locked in position. The lock assembly adapter (ACME threaded nose cone which serves as the point of attachment for the retrieval tool) was intact.

Following the video inspection, a retrieval tool was attached to the W-97 capsule adapter to disengage the latches, and the capsule was withdrawn from its holder and out of the reactor vessel. The W-97 capsule was transferred to the spent fuel pool where it was sectioned into lengths for insertion into a shipping cask. Sectioning was accomplished by drilling to separate the wedge assembly halves, leaving the specimen compartments intact.

The surveillance capsule was shipped to Neutron Products, Inc. in Dickerson, Maryland, for inspection, disassembly and specimen removal in the hot cell facility. No unusual features or damage were revealed by visual inspection. A remote control circular saw was used to open the capsule compartments. Each compartment was identified and inspected prior to cutting, and the contents were removed and verified against the original loading records. An inventory of the mechanical test specimens removed from the W-97 capsule is given in Table IV-1.

TABLE IV-1

MECHANICAL TEST SPECIMENS

REMOVED FROM W-97 CAPSULE

Compartment Number	Material and Specimen Type	Specimen Identification
6214	HAZ Tension	4K7, 4J2, 4KA
6224	HAZ Charpy	435, 43U, 455 44D, 464, 432 447, 451, 42D 45A, 44M, 45M
6232	Base Metal Charpy (Transverse)	23U, 25C, 252 23M, 23K, 21K 251, 25J, 21M 21E, 23T, 23A
6241	Base Metal Tension	1KC, 1JU, 1JA
6251	Base Metal Charpy (Longitudinal)	147, 122, 14D 135, 11B, 11Y 14P, 137, 16B 14M, 14U, 114
6263	Weld Metal Charpy	31L, 352, 31D 33J, 34D, 34A 31C, 36U, 317 33B, 36M, 33C
6273	Weld Metal Tension	3JY, 3J2, 3JJ

V. TEST RESULTS

A. Irradiation Environment

1. Temperature Monitors

Each Tensile-Monitor Compartment (Figures III-1 and III-3) in the capsule assembly contained a set of four temperature monitors to provide an indication of the maximum temperature in the capsule during irradiation. The composition and melting point of each eutectic alloy monitor is given in Table V-1. Each monitor consisted of a helix of the eutectic alloy and a stainless steel weight encapsulated in a quartz tube. Each set of four temperature monitors was inserted into a stainless steel housing, and the temperature monitors were irradiated in the top, middle and bottom surveillance capsule compartments.

Post-irradiation examination of the temperature monitors was performed at C-E's Windsor, Connecticut facility. Each temperature monitor was identified by length, photographed, and inspected to determine whether the eutectic alloy helix had melted and been crushed by the weight. Photographs of the three sets of monitors at 5X are shown in Figures V-1 through V-3. The 536°F monitors (80% Au - 20% Sn) were completely melted. The 558°F monitors (90% Pb - 5% Sn - 5% Ag) helices were distorted but exhibited only localized melting. The 580°F and 590°F monitors were intact and exhibited no distortion. A 558°F monitor is compared with a 590°F monitor in Figure V-4 to illustrate the differences in behavior. Each set of monitors exhibited similar features, indicating that the maximum irradiation temperature was in the 550°F - 558°F range and uniform along the length of the surveillance capsule.

TABLE V-1

COMPOSITION AND MELTING POINTS

OF TEMPERATURE MONITOR MATERIALS

Composition (Weight %)	Melting Temperature °F
80 Au, 20 Sn	536
90 Pb, 5 Sn, 5 Ag	558
97.5 Pb, 2.5 Ag	580
97.5 Pb, 0.75 Sn, 1.75 Ag	590

FIGURE V-1 TEMPERATURE MONITORS
COMPARTMENT 6214 (5x)

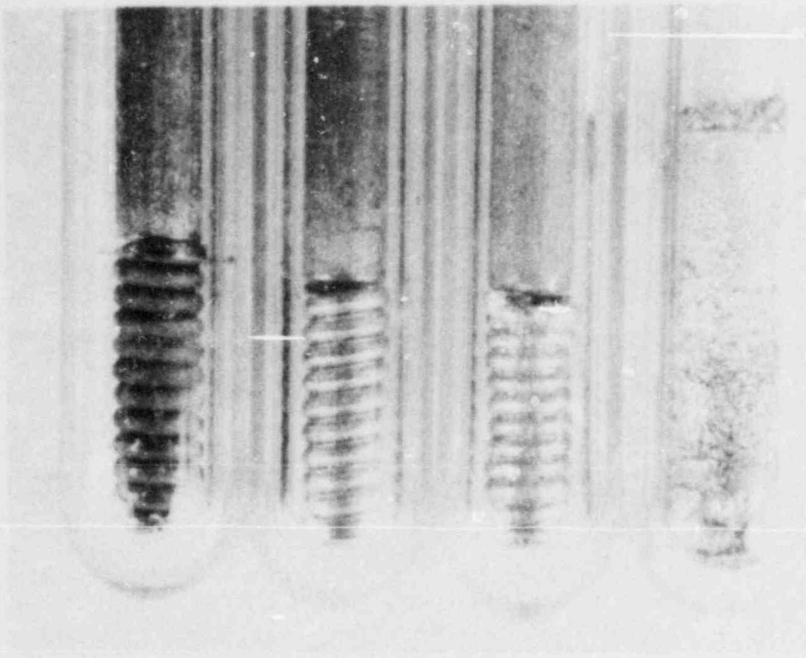

590F 580F 558F 536F

FIGURE V-2 TEMPERATURE MONITORS
COMPARTMENT 6241 (5x)

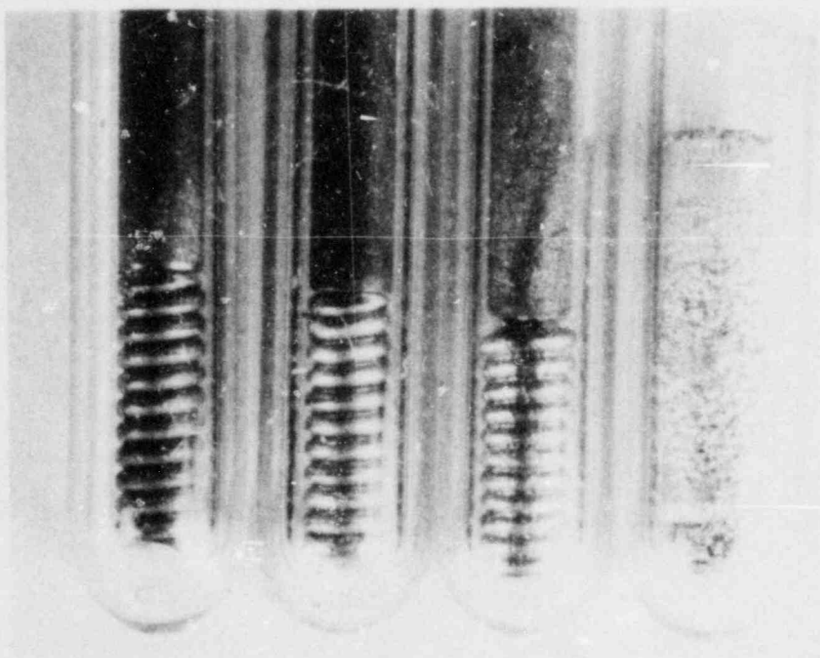

590F 580F 558F 536F

FIGURE V-3 TEMPERATURE MONITORS
COMPARTMENT 6273 (5x)

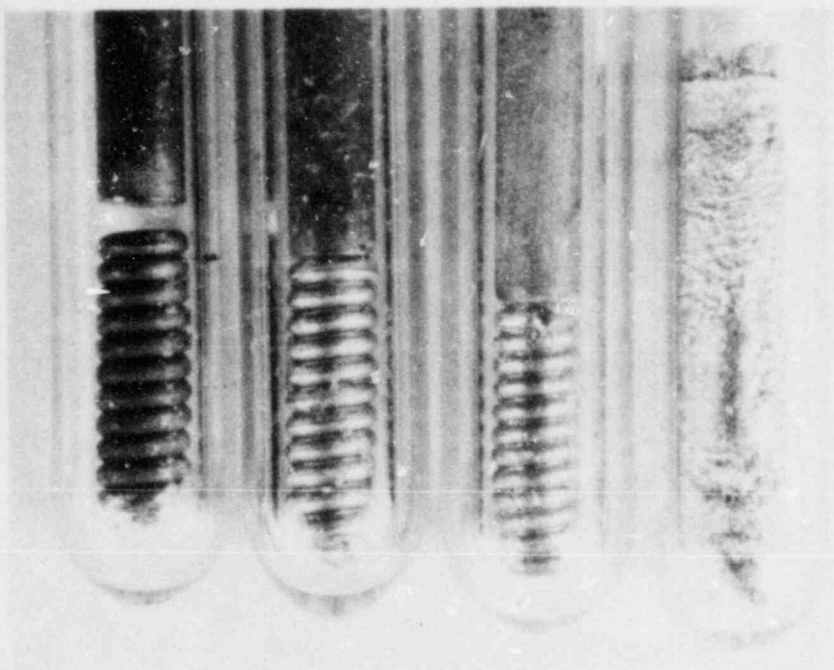

590F 580F 558F 536F

FIGURE V-4 558F AND 590F MONITORS
COMPARTMENT 6214 (7x)

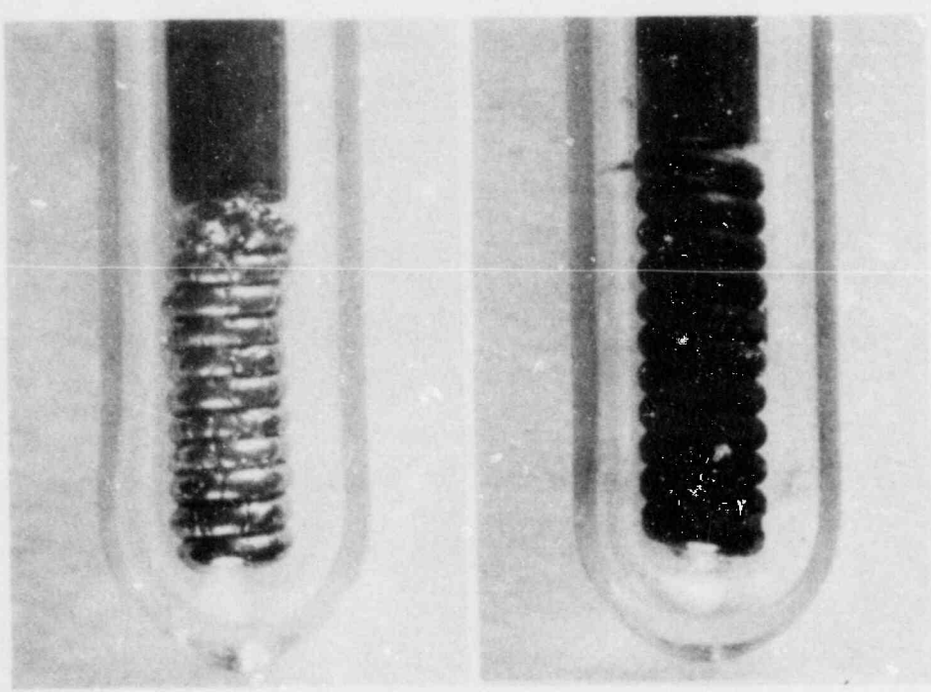

558F 590F

2. Neutron Dosimetry

Each Tensile-Monitor compartment (Figures III-1 and III-3) in the capsule assembly contained two sets of neutron flux monitors as described in Table V-2. Each flux monitor was encapsulated in a stainless steel sheath (except for the sulfur which had a quartz sheath); in addition, cadmium covers were placed around the uranium, cobalt, nickel and copper monitors which have competing thermal activities. Each set of nine flux monitors was inserted into two stainless steel housings, one set for each of the top, middle and bottom surveillance capsule compartments.

The flux monitors were removed from the capsule compartments in the hot cell. Each monitor was inspected and its position in the housing verified by the number of grooves in the stainless steel sheath. The monitors were then repackaged and shipped to C-E's Windsor, Connecticut facility for radiochemical analysis.

a. Radiochemical Analysis

Radiochemical analysis of the flux monitors was performed in accordance with C-E Procedure 00000-FMD-401, Rev. 0, November 1, 1978 ("Standard Method for the Analysis of Radioisotopes in Reactor Irradiation Surveillance Detectors and Flux Distribution Monitors"). Each monitor was removed from its sheath and inserted in a glass vial. Recovery of the uranium, titanium and cadmium shielded monitors was complicated by oxidation and contamination of the monitors. In order to assure that the subsequent activity measurements from these monitors would be accurate, specific steps were taken to either remove or identify the source of the contamination.

TABLE V-2

NEUTRON FLUX MONITORS

Material	Reaction	Threshold Energy (Mev)	Half-Life
Cobalt (Cadmium Shielded)	$Co^{59}(n,\gamma)Co^{60}$	Thermal	5.3 Years
Uranium*	$U^{238}(n,f)\ Cs^{137}$	0.7	30.2 Years
Titanium	$Ti^{46}(n,p)Sc^{46}$	8.0	84 days
Iron	$Fe^{54}(n,p)Mn^{54}$	4.0	314 days
Cobalt	$Co^{59}(n,\gamma)Co^{60}$	Thermal	5.3 Years
Uranium * (Cadmium Shielded)	$U^{238}(n,f)\ Cs^{137}$	0.7	30.2 years
Nickel (Cadmium Shielded)	$Ni^{58}(n,p)\ Co^{58}$	5.0	71 days
Copper (Cadmium Shielded)	$Cu^{63}(n,\alpha)\ Co^{60}$	7.0	5.3 years
Sulfur	$S^{32}(n,p)\ P^{32}$	2.9	14.3 days

*U-238 foil depleted in U-235 to .05 w/o

The uranium foil had converted to a black powder, assumed to be U_3O_8. Therefore, instead of using a simple gravimetric measurement, the amount of uranium recovered was determined by atomic absorption spectroscopy. The titanium wires were embrittled, but otherwise they presented no handling or counting problems. The cadmium shield on the cobalt, copper and nickel wires had apparently melted and fused to the wire during irradiation. The cadmium shields were mechanically removed by stripping, scraping and filing. Final monitor weights were based on elemental analysis using atomic absorption spectroscopy. The sulfur monitor from compartment 6241 contained hydrogen sulfide gas at a pressure high enough to cause a violent separation of the glass capsule during the opening process. As a result, the data were not used for analysis since it was not certain that the sulfur which remained in the capsule was a representative sample; the phosphorus-32 activity was about a decade lower than that found for the other two sulfur monitors. The remainder of the samples for radio-chemical analysis were prepared using standard methods.

Gamma counting was performed with a 4096 channel gamma spectrometer system coupled with a hyperpure germanium detector. The system was calibrated at 0.5 Kev per channel to span the gamma energy range from 0.05 to 2 Mev. Efficiency calibration was performed using eight (8) gamma energies emitted from an NBS traceable mixed isotope standard. Phosphorus-32 beta activity was measured on a gas flow proportional counter which was calibrated with NBS traceable beta standards.

Physical constants used in the calculation of radioisotope activity levels are as follows:

Isotope	Half-Life	Gamma Energy (Mev)	Intensity
Cobalt-58	70.8 days	0.8108	0.99
Cobalt-60	5.27 years	1.3325	1.00
Cesium-137	30.2 years	0.6616	0.85
Manganese-54	312.5 days	0.8348	1.00
Scandium-46	83.8 days	0.8890	1.00
Phosphorus-32	14.3 days	------	1.00

Flux spectrum monitor activity levels are presented in Tables V-3 through V-5. All values are decay corrected to the time of reactor shutdown, 0800 hours, August 17, 1980. The uncertainty listed with each result is the 2-sigma counting error only. An additional error of ±20% for uranium monitors and ±5% for all other metal monitors is estimated from volumetric and gravimetric operations and from the certified uncertainties of calibration isotopes. The additional error associated with the sulfur monitor results is ± 8%.

The shutdown activities determined from gamma ray emission rates were calculated as follows:

$$A = \frac{N_p}{EWBC\ (\exp-\lambda t)}$$

where: A = shutdown activity in disintegrations per minute per milligram of material (dpm/mg)

Np = radioisotope net counts per minute

E = full energy peak effiency (counts per gamma ray emitted)

W = weight of monitor sample (milligrams)

B = radioisotope gamma ray branching ratio (gamma rays per disintegration)

C = correction for coincident or random summing

λ = radioisotope decay constant

t = elapsed time between plant shutdown and counting

TABLE V-3

MILLSTONE UNIT 2 FLUX SPECTRUM MONITOR ACTIVITIES, COMPARTMENT 6214

Monitor Material	Number of Grooves	Weight (mg)	Measured Isotope	Activity at End Irradiation (Dpm/mg)
Cobalt (shielded)	0	7.7	Co-60	$1.76 \pm 0.01 \times 10^5$
Uranium	1	17.5	Cs-137	$2.70 \pm 0.02 \times 10^4$
Titanium	2	9.9	Sc-46	$3.69 \pm 0.08 \times 10^4$
Iron	3	24.3	Mn-54	$1.121 \pm 0.004 \times 10^5$
Cobalt	4	8.1	Co-60	$1.331 \pm 0.006 \times 10^6$
Uranium (shielded)	5	15.6	Cs-137	$1.06 \pm 0.01 \times 10^4$
Nickel (shielded)	6	21.4	Co-58	$1.803 \pm 0.002 \times 10^6$
Copper (shielded)	7	20.0	Co-60	$6.7 \pm 0.1 \times 10^3$
Sulfur	--	18.5	P-32	$2.167 \pm 0.009 \times 10^6$

TABLE V-4

MILLSTONE UNIT 2 FLUX SPECTRUM MONITOR

ACTIVITIES, COMPARTMENT 6241

Monitor Material	Number of Grooves	Weight (mg)	Measured Isotope	Activity at End of Irradiation (D/M/mg)
Cobalt (shielded)	0	8.3	Co-60	$1.81 \pm 0.01 \times 10^5$
Uranium	1	31.9	Cs-137	$2.37 \pm 0.03 \times 10^4$
Titanium	2	13.4	Sc-46	$3.29 \pm 0.06 \times 10^4$
Iron	3	26.5	Mn-54	$1.055 \pm 0.004 \times 10^5$
Cobalt	4	8.4	Co-60	$1.514 \pm 0.007 \times 10^6$
Uranium (shielded)	5	11.1	Cs-137	$1.15 \pm 0.02 \times 10^4$
Nickel (shielded)	6	22.5	Co-58	$1.668 \pm 0.002 \times 10^6$
Copper (shielded)	7	25.0	Co-60	$6.6 \pm 0.1 \times 10^3$
Sulfur	---	10.7	P-32	$2.84 \pm 0.04 \times 10^5$

TABLE V-5

MILLSTONE UNIT 2 FLUX SPECTRUM

MONITOR ACTIVITIES, COMPARTMENT 6273

Monitor Material	Number of Grooves	Weight (mg)	Measured Isotope	Activity at End of Irradiation (D/M/mg)
Cobalt (shielded)	0	7.9	Co-60	$1.84 \pm 0.01 \times 10^5$
Uranium	1	4.9	Cs-137	$2.23 \pm 0.04 \times 10^4$
Titanium	2	12.5	Sc-46	$3.43 \pm 0.07 \times 10^4$
Iron	3	24.8	Mn-54	$1.116 \pm 0.004 \times 10^5$
Cobalt	4	8.3	Co-60	$1.022 \pm 0.006 \times 10^6$
Uranium (shielded)	5	5.6	Cs-137	$1.12 \pm 0.03 \times 10^4$
Nickel (shielded)	6	20.2	Co-58	$1.828 \pm 0.002 \times 10^6$
Copper (shielded)	7	23.2	Co-60	$7.6 \pm 0.1 \times 10^3$
Sulfur	---	17.3	P-32	$1.927 \pm 0.008 \times 10^6$

b. Threshold Detector Analysis

The SAND-II[3] and DOT-III[4] computer codes were used to calculate the fast flux and fluence at the surveillance capsule assembly location and at the reactor vessel.

The SAND-II computer code is used to calculate a neutron flux spectrum from the measured activities of the flux monitors. SAND-II requires an initial flux spectrum estimate; this is calculated using DOT-III. The measured activities must be adjusted before they can be put into SAND. The various steps of the procedure are described below.

The measured activities were decay corrected to reactor shutdown. The foils irradiated and the shutdown activities are shown in Table V-6. Before being used by SAND, the foil activities must be converted to saturated activity with units of disintegrations per second per target atom (dps/a). The following equation was used for the conversion:

$$A_{sat} = \frac{M\ A\ 16.67}{N\ I\ S}$$

where

A_{sat} = Saturated activity (dps/a)
M = Measured activity at shutdown (dpm/mg)
A = Atomic weight
N = Avogadro's number
I = Isotopic abundance of target isotope
S = Saturation factor, explained below

For U^{238} fission product activities, the required SAND input has dimensions of fissions per second per U^{238} atom (fps/a).

TABLE V-6

FLUX MONITOR ACTIVITIES

Monitor	Material	Measured Isotope
1	Cobalt (shielded)	Co-60
2*	Uranium	Cs-137
3	Titanium	Sc-46
4	Iron	Mn-54
5	Cobalt	Co-60
6	Uranium (shielded)	Cs-137
7	Nickel (shielded)	Co-58
8	Copper (shielded)	Co-60
9*	Sulfur	P-32

*These monitors were not included in the SAND analysis.

TABLE V-6 (cont'd)

FLUX MONITOR ACTIVITIES

Compartment[c]	Monitor	Shutdown Activity (dpm/mg)[a]	Saturated Activity (dps/a)[b]
6214	1(d)	1.76+5	9.475-16
	2	2.70+4	4.344-14
	3	3.69+4	9.154-16
	4	1.121+5	4.638-15
	5	1.331+6	7.165-15
	6	1.06+4	1.706-14
	7	1.803+6	6.348-15
	8	6.7+3	5.629-17
	9	2.167+6	2.166-15
6241	1(d)	1.81+5	9.745-16
	2	2.37+4	3.813-14
	3	3.29+4	8.162-16
	4	1.055+5	4.365-15
	5	1.514+6	8.151-15
	6	1.15+4	1.850-14
	7	1.668+6	5.873-15
	8	6.60+3	5.545-17
	9	2.84+5	2.838-16
6273	1(d)	1.84+5	9.906-16
	2	2.23+4	3.587-14
	3	3.43+4	8.509-16
	4	1.116+5	4.618-15
	5	1.022+6	5.502-15
	6	1.12+4	1.801-14
	7	1.828+6	6.436-15
	8	7.6+3	6.386-17
	9	1.927+6	1.926-15

(a) Denotes power of 10

(b) Uranium Foils are (fps/a)

(c) Used compartment number 6273 to obtain the fast flux in the surveillance capsule given in Table V-7. The relative axial variation in the unfolded fast flux was as follows: 6214/6273 = 0.94; 6241/6273 = 0.985

(d) U-238 fission yield of Cs-137 = .0626

This is obtained by dividing A_{sat} by the fractional fission yield of the fission product whose activity was measured.

The saturation factor, S, converts the measured activity to a saturated activity. The actual reactor operating history was used to calculate the saturation factor. The reactor was assumed to operate for several periods of constant power. Then, for each isotope, S was calculated.

$$S = \sum_i \frac{Pi}{Po} \exp(-\lambda T_i) [1 - \exp(-\lambda t_i)]$$

where

Pi = Power of ith interval

Po = Full Power

λ = isotope decay constant

T_i = Time between end of ith operating period to reactor shutdown

t_i = length of ith operating period

The saturated activities are given in Table V-6.

The combination of a cadmium shielded and unshielded U-238 foil is included in the flux monitor set. The activity of the unshielded foil is used to correct for U-235 fissions in the shielded foil. As a result of this calculation, the U-238 fission rate was determined to be 94% of the shielded uranium foil activity in Table V-6. No correction for photo fission of U-238 was included.

SAND requires an initial estimate of the neutron flux spectrum. This initial estimate was calculated using DOT-III, a two-dimensional discrete ordinate code. The DLC-23 CASK, 22

group neutron cross section library was used. The reactor geometry is shown in Figure V-5. Dimensions[5] and power distributions used are as shown in Figure V-6. The distribution of pin power was obtained from an end of cycle 3 PDQ calculated with the assembly power distribution adjusted to correspond to an average over the time from startup to the end of cycle 3. Figure V-7 shows the surveillance capsule detail used in the DOT model.

SAND uses an iterative technique to calculate the neutron flux spectrum. The activities of the set of flux monitors and an initial flux spectrum are the input required by SAND. Activities are calculated for each foil for the flux spectrum using the following equation

$$A = \sum_i \sigma(E_i)\emptyset(E_i)\Delta E_i$$

where

$\sigma(E_i)$ is reaction cross section at energy E_i, barns.
$\emptyset(E_i)$ is the flux at E_i, n/cm^2-s,mev
ΔE_i is width of energy band at E_i, mev.

The flux spectrum is adjusted by an iterative technique until the calculated and measured activities agree within a standard deviation of five percent. The result of this is a 620 group neutron flux.

In addition to DOT-III being used for the initial flux estimate for SAND, it was also used to determine the azimuthal flux distribution on and in the vessel relative to that at the surveillance capsule. With the DOT-III results, Lead Factors were calculated as the ratio of the peak fast flux (En > 1.0 MeV) at the surveillance capsule assembly to the peak fast flux at the vessel-clad interface and 1/4 and 3/4

Figure V-5

MILLSTONE UNIT 2 GEOMETRY USED IN DOT (SEE Figure V-6 FOR DIMENSIONS AND POWER DISTRIBUTIONS)

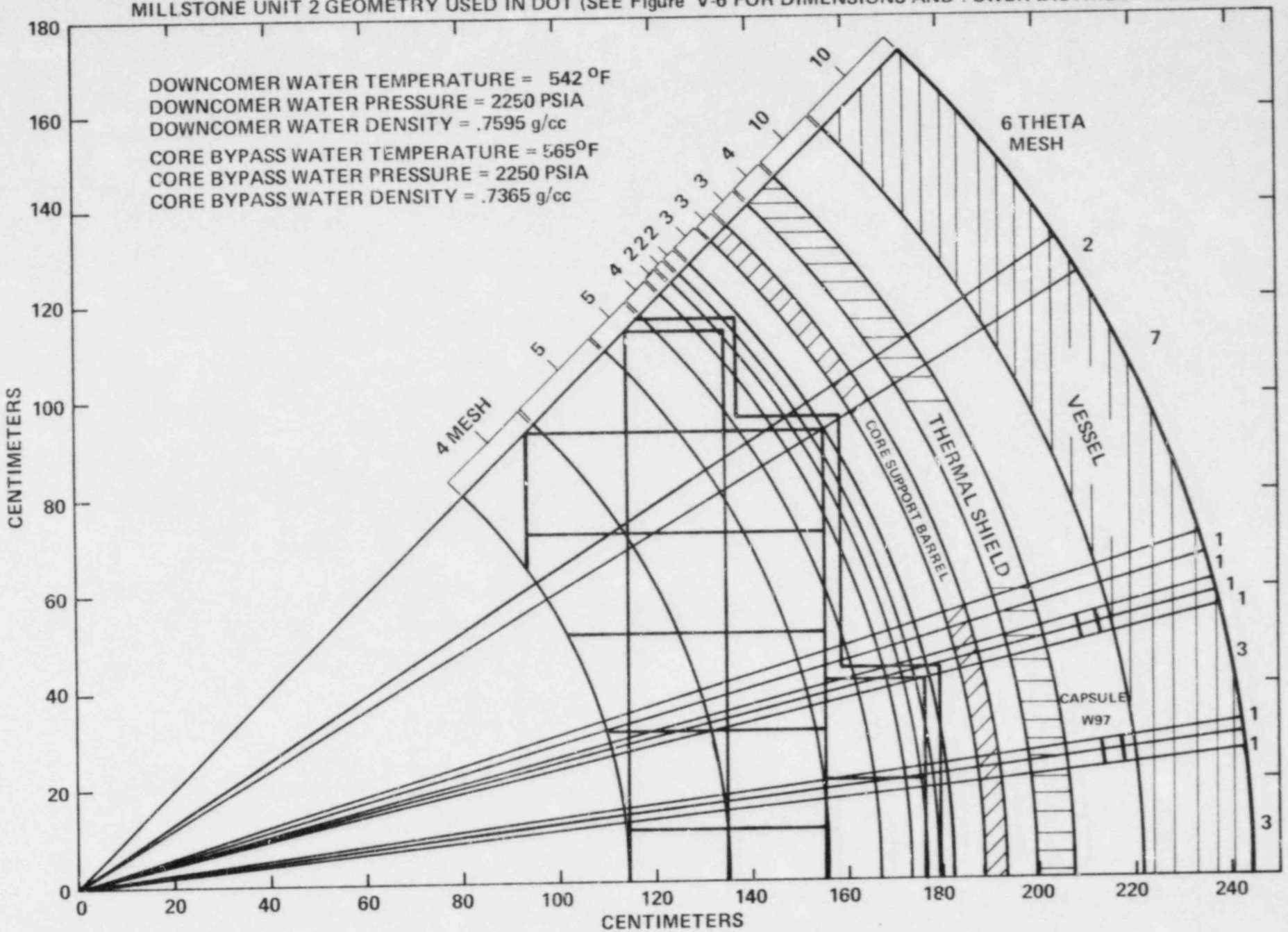

Figure V-6

MILLSTONE UNIT 2 DIMENSIONS AND POWER DISTRIBUTIONS USED IN DOT

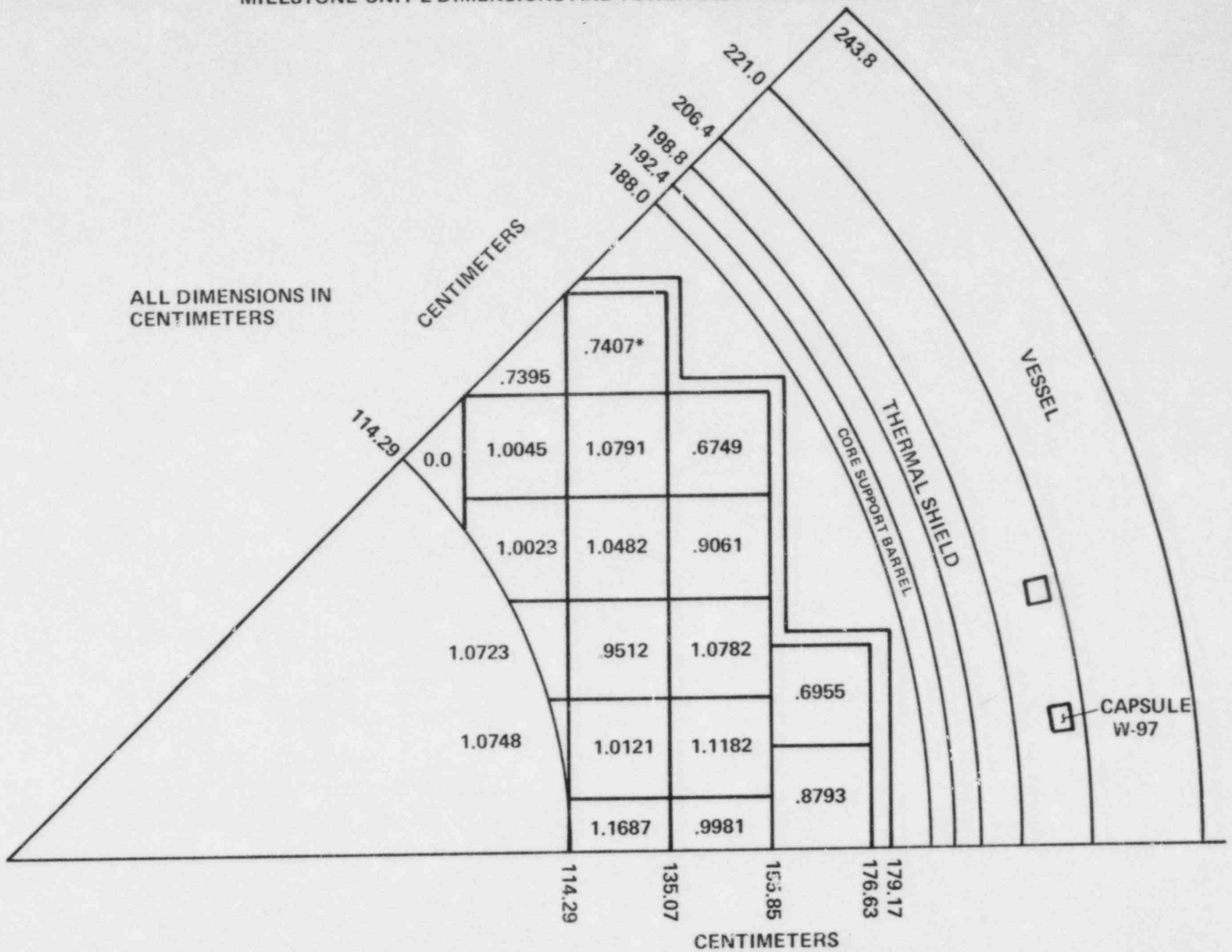

Figure V-7

MILLSTONE UNIT 2 SURVEILLANCE CAPSULE LOCATION

CAPSULE W-97

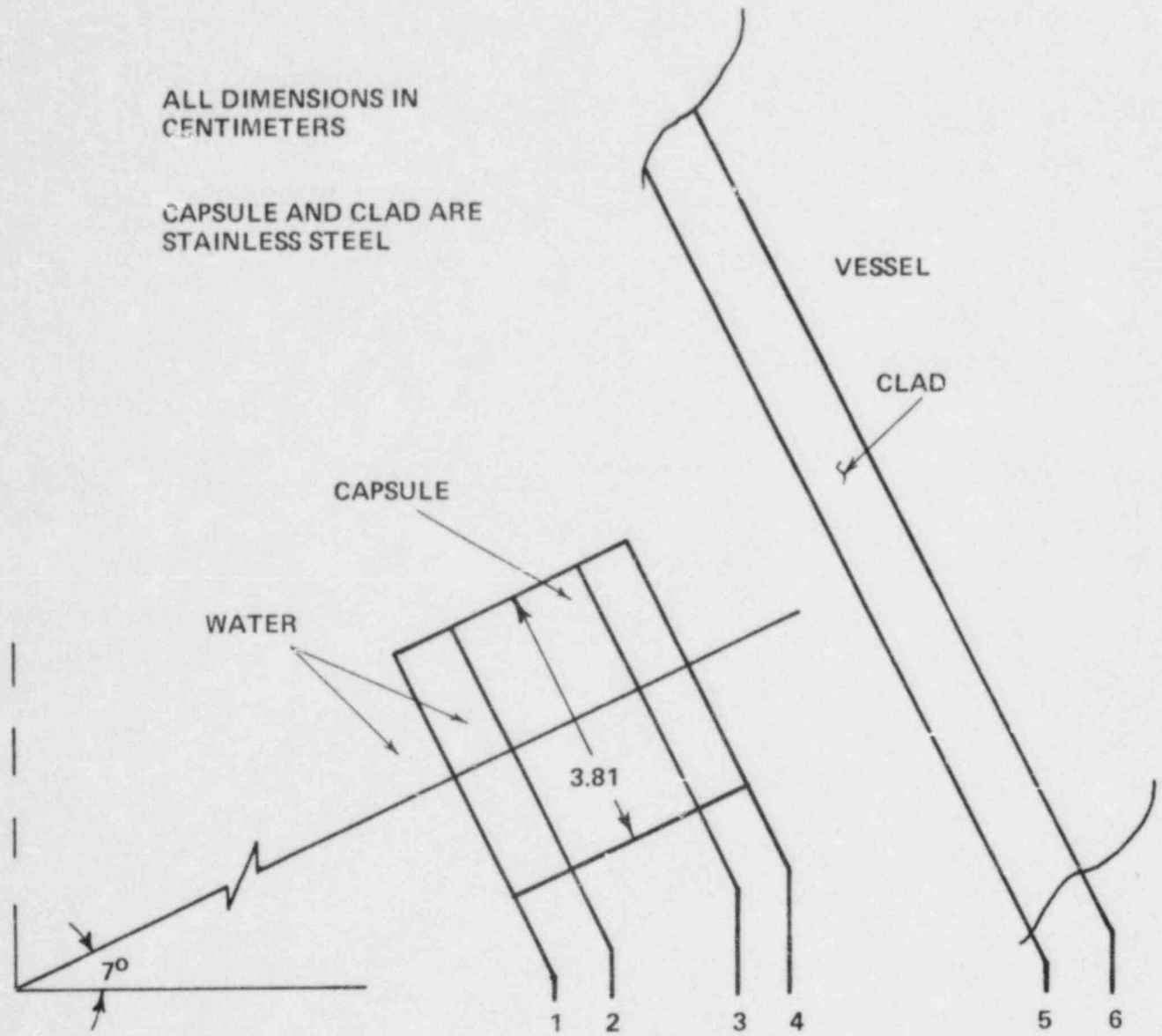

RADIAL DISTANCE (CENTIMETERS)

1	214.65
2	215.69
3	217.57
4	218.46
5	220.0475
6	221.0

vessel thickness locations. These Lead Factors (1.36, 2.62 and 13.9, respectively) were then multiplied by the fast flux generated by SAND to give us the fast flux and fluence at the vessel-clad interface and 1/4 and 3/4 thickness into the vessel respectively. The fluence was calculated for the end of cycle 3 (3.0 Effective Full Power Years at 2700 MWt) and end of life (32 EFPY at 2700 MWt).

The maximum fast flux at the Millstone-II W-97 Surveillance capsule assembly location is $4.0 \times 10^{+10}$ n/cm^2-s. The highest flux was measured in the bottom compartment (6273). The neutron flux in the top compartment (6214) and middle compartment (6241) was approximately 3.76×10^{10} and 3.94×10^{10} n/cm^2-s, respectively. The maximum fast flux at the vessel-clad interface is deduced from this analysis to be $2.94 \times 10^{+10}$ n/cm^2-s thus resulting in an updated estimate of the end of life fluence of $2.96 \times 10^{+19}$ n/cm^2. This assumes a 40 year life with an 80% capacity factor.

TABLE V-7

MILLSTONE UNIT 2 FAST NEUTRON FLUX AND FLUENCE VALUES[a]

Fast Flux (E>1.0 Mev)

Location	Maximum Flux (n/cm^2-s)
Surveillance Capsule	4.00(+10)[b]
Vessel-clad interface	2.94(+10)
1/4 thickness of vessel	1.53(+10)
3/4 thickness of vessel	2.88(+9)

Fast Fluences (E>1.0 MeV)

Location	End of Cycle 3[c]	End of Life[d]
Surveillance Capsule	3.78(+18)	4.03(+19)
Vessel-clad interface	2.78(+18)	2.96(+19)
1/4 thickness of vessel	1.44(+18)	1.54(+18)
3/4 thickness of vessel	2.72(+17)	2.90(+18)

(a) Uncertainty in fluence values ±30%
(b) Denotes power of 10
(c) 3.0 Effective Full Power Years (EFPY) (2700 mwt)
(d) 32.0 EFPY (2700 mwt)

This updated estimate of the end of life fluence at the vessel-clad interface is a factor of 1.55 times higher than the original FSAR predicted value of 1.91×10^{19} n/cm^2. The increase in predicted vessel fluence is the result of a number of factors such as stretch power level (2700 Mwt versus 2560 Mwt), differences in assumed coolant temperature conditions, vessel dimensions, and core wide power distributions (i.e., fuel management strategies). It should be noted that the end of life vessel fluence predicted as a result of using those updated parameters in a predictive mode calculation yields a vessel fluence of 4.0×10^{19} n/cm^2 (assuming a 1.15 time-averaged axial peak), which differs from that inferred from the surveillance capsule by 35%. See Table V-7 for additional fluence data.

Reference 3 states that the SAND code will give fluxes that are accurate to within $\pm$ 10% to $\pm$ 30% if the errors in the measured activities are within similar limits. In Tables V-3 through V-5, the quoted uncertainties are at a 2-Sigma level and are determined from counting statistics. An additional error of $\pm$ 20% for uranium monitors and $\pm$ 5% for all other metal monitors is estimated from volumetric and gravimetric operations and from the certified uncertainties of calibration isotopes. The additional error associated with the sulfur monitor results in $\pm$ 8%. Therefore, it is estimated that the uncertainty in the measured flux at the surveillance capsule location is about $\pm$ 20% to $\pm$ 30%. The extrapolated flux in the vessel will be slightly higher, so a reasonable value to use for the uncertainty of the fluence at the vessel ID is $\pm$ 30%. This uncertainty does not include variations that may occur in the Lead Factor due to changes in the azimuthal distributions which could result from different fuel management strategies.

B. Chemical Analysis

Six Charpy specimens each of the base metal (transverse orientation) and weld metal were chemically analyzed by X-ray fluorescence for molybdenum, copper, nickel, manganese, silicon, sulfur and phosphorous content. Each Charpy specimen was placed in a carrier with a graphite mask for analysis. Calibration curves were initially established for the seven elements using nine plate and weld specimens with a known chemical content. One of these specimens (11E) was used to check for reproducibility with copper and phosphorous as the selected elements. Twelve separate measurements yielded a copper reproducibility of $\pm$ 1% and a phosphorous reproducibility of $\pm$ 7% at one standard deviation. Specimen 11E was also used as a control for each set of irradiated specimen measurements.

Results of the analysis of the irradiated specimens and the control specimen are given in Table V-8. The base metal specimens represent four different sections of the surveillance plate; specimens 23A, 23K and 23M represent the same plate section. The weld metal specimens represent six separate layers through the thickness of the weld.

C. Strength and Toughness Properties

1. Tension Tests

Tension tests were conducted in accordance with applicable ASTM standards and C-E laboratory procedures. The test method and equipment are described in Appendix A.

The three irradiated specimens from each material (base metal, weld metal and heat-affected zone) were tested at

TABLE V-8

IRRADIATED PLATE AND WELD

MATERIAL CHEMICAL ANALYSIS

Specimen ID	Lab Number	Material	Chemical Content(Weight Percent)						
			Mo	Cu	Ni	Mn	Si	S	P
21E	6025	Plate(WR)	0.60	0.15	0.61	1.28	0.20	0.016	0.008
23A	6026	Plate(WR)	0.59	0.14	0.60	1.26	0.38	0.015	0.007
23K	6020	Plate(WR)	0.59	0.14	0.60	1.28	0.28	0.016	0.008
23M	6019	Plate(WR)	0.59	0.14	0.60	1.27	0.28	0.15	0.007
25I	6015	Plate(WR)	0.60	0.14	0.60	1.27	0.61	0.017	0.009
25C	6018	Plate(WR)	0.59	0.14	0.59	1.29	0.51	0.017	0.008
31I	6023	Weld	0.54	0.23	0.065	1.12	0.17	0.015	0.014
31L	6024	Weld	0.52	0.24	0.071	1.14	0.34	0.016	0.014
33B	6022	Weld	0.54	0.28	0.059	1.09	0.24	0.015	0.012
34D	6021	Weld	0.54	0.29	0.055	1.08	0.40	0.015	0.014
352	6016	Weld	0.54	0.30	0.057	1.07	0.21	0.015	0.013
36M	6017	Weld	0.53	0.31	0.044	1.10	0.20	0.015	0.012
11E	#1	Control	0.57	0.16	0.57	1.27	0.21	0.014	0.008
11E	#2	Control	0.57	0.16	0.54	1.24	0.20	0.014	0.008
11E	#3	Control	0.57	0.16	0.55	1.24	0.20	0.014	0.007
11E	#4	Control	0.56	0.16	0.54	1.25	0.20	0.014	0.008

room temperature, 250°F and 550F. The tensile properties are listed in Table V-9, and the stress-strain curves are shown in Figure V-8 through V-16. The pre-irradiation tensile properties[2] are summarized in Table V-10 (each value average of three tests). Photographs of the fracture surface of the broken irradiated specimens are shown in Figure V-17.

2. Charpy V-Notch Impact Tests

Charpy V-notch impact tests were conducted in accordance with applicable ASTM standards and CE laboratory procedures. The test method and equipment are described in Appendix B.

Twelve irradiated specimens from each material (transverse and longitudinal base metal, weld metal and heat-affected zone) were tested at a series of temperatures to establish the transition temperature behavior. The impact data (impact energy, lateral expansion and fracture appearance as a function of test temperature) are shown in Tables V-11 through V-14 and Figures V-18 through V-29. (Also shown in each of the figures is the unirradiated transition temperature curve from the baseline evaluation.[2]) Fracture surface photographs of the broken irradiated specimens are shown in Figures V-30 through V-33.

Each impact test was instrumented. Additional data related to instrumented impact testing are presented in Appendix C.

TABLE V-9

POST-IRRADIATION TENSION TEST PROPERTIES

Material	Specimen Code	Test Temp. (°F)	Yield Strength 0.2% Offset (ksi)	Ultimate Tensile Strength (ksi)	Fracture Load (lb)	Fracture Strength[a] (ksi)	Fracture Stress[b] (ksi)	Reduction of Area (%)	Elongation (1-inch gage) TE/UE (%)
Base Metal	1KC	72	73.3	96.0	2940	59.9	181	67	26/9.3
	1JA	250	70.9	92.5	2880	58.7	174	66	26/10.0
	1JU	550	61.7	86.7	2820	57.5	158	64	27/9.3
Weld Metal	3JY	72	86.8	102.1	3180	64.8	213	70	27.5/9.0
	3JJ	250	79.5	92.8	2880	58.7	174	66	25/8.8
	3J2	550	72.8	90.4	2820	57.0	168	66	22.5/8.5
HAZ	4K7	72	75.8	100.1	2940	59.9	185	68	27/7.0
	4KA	250	69.3	92.2	2940	59.9	181	67	22.5/8.5
	4J2	550	68.4	87.8	2820	57.9	168	66	22/6.6

a - Fracture strength is the fracture load divided by initial cross sectional area

b - Fracture stress is the fracture load divided by final cross sectional area

TABLE V-10

PRE-IRRADIATION TENSION TEST PROPERTIES

Material	Test Temp. (°F)	Yield Strength 0.2% Offset[a] (ksi)	Ultimate Tensile Strength (ksi)	Fracture Load (lb)	Fracture Strength[b] (ksi)	Fracture Stress[c] (ksi)	Reduction of Area (%)	Elongation (1-inch gage) TE/UE (%)
Base Metal	71	67.1/63.5	85.7	2620	53.5	183	71	29/11.7
	250	61.4/59.4	79.3	2500	51.0	171	70	26/10.2
	550	56.3	82.9	2680	54.3	179	69	26/10.1
Weld Metal	71	76.1/73.0	85.8	2540	51.8	201	74	28/11.2
	250	73.7/69.1	80.5	2460	50.2	176	71	25/9.3
	550	66.8	84.9	2880	58.8	169	65	25/9.9
HAZ	71	67.8/63.7	87.6	2760	56.3	188	70	24/9.2
	250	60.4/59.0	80.4	2540	51.8	186	72	25/7.8
	550	61.7	83.1	2700	55.1	173	68	21/7.3

a - Upper/Lower yield strength where observed.

b - Fracture strength is the Fracture Load divided by initial cross sectional area.

c - Fracture stress is the Fracture Load divided by final cross sectional area.

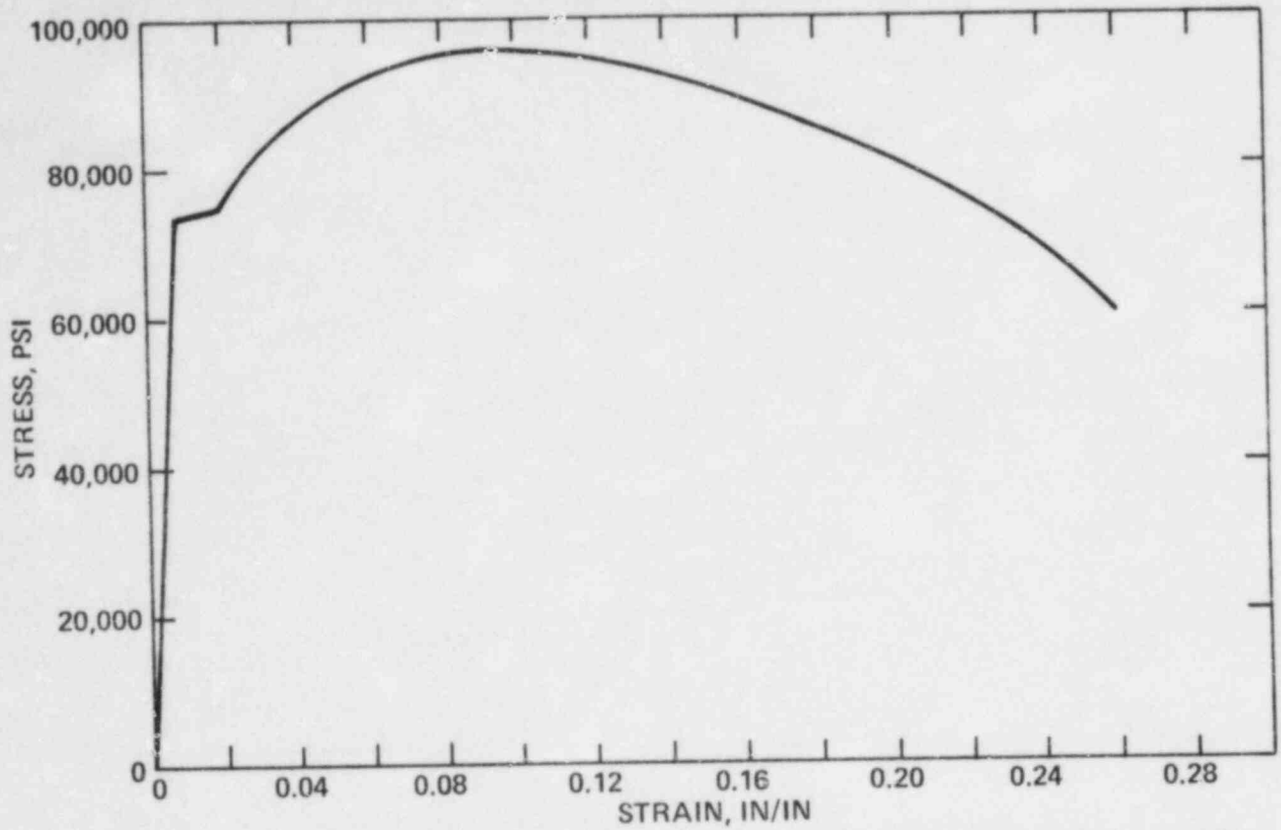

Figure V-8 STRESS STRAIN RECORD OF TENSION TEST, BASE METAL PLATE C-506-1 SPECIMEN No. 1KC, TEST TEMPERATURE R.T. ^{o}F

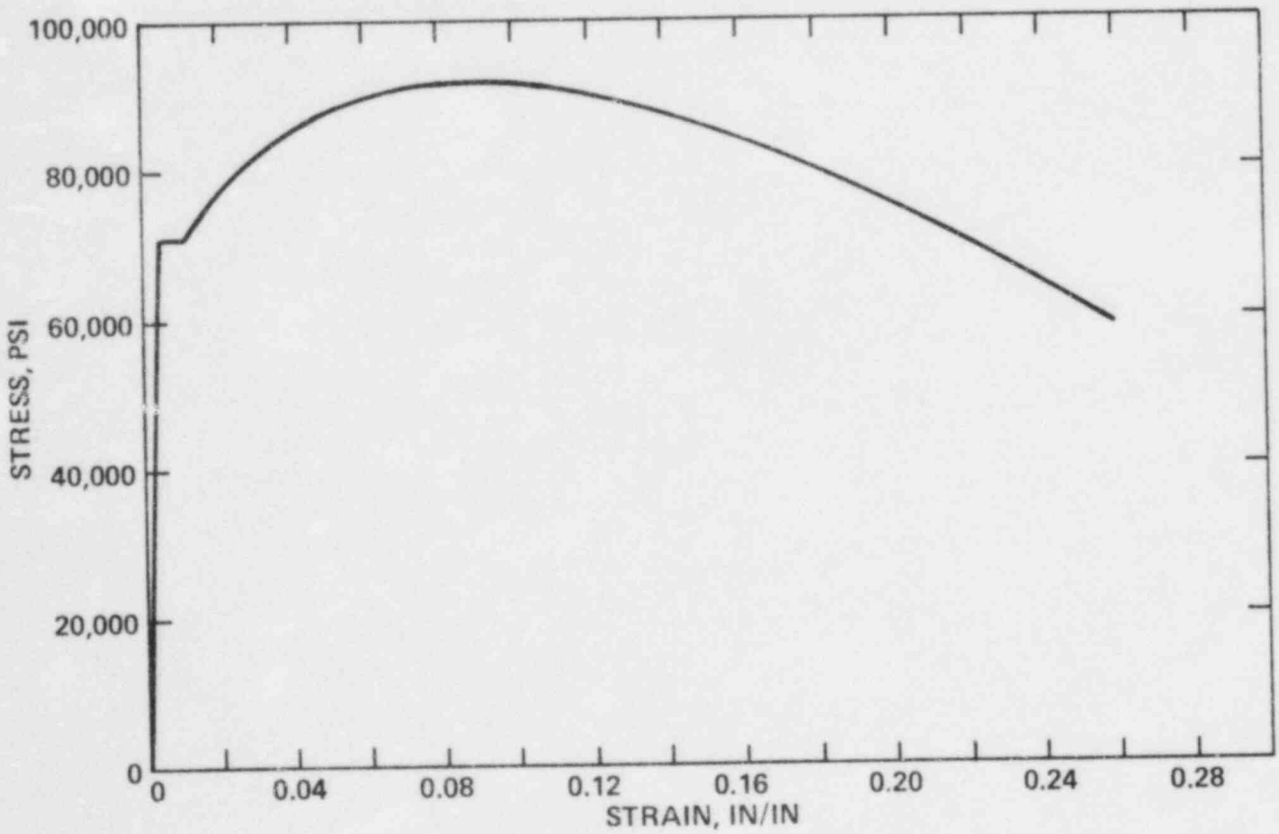

Figure V-9 STRESS STRAIN RECORD OF TENSION TEST, BASE METAL PLATE C-506-1 SPECIMEN No. 1JA, TEST TEMPERATURE 250^{o}F

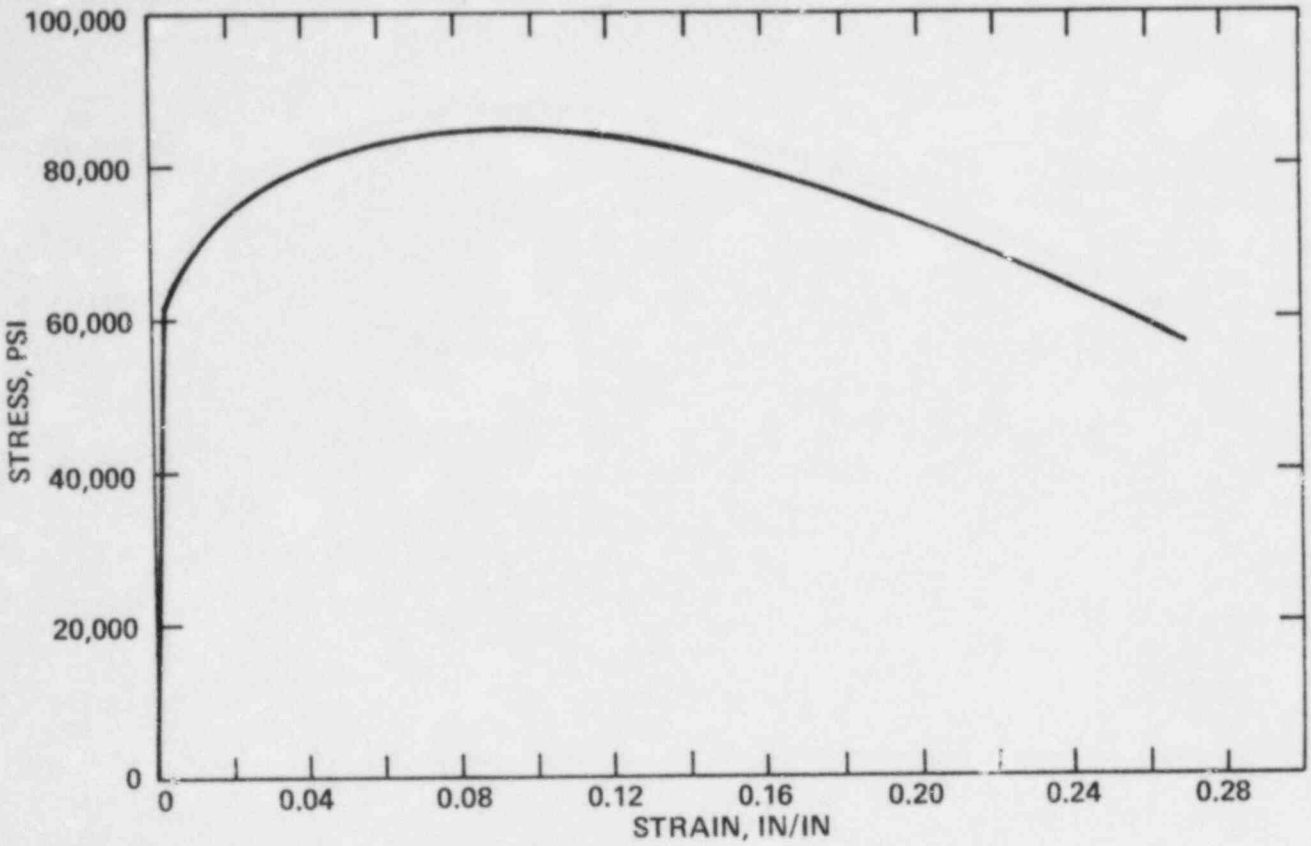

Figure V-10 STRESS STRAIN RECORD OF TENSION TEST, BASE METAL PLATE C-506-1 SPECIMEN No. 1JU, TEST TEMPERATURE 550°F

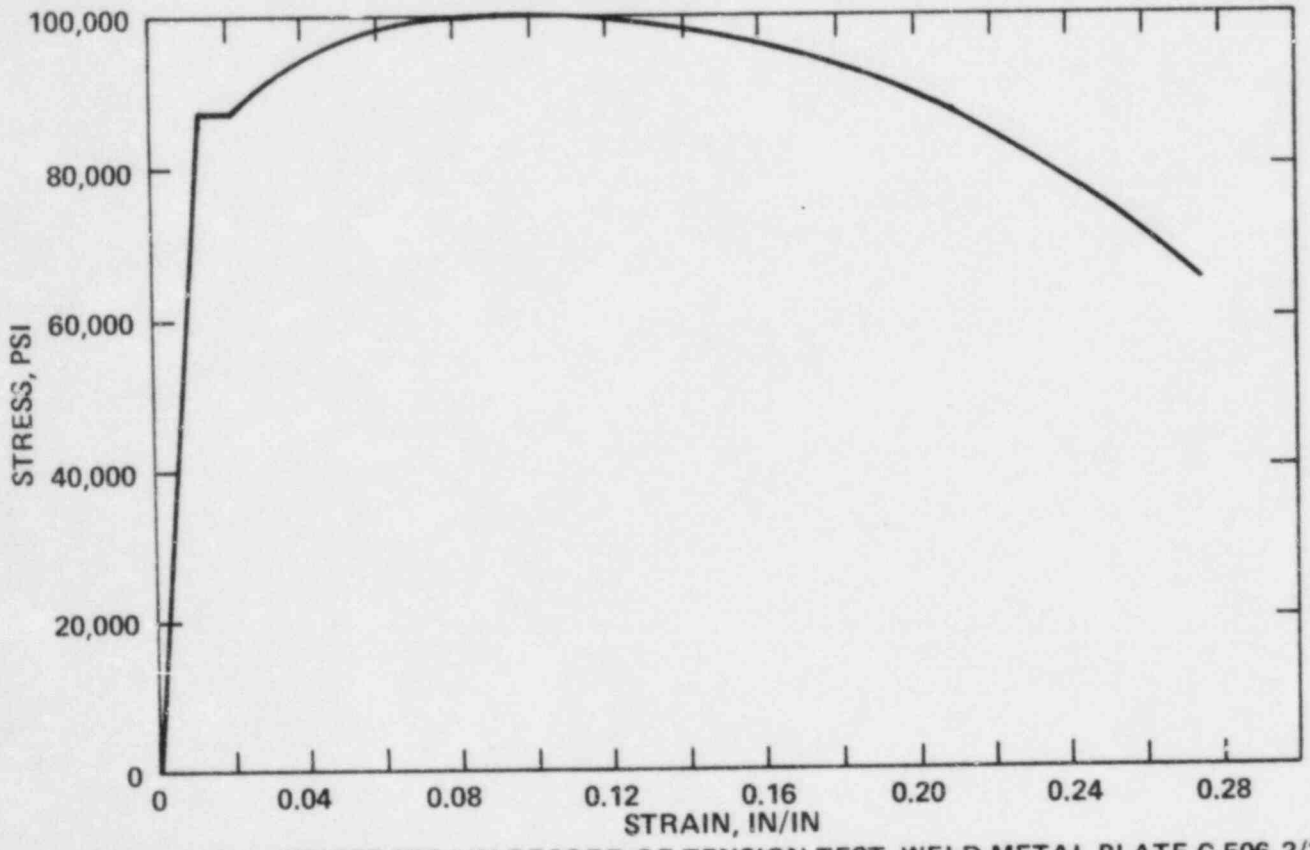

Figure V-11 STRESS STRAIN RECORD OF TENSION TEST, WELD METAL PLATE C-506-2/3 SPECIMEN No. 3JY, TEST TEMPERATURE R.T. °F

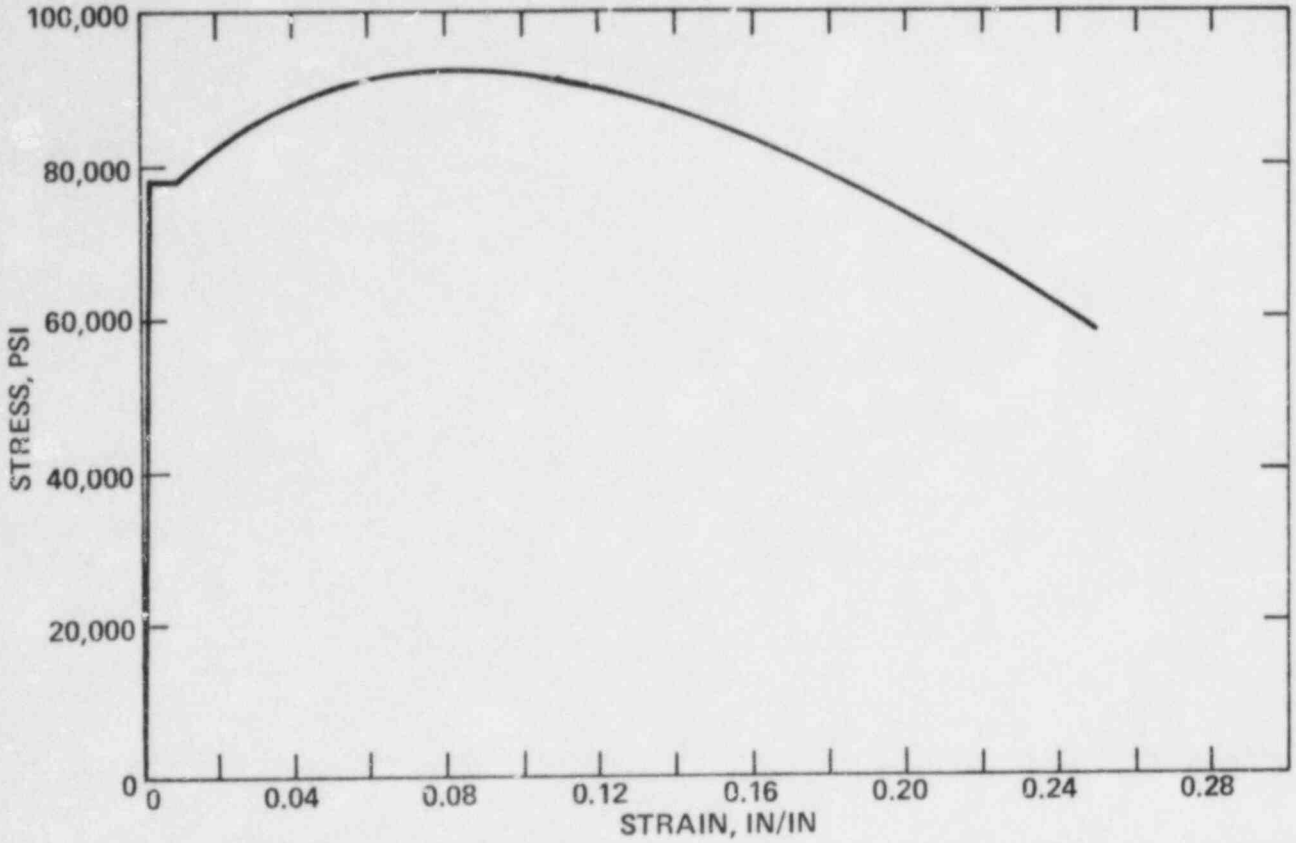

Figure V-12 STRESS STRAIN RECORD OF TENSION TEST, WELD METAL PLATE C-506-2/3 SPECIMEN No. 3JJ, TEST TEMPERATURE 250°F

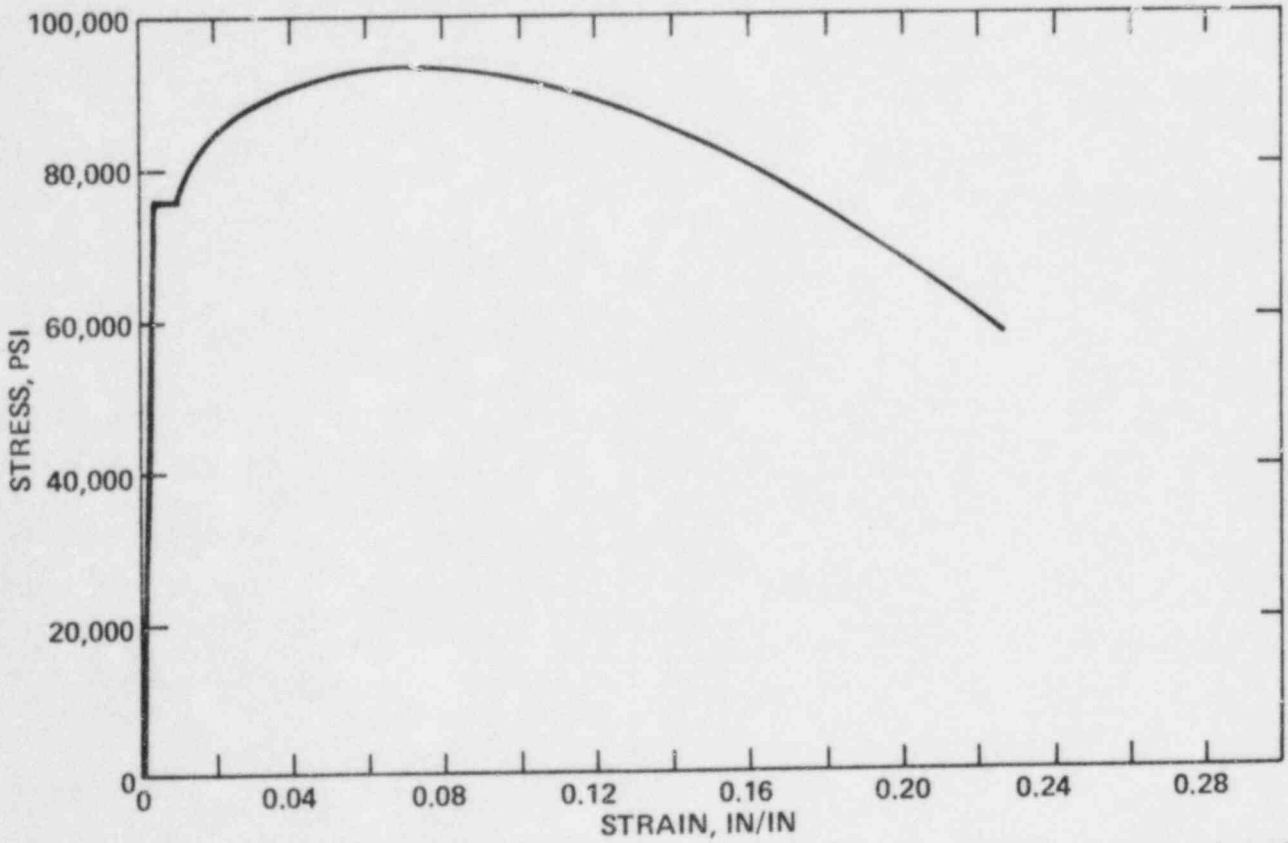

Figure V-13 STRESS STRAIN RECORD OF TENSION TEST, WELD METAL PLATE C-506-2/3 SPECIMEN No. 3J2, TEST TEMPERATURE 550°F

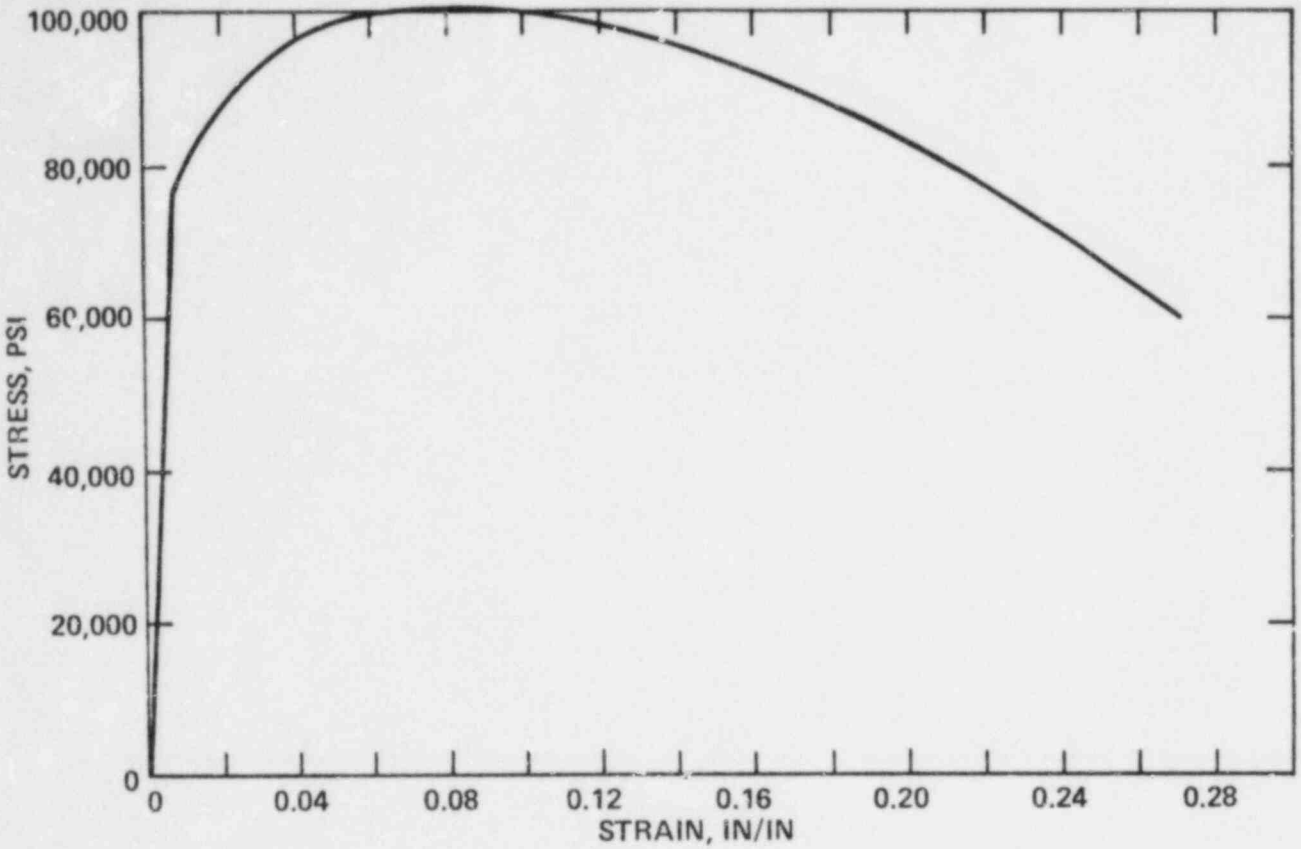

Figure V-14 STRESS STRAIN RECORD OF TENSION TEST, HAZ METAL PLATE C-506-1 SPECIMEN No. 4K7, TEST TEMPERATURE, R.T. ^{O}F

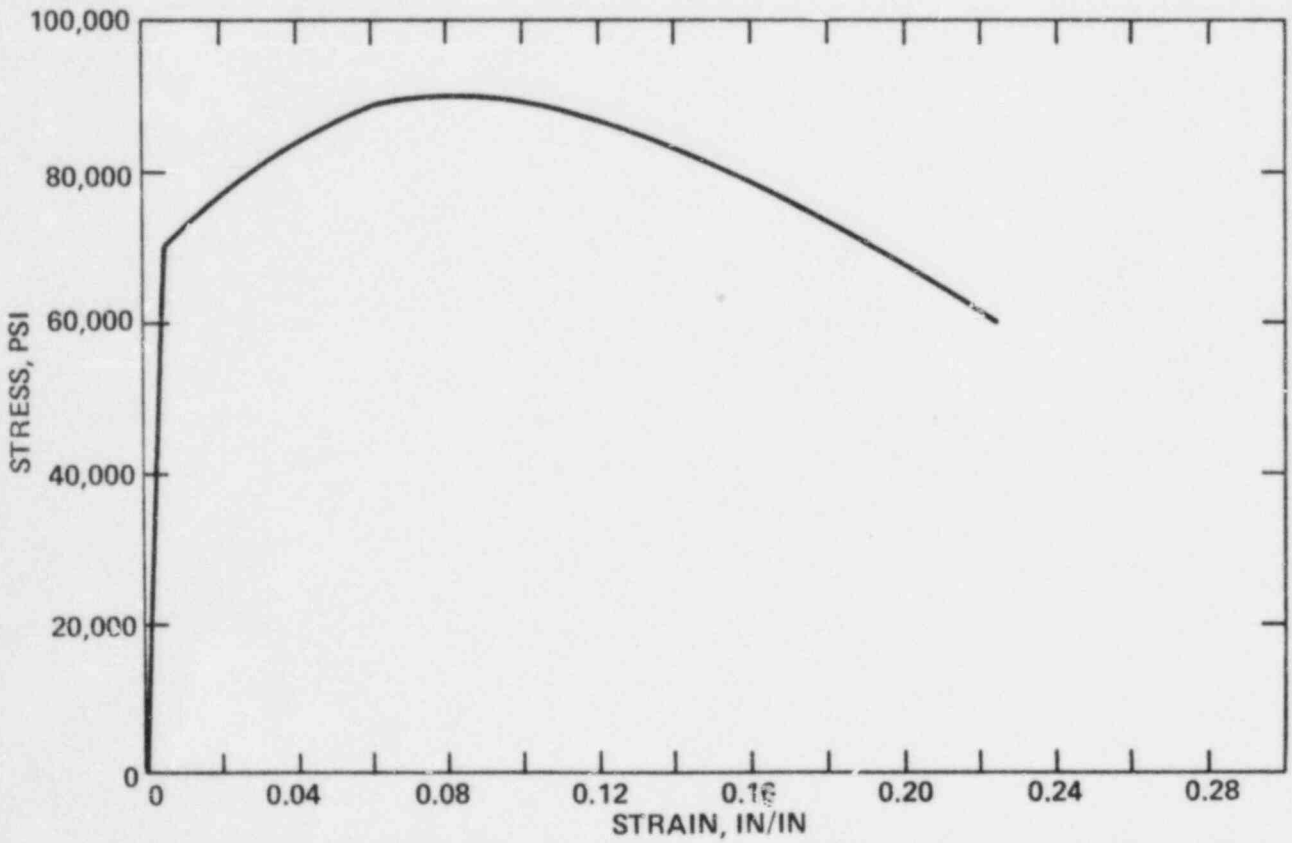

Figure V-15 STRESS STRAIN RECORD OF TENSION TEST, HAZ METAL PLATE C-506-1 SPECIMEN No. 4KA, TEST TEMPERATURE 250^{O}F

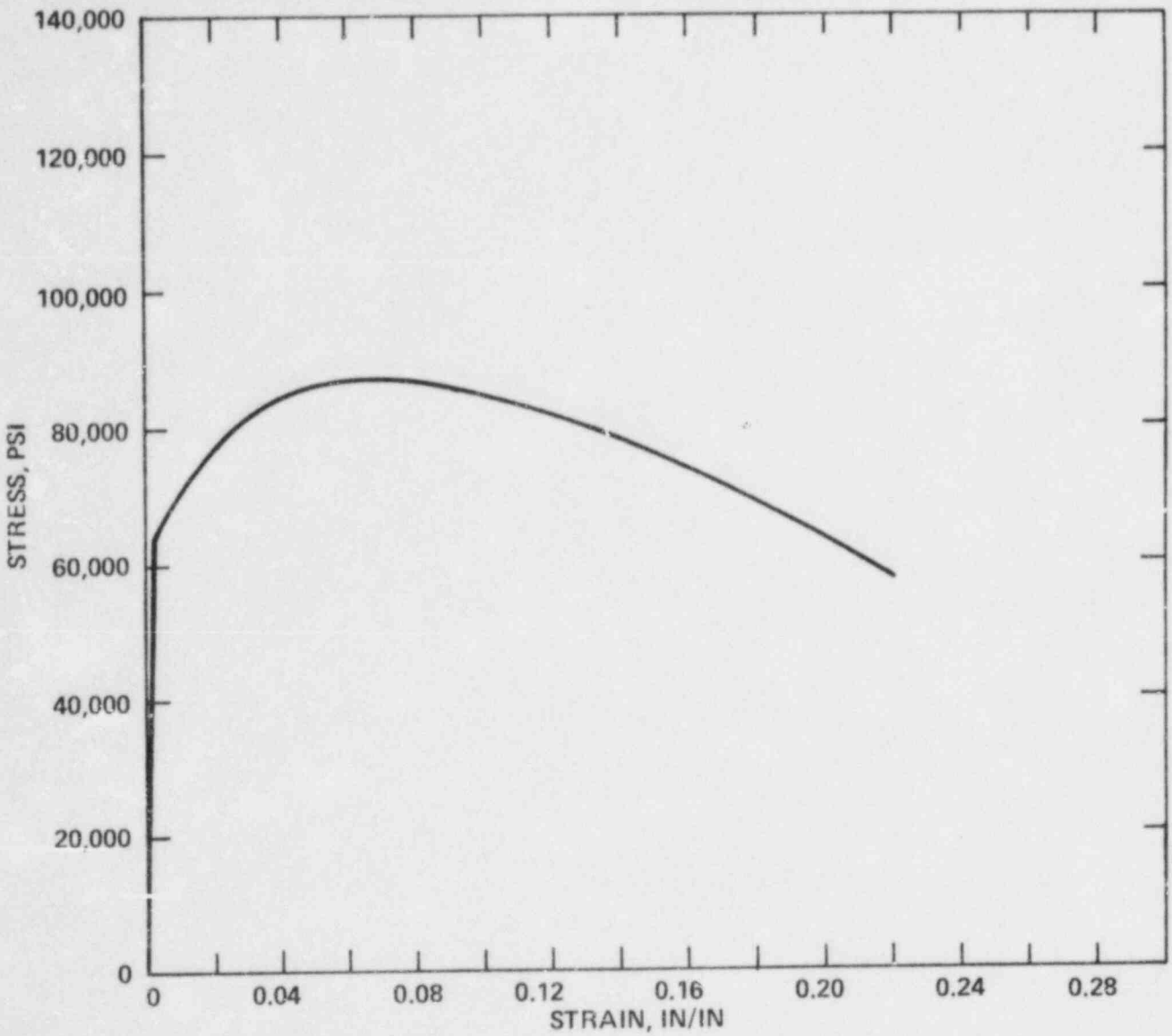

Figure V-16 STRESS STRAIN RECORD OF TENSION TEST, HAZ METAL PLATE C-506-1 SPECIMEN No. 4J2, TEST TEMPERATURE 550°F

FIGURE V-17
FRACTURE SURFACE OF IRRADIATED
TENSION SPECIMENS

Base Metal

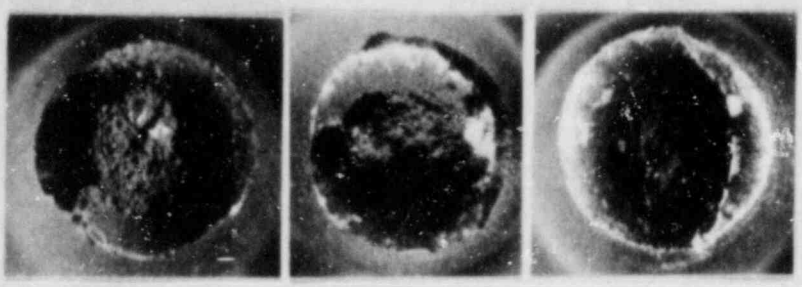

Specimen No:	1KC	1JA	1JU
Test Temp.:	72°F	250°F	550°F

Weld Metal

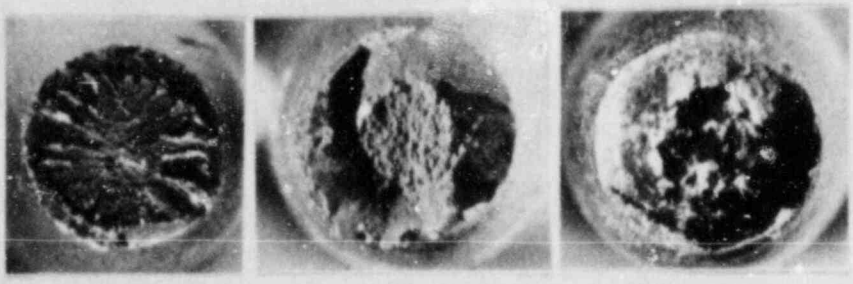

Specimen No:	3JY	3JJ	3J2
Test Temp.:	72°F	250°F	550°F

Heat-Affected Zone

Specimen No:	4K7	4KA	4J2
Test Temp.:	72°F	250°F	550°F

TABLE V-11

CHARPY V-NOTCH IMPACT RESULTS

IRRADIATED BASE METAL (TRANSVERSE)

(PLATE C-506-1)

Specimen Identification Number	Test Temperature (°F)	Impact Energy (Ft-lbs.)	Lateral Expansion (mils)	Fracture Appearance (% Shear)
25Z	0	10	9	0
21M	60	13	16	10
21E	100	26	26	20
23U	100	30	30	20
21K	160	44	44	40
23M	180	54	49	40
23T	200	64	62	70
25J	240	71	64	100
23A	240	83	74	100
25I	280	76	72	100
23K	280	80	72	100
25C	320	87	75	100

TABLE V-12

CHARPY V-NOTCH IMPACT RESULTS

IRRADIATED BASE METAL (LONGITUDINAL)

(PLATE C-506-1)

Specimen Identification Number	Test Temperature (°F)	Impact Energy (Ft-lbs.)	Lateral Expansion (mils)	Fracture Appearance (% Shear)
114	40	11	11	0
16B	80	29	28	20
11Y	120	33	36	20
14P	120	36	36	20
135	160	48	45	30
147	160	52	45	30
122	160	53	51	30
14M	200	72	66	70
137	240	98	83	100
11B	280	92	78	100
14U	280	97	79	100
14D	350	90	80	100

TABLE V-13

CHARPY V-NOTCH IMPACT RESULTS

IRRADIATED WELD METAL

Specimen Identification Number	Test Temperature (°F)	Impact Energy (Ft-lbs.)	Lateral Expansion (mils)	Fracture Appearance (% Shear)
33B	0	17	15	0
33J	40	23	24	20
31D*	40	47	41	30
33C	60	38	37	40
31L*	80	74	57	60
36M	80	80	66	70
352	120	71	59	80
317*	120	99	78	90
34A	160	95	78	100
31C*	160	105	83	100
34D	200	93	79	100
36U	240	106	85	100

* Specimens from outside diameter region of weldment; all other from inside diameter region.

TABLE V-14

CHARPY V-NOTCH IMPACT RESULTS

IRRADIATED HAZ METAL

(BASE METAL PLATE C-506-1)

Specimen Identification Number	Test Temperature (°F)	Impact Energy (Ft-lbs.)	Lateral Expansion (mils)	Fracture Appearance (% Shear)
455	0	14	14	10
45A	40	19	18	20
43U	40	20	19	10
45M	60	26	25	20
42D	80	47	43	50
44D	100	48	41	40
451	100	51	47	60
435	120	76	51	60
464	160	92	75	90
447	200	89	70	100
44M	200	92	73	100
432	240	92	72	100

Figure V-18 CHARPY IMPACT ENERGY, BASE METAL PLATE C-506-1 (TRANSVERSE)

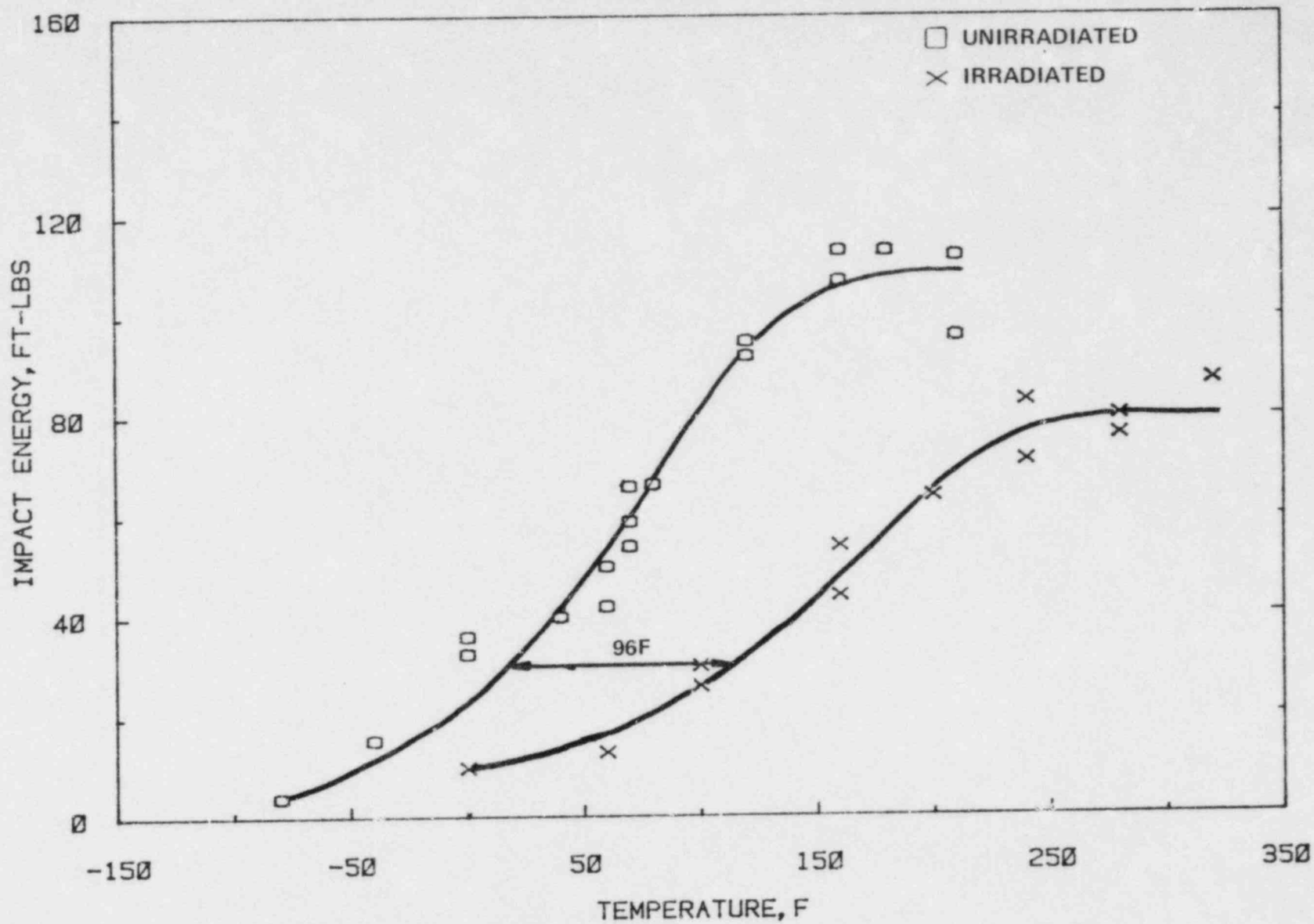

Figure V-19 CHARPY LATERAL EXPANSION, BASE METAL PLATE C-506-1 (TRANSVERSE)

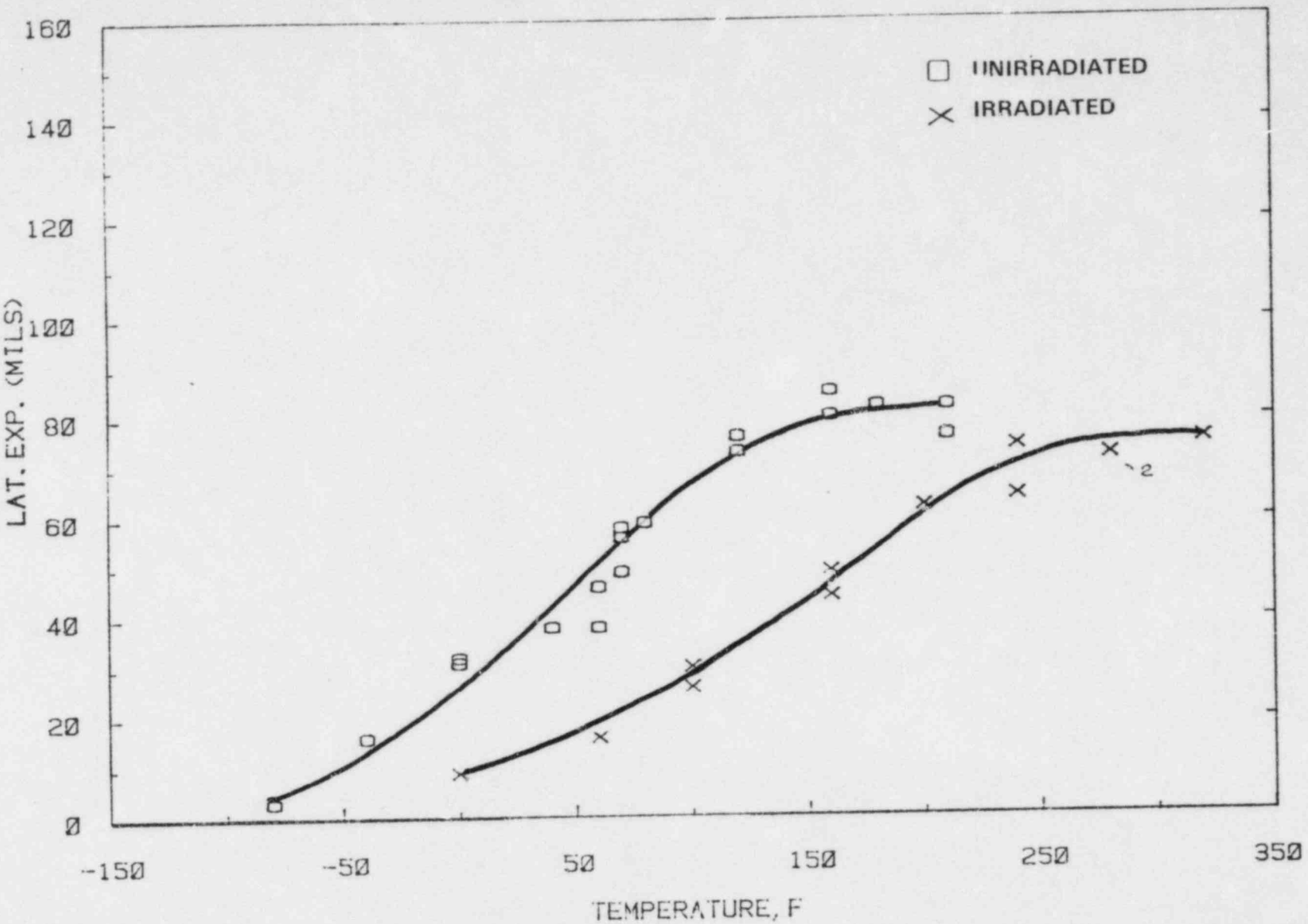

Figure V-20 CHARPY SHEAR FRACTURE, BASE METAL PLATE C-506-1 (TRANSVERSE)

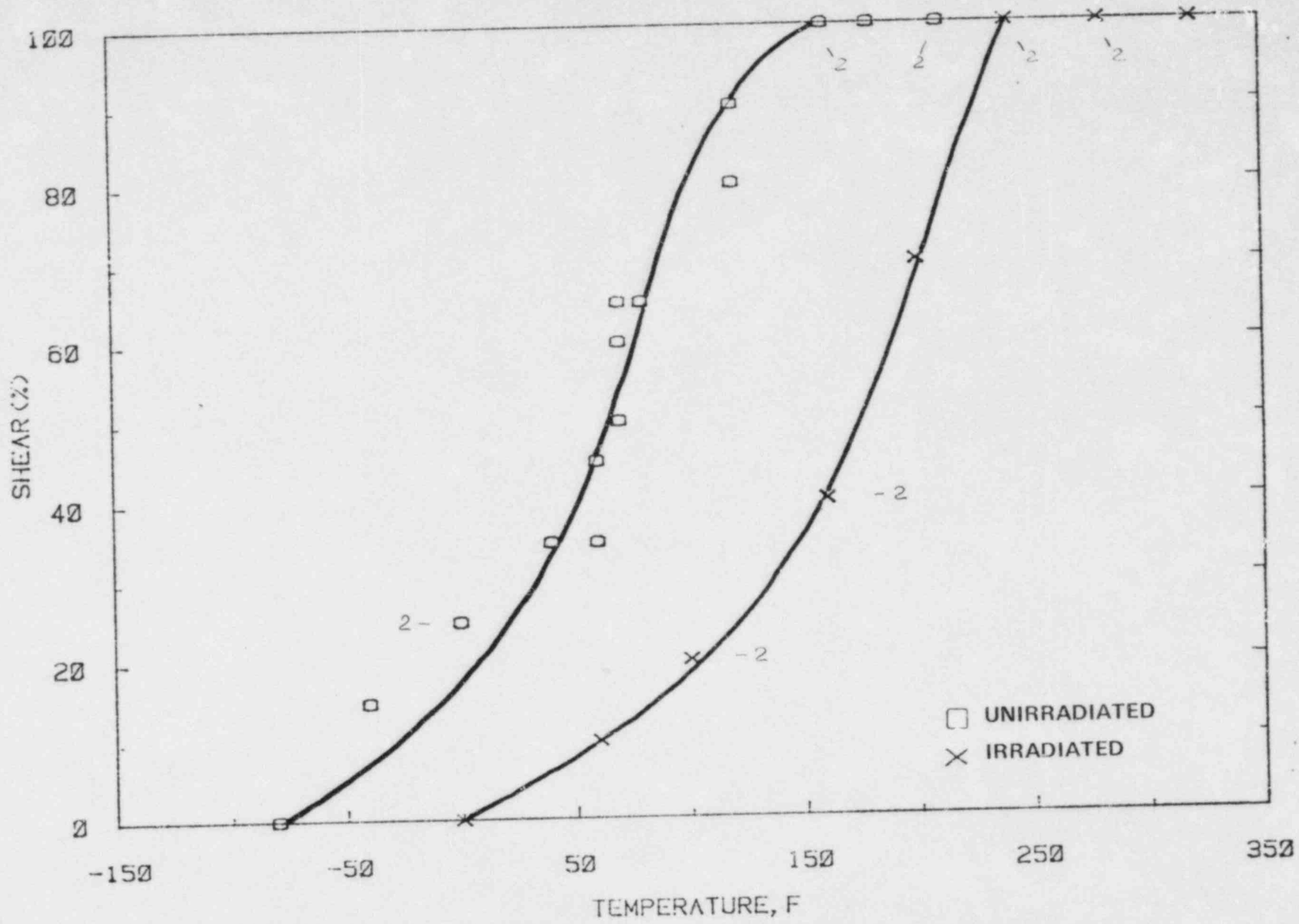

Figure V-21 CHARPY IMPACT ENERGY, BASE METAL PLATE C-506-1 (LONGITUDINAL)

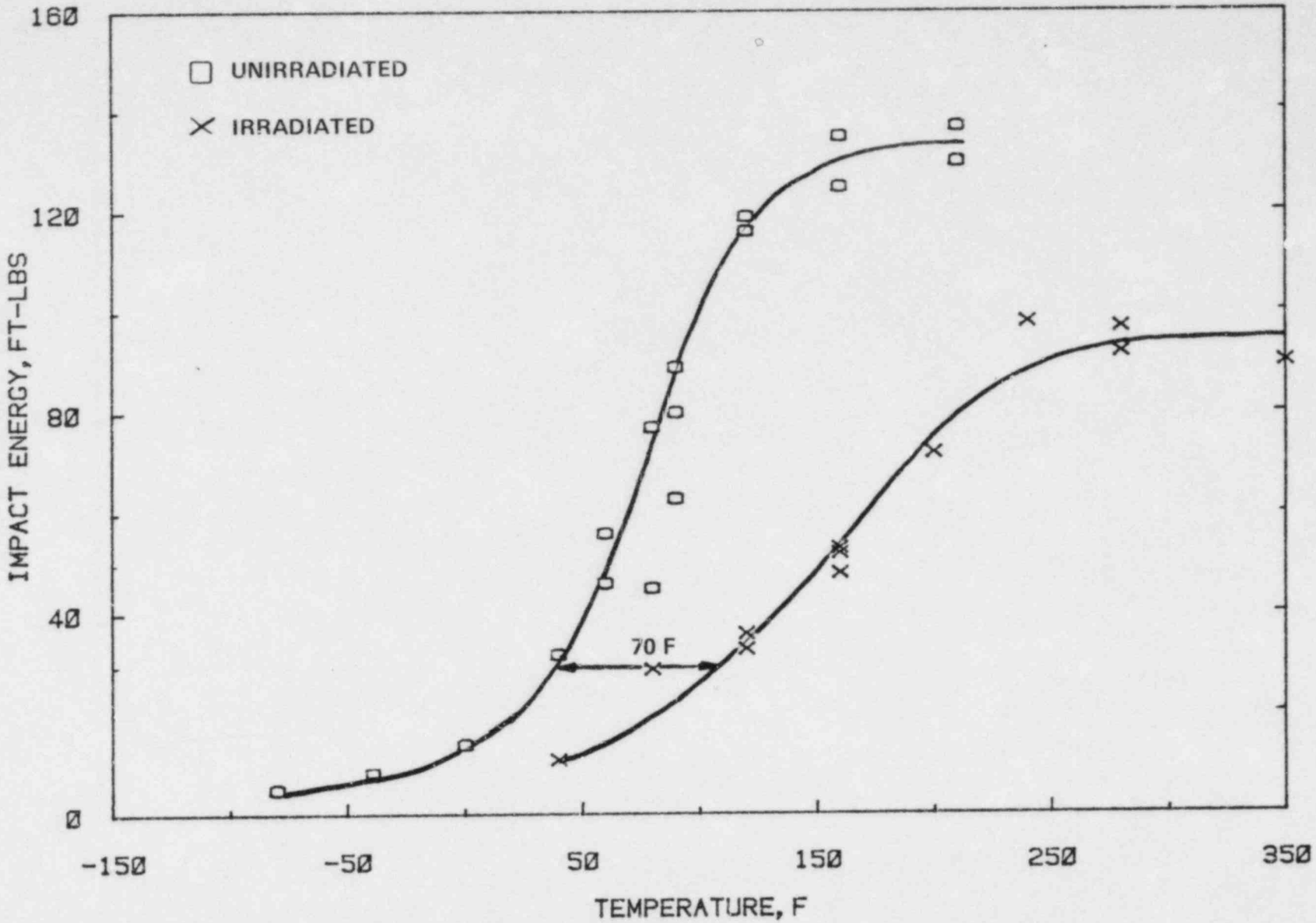

Figure V-22 CHARPY LATERAL EXPANSION, BASE METAL PLATE C-506-1 (LONGITUDINAL)

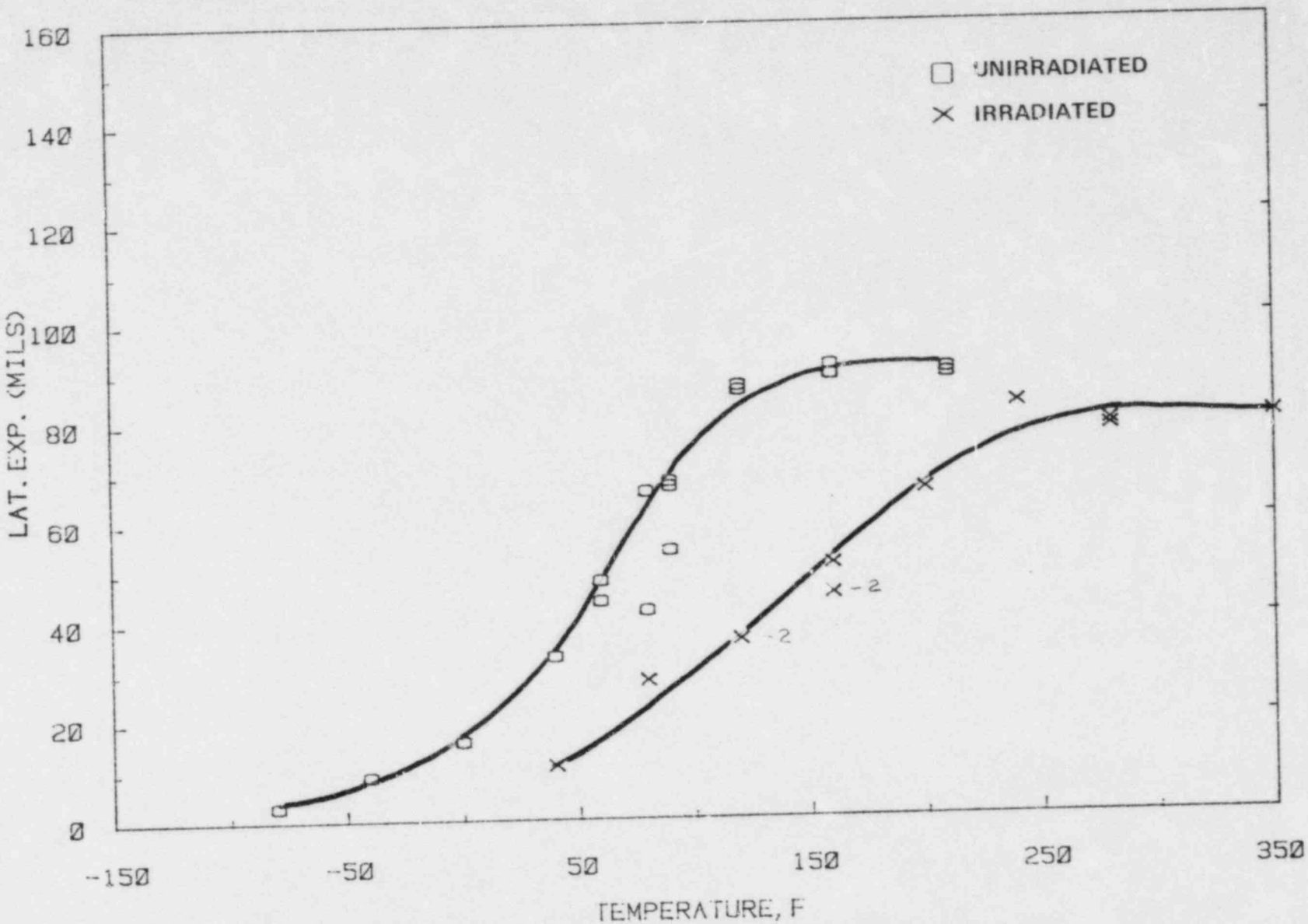

Figure V-23 CHARPY SHEAR FRACTURE, BASE METAL PLATE C-506-1 (LONGITUDINAL)

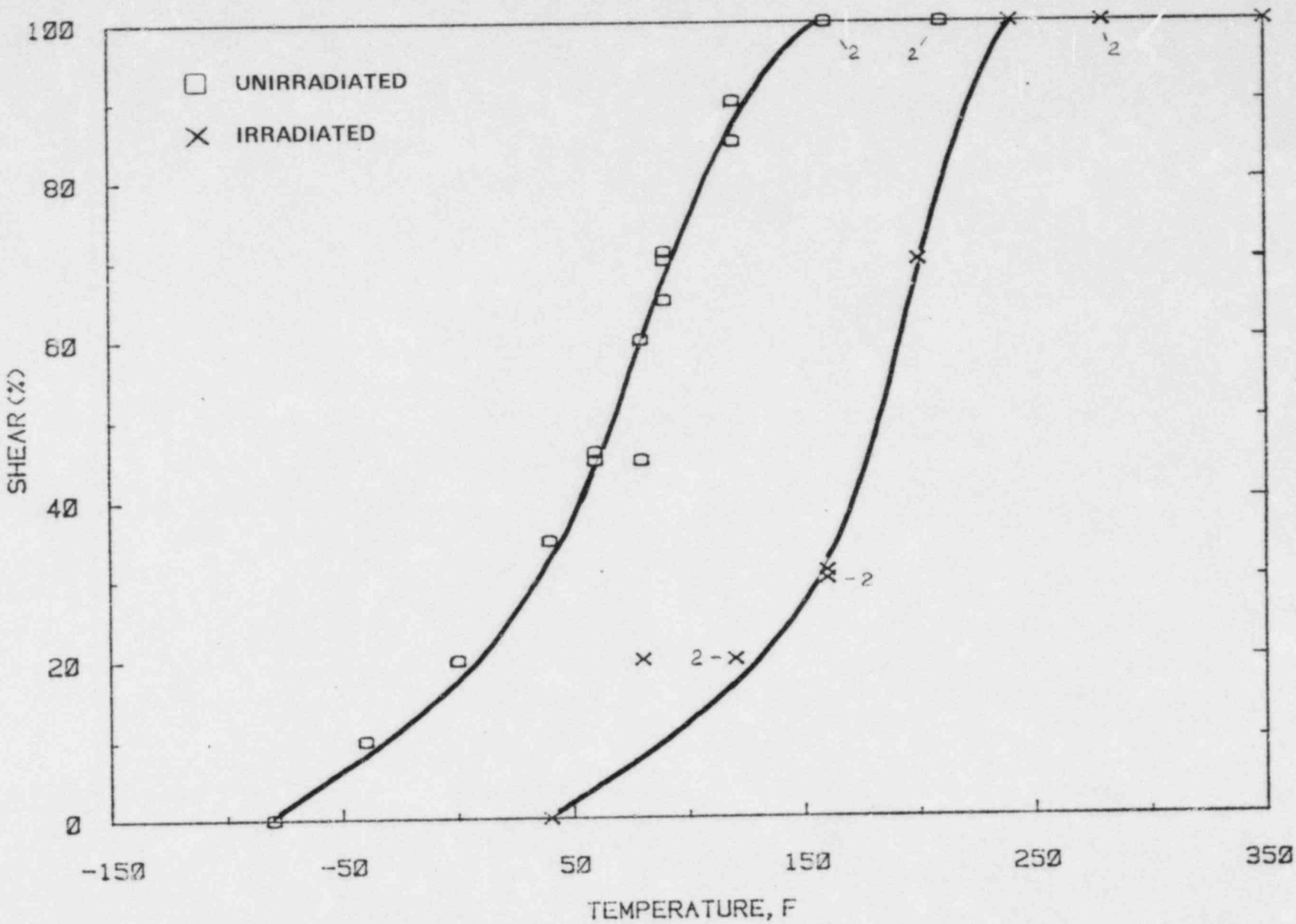

Figure V-24 CHARPY IMPACT ENERGY WELD METAL

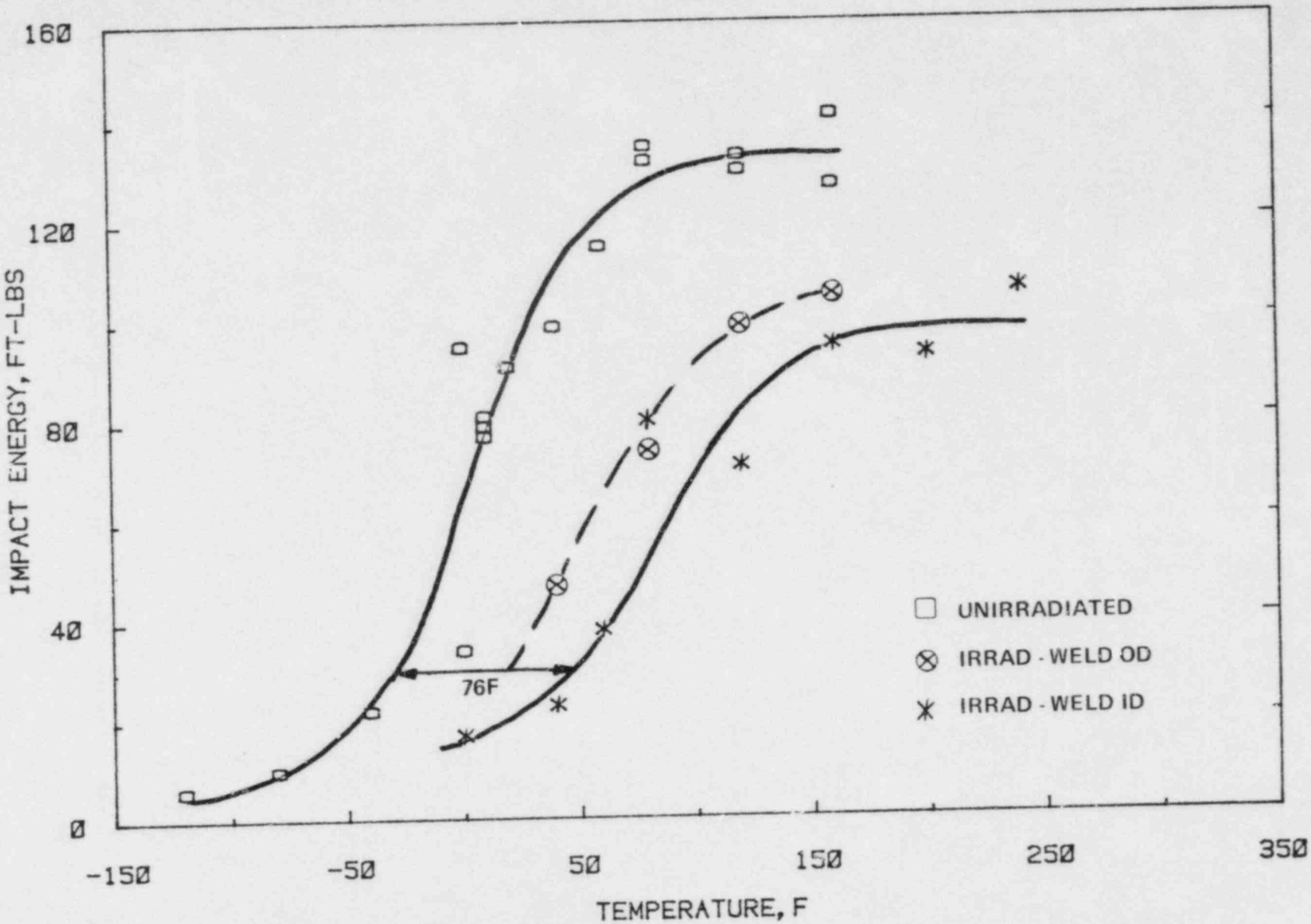

Figure V-25 CHARPY LATERAL EXPANSION WELD METAL

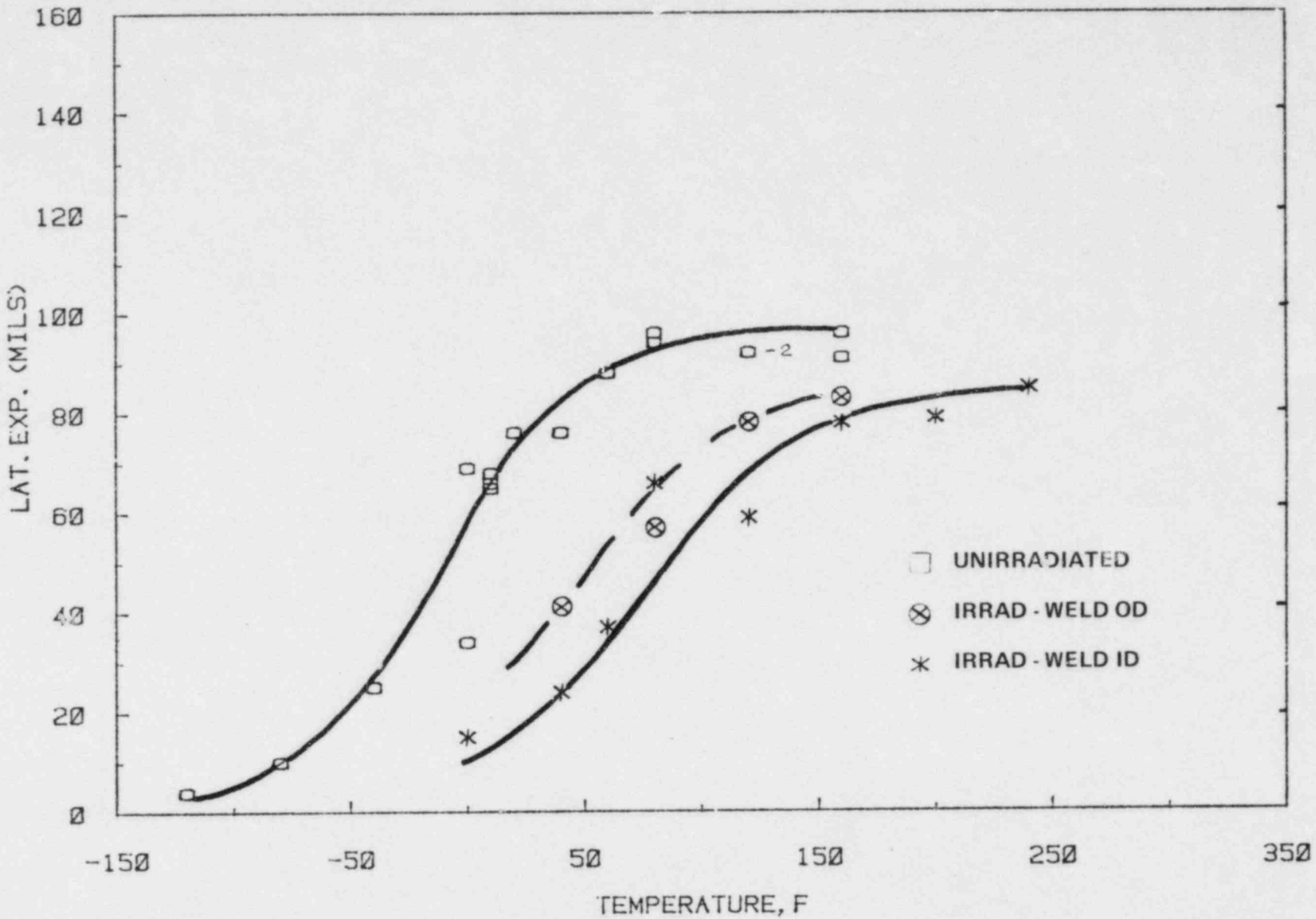

Figure V-26 CHARPY SHEAR FRACTURE WELD METAL

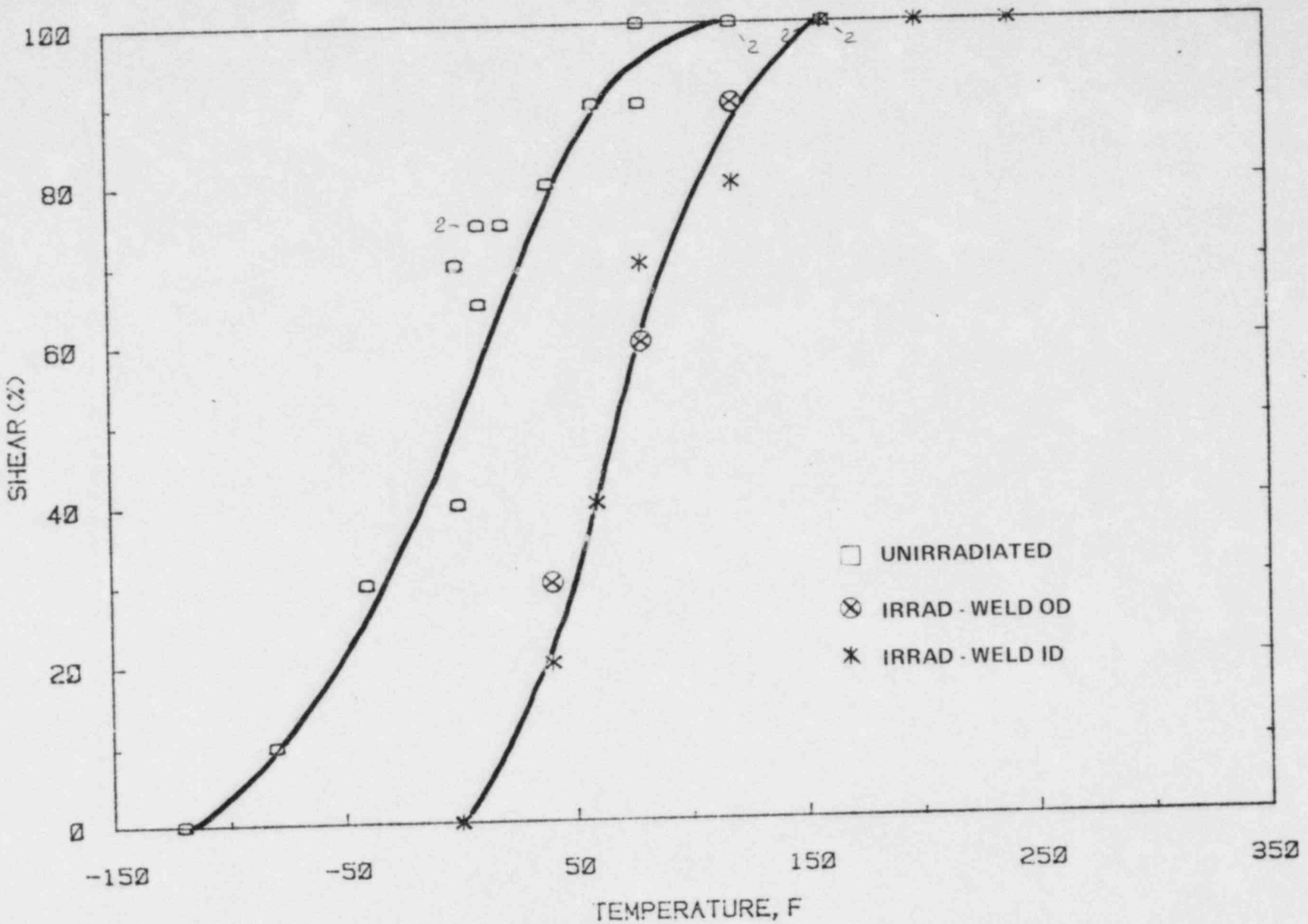

Figure V-27 CHARPY IMPACT ENERGY HEAT-AFFECTED ZONE

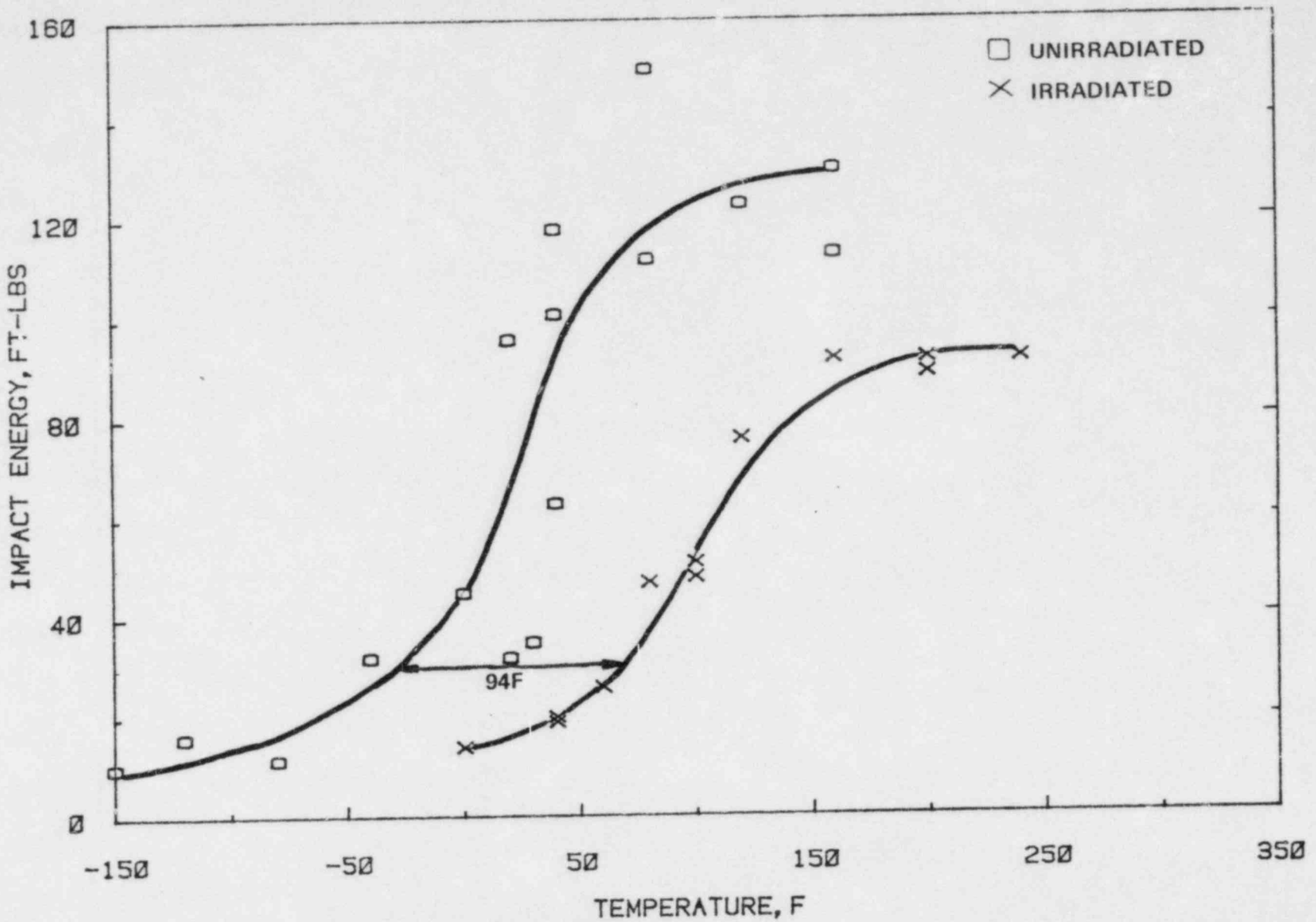

Figure V-28 CHARPY LATERAL EXPANSION HEAT-AFFECTED ZONE

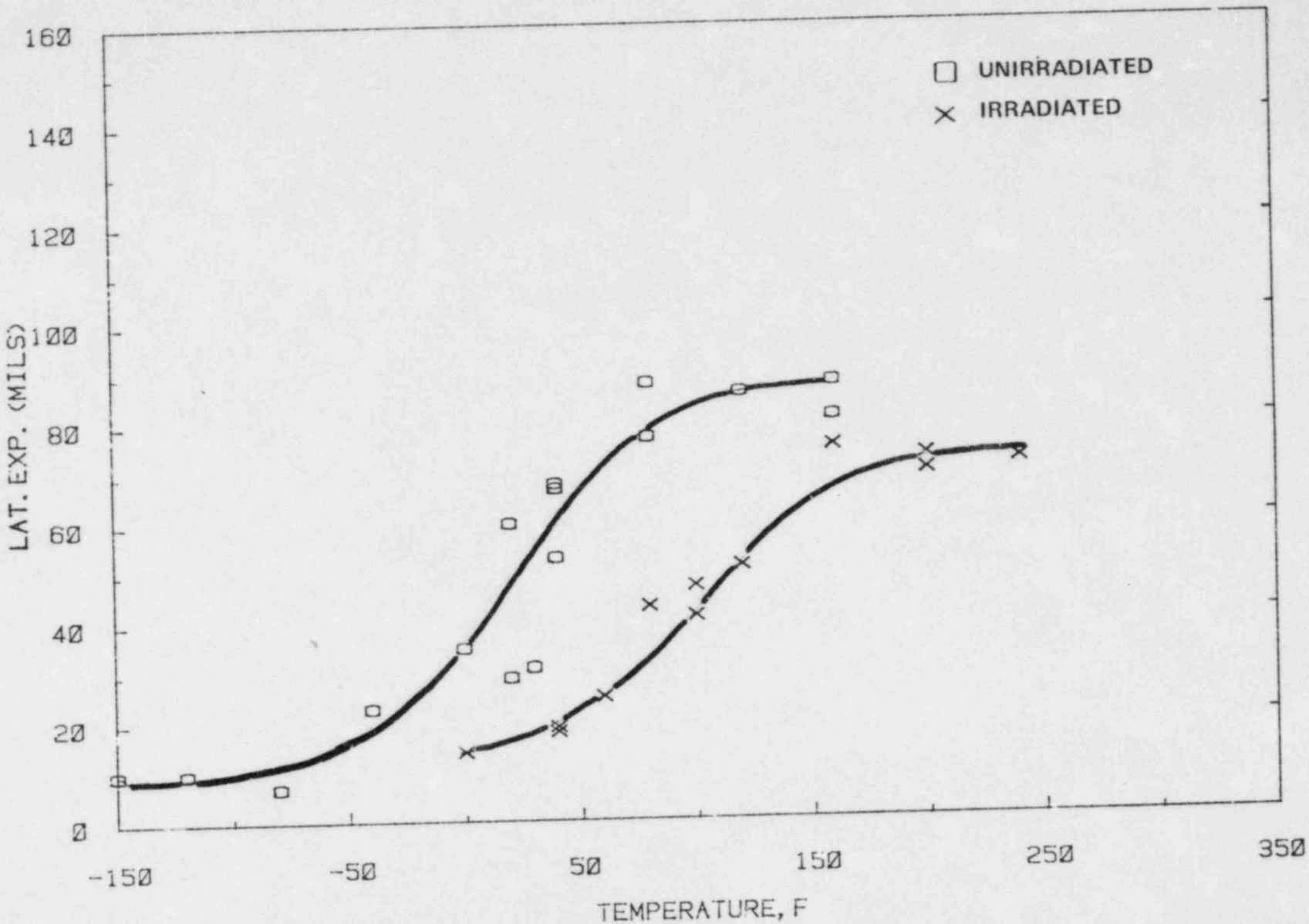

Figure V-29 CHARPY SHEAR FRACTURE HEAT-AFFECTED ZONE

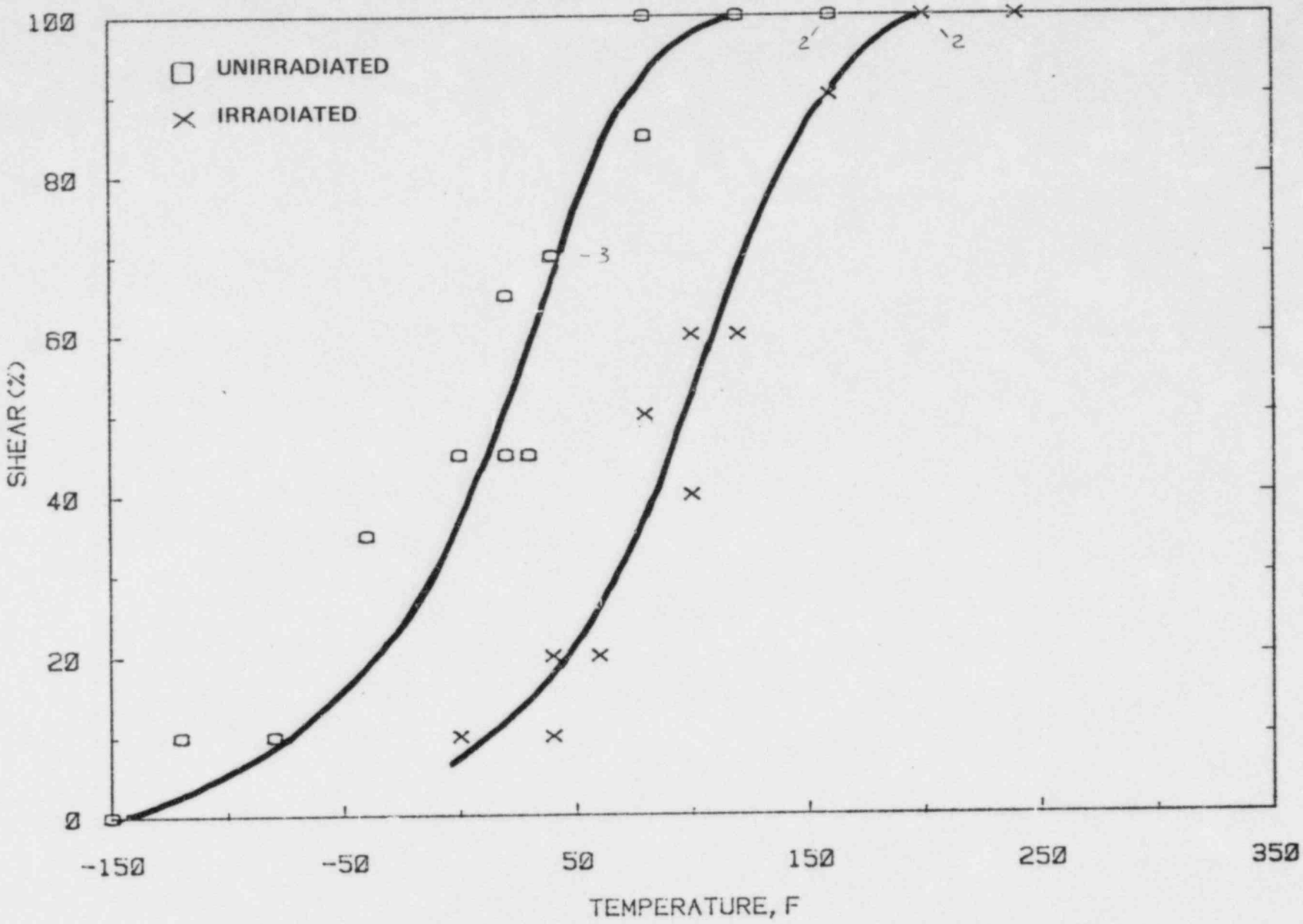

FIGURE V-30

FRACTURE SURFACES OF
CHARPY V-NOTCH IMPACT TEST SPECIMENS
BASE METAL (TRANSVERSE)

Specimen No.: 252
Test Temperature: 0°F

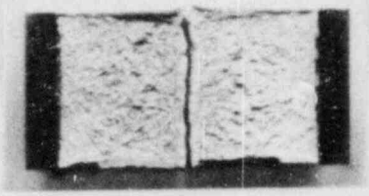

21M
60°F

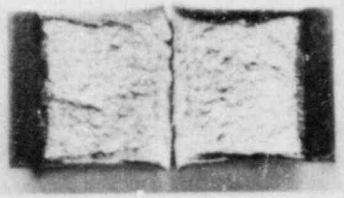

21E
100°F

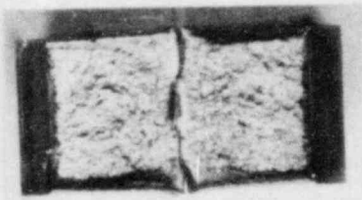

Specimen No.: 23U
Test Temperature: 100°F

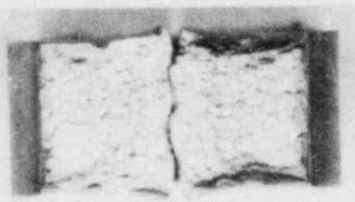

21K
160°F

23M
160°F

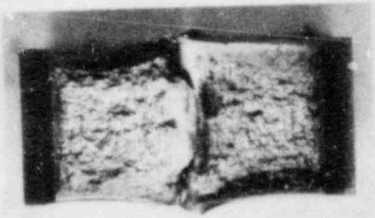

Specimen No.: 23T
Test Temperature: 200°F

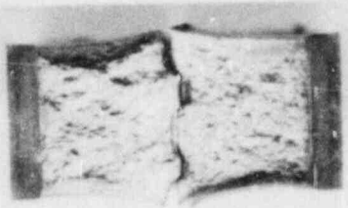

25J
240°F

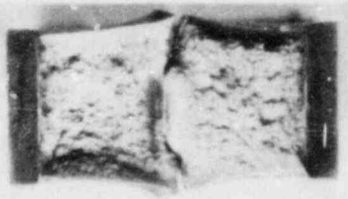

23A
240°F

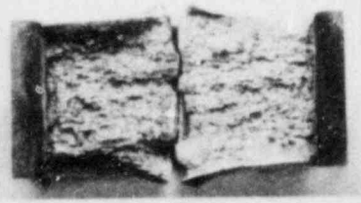

Specimen No.: 25I
Test Temperature: 280°F

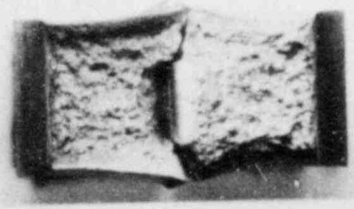

23K
280°F

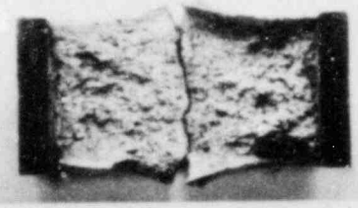

25C
320°F

FIGURE V-31

FRACTURE SURFACES OF
CHARPY V-NOTCH IMPACT TEST SPECIMENS
BASE METAL (LONGITUDINAL)

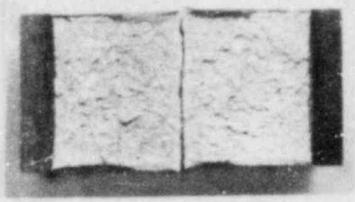

Specimen No.: 114
Test Temperature: 40°F

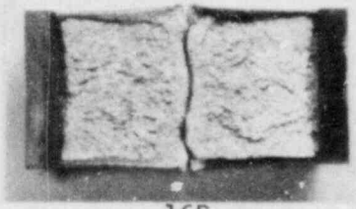

16B
80°F

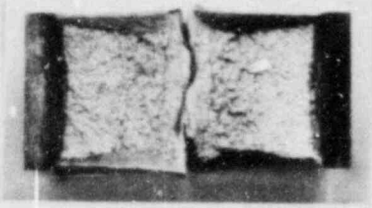

11Y
120°F

Specimen No.: 14P
Test Temperature: 120°F

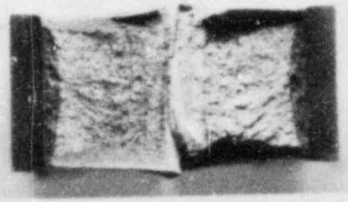

135
160°F

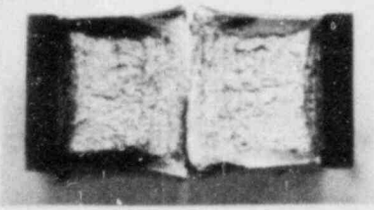

147
160°F

Specimen No.: 122
Test Temperature: 160°F

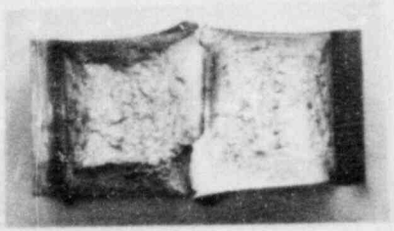

14M
200°F

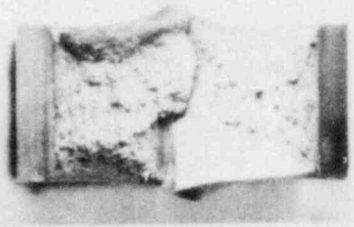

137
240°F

Specimen No.: 11B
Test Temperature: 280°F

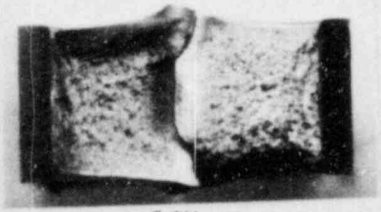

14U
280°F

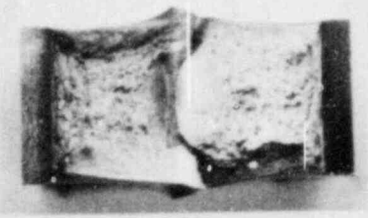

14D
350°F

FIGURE V-32

FRACTURE SURFACES OF
CHARPY V-NOTCH IMPACT TEST SPECIMENS
WELD METAL

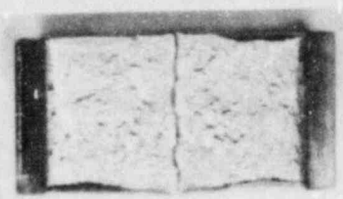

Specimen No.: 33B
Test Temperature: 0°F

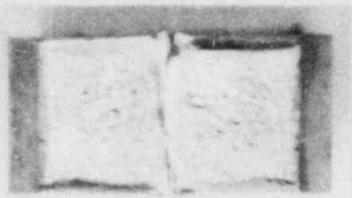

33J
40°F

31D
40°F

Specimen No.: 33C
Test Temperature: 60°F

31L
80°F

36M
80°F

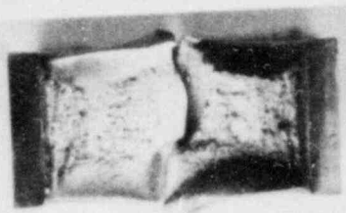

Specimen No.: 352
Test Temperature: 120°F

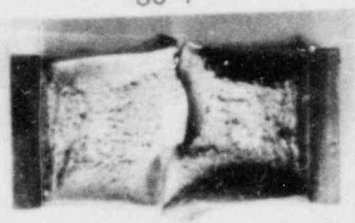

317
120°F

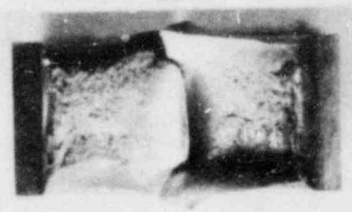

34A
160°F

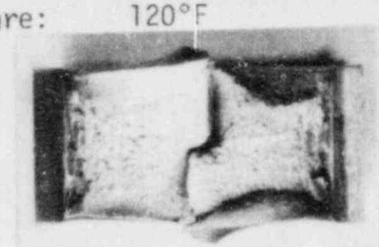

Specimen No.: 31C
Test Temperature: 160°F

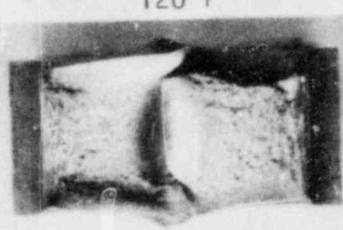

34D
200°F

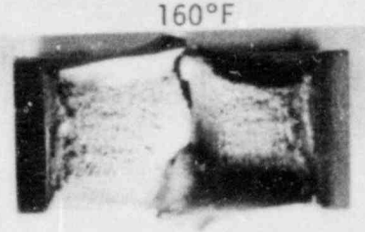

36U
240°F

FIGURE V-33

FRACTURE SURFACES OF
CHARPY V-NOTCH IMPACT TEST SPECIMENS
HEAT-AFFECTED-ZONE

Specimen No.: 455
Test Temperature: 0°F

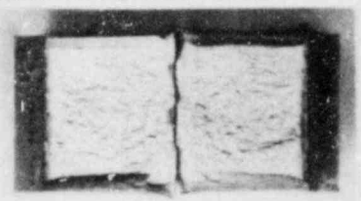

Specimen No.: 45A
Test Temperature: 40°F

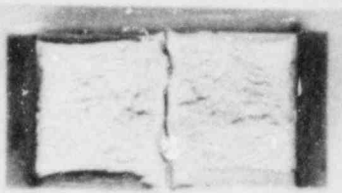

Specimen No.: 43U
Test Temperature: 40F

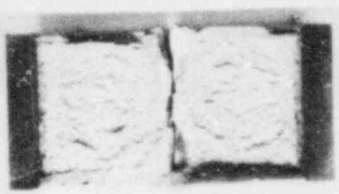

Specimen No.: 45M
Test Temperature: 60°F

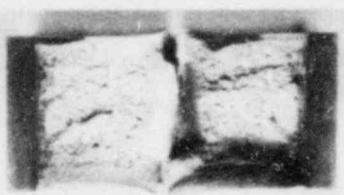

Specimen No.: 42D
Test Temperature: 80°F

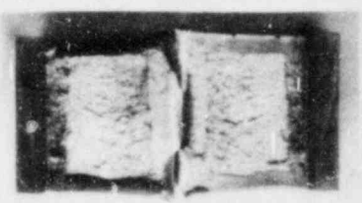

Specimen No.: 44D
Test Temperature: 100°F

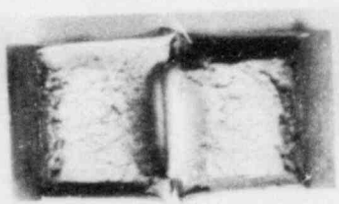

Specimen No.: 451
Test Temperature: 100°F

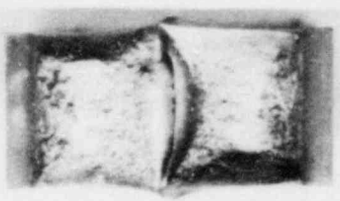

Specimen No.: 435
Test Temperature: 120°F

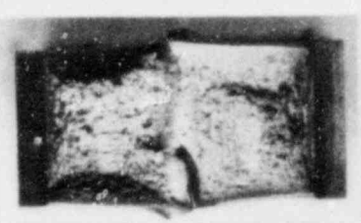

Specimen No.: 464
Test Temperature: 160°F

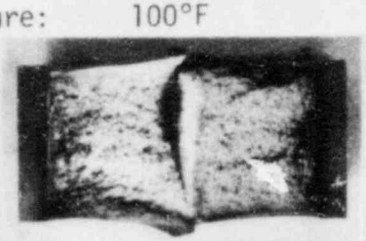

Specimen No.: 447
Test Temperature: 200°F

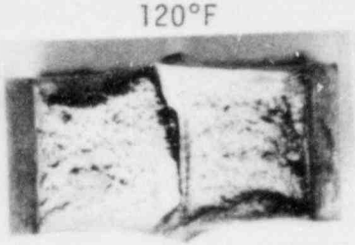

Specimen No.: 44M
Test Temperature: 200°F

Specimen No.: 432
Test Temperature: 240°F

VI. DATA ANALYSIS

A. Irradiation Exposure

The W-97 surveillance capsule was removed from the Millstone Unit 2 reactor vessel following plant shutdown on August 17, 1980, 0800 hours. The surveillance specimens were irradiated at approximately 550°F; the temperature variation along the length of the capsule was negligible based on the similarity in appearance of the three 558°F monitors.

The surveillance capsule was exposed to a maximum neutron flux of 4.0×10^{10} n/cm^2-s (E>1.0 MeV). The highest flux was measured in the bottom compartment (6273). The neutron flux in the top compartment (6214) and middle compartment (6241) was approximately 3.76×10^{10} n/cm^2-s and 3.94×10^{10} n/cm^2-s, respectively, indicating a total axial variation of 6%. The maximum surveillance capsule fluence after 3.0 effective full power years (EFPY) operation at 2700 MWT was, therefore, 3.78×10^{18} n/cm^2(E>1.0 MeV).

Lead factors between the surveillance capsule and the maximum azimuthal position on the reactor vessel were calculated to be 1.36 at the vessel-clad interface, 2.62 at the quarter thickness location in the vessel, and 13.9 at the three-quarter thickness location. The maximum neutron flux at the vessel-clad interface was, therefore, 2.94×10^{10} n/cm^2-s. The predicted end-of-life fluence at the vessel-clad interface is 2.96×10^{19} n/cm^2 ($\pm$30%), using the same power level (2700 Mwt), coolant inlet temperature*, and fuel management strategy as for the first 3.0 EFPY of operation. This projected estimate is only 55% higher than the FSAR estimate of 1.91×10^{19} n/cm^2 which was based on 2560 Mwt power level and assumed

* Coolant inlet temperature increased from 542F in Cycle 2 to 549F in Cycle 3. Although the projected fluence is based on the lower temperature, the higher inlet temperature will not cause a significant increase in vessel wall fluence.

design parameters. As noted previously, when the DOT-III computer code and the DLC-23 CASK cross section library were used in a predictive mode (ie, without using the surveillance dosimeter measurements for normalization) and actual operating parameters were factored in, the end-of-life fluence was conservatively predicted to be 4.0×10^{19} n/cm^2.

B. Chemical Analysis

Chemical analysis of the irradiated base metal and weld metal Charpy specimens demonstrated that the encapsulated surveillance specimens had the same chemical composition as that originally reported in the baseline evaluation. (2) Furthermore, analysis of the weld specimens enabled delineation between the high copper (inner) and low copper (outer) sections of the surveillance weldment. As can be noted in Table V-8, the copper content of the first two specimens (31I and 31L) is significantly lower than for the remaining four. The weld metal specimen layout drawing (6) was then used to identify which of the six remaining irradiated Charpy specimens were from the lower copper portion of the weldment - specimen number 31I, 31C, 31D and 31L were all from the first two layers on the outside of the weld.

C. Uniaxial Tension Properties

Radiation induced changes in uniaxial tension properties of the Millstone Unit 2 surveillance materials were determined from a comparison of Tables V-9 and V-10. The yield strength and ultimate strength increased approximately 11% following irradiation to 3.78×10^{18} n/cm^2. Uniform elongation decreased approximately 11% following irradiation, while reduction in area and total elongation decreased only 3 to 5%. Fracture stress (fracture load divided by final cross

sectional area) was not changed significantly by irradiation. In general, property changes were similar for each of the materials despite the large difference in copper content between base metal and weld metal.

Post-irradiation room temperature yield strength values ranged from 73,300 psi for the base metal to 86,800 psi for the weld metal. Total elongation of the irradiated materials ranged from 22% to 27.5%.

D. Charpy Impact Toughness Properties

The radiation induced changes in toughness of the Millstone Unit 2 surveillance materials are summarized in Table VI-1. Index temperature shifts were measured using the average curves at the 30 ft-lb level (Cv30), 50 ft-lb level (Cv50), and 35 mils lateral expansion level (Cv35). Upper shelf energy changes were based on the average impact energy for each set of test specimens exhibiting 100% shear fracture measured before and after irradiation. The unirradiated Charpy impact data were obtained from the baseline evaluation report. [2]

The base metal (transverse orientation) exhibited the greatest shift in the 30 ft-lb index temperature (96°F). The shift for the heat-affected-zone material was similar (94°F), whereas the weld metal shift was only 76°F at the 30 ft-lb level. The decrease in upper shelf energy was similar for each of the irradiated materials, ranging from 26 to 29%.

The Millstone Unit 2 design curve for prediction of transition temperature shift as a function of neutron fluence is given in Figure B3/4.4-1 of the Technical Specifications. [7] The design curve prediction for the surveillance capsule exposure of 3.78×10^{18} n/cm^2 is 120°F, or 25% higher than the base

metal shift and 58% higher than the weld metal shift. In contrast, shifts predicted using NRC Regulatory Guide 1.99[8] based on measured copper and phosphorus content are 61°F for the base metal (35% less than measured) and 181°F for the weld metal (140% more than measured).

In order to provide an improved means of predicting transition temperature shift of the controlling beltline material for Millstone Unit 2, Figure VI-1 was developed. This figure should be used to adjust the reactor coolant system pressure-temperature operating limit curves in place of the current Figure B3/4.4-1 of the Millstone Unit 2 Technical Specifications. Figure VI-1 was developed based on the methodology of Regulatory Guide 1.99[8] using the measured value of shift at the 30 ft-lb level for the base metal (96°F) at 3.78×10^{18} n/cm^2. The shift versus neutron fluence relationship is as follows:

$$\Delta NDTT = 156 \left(\frac{\phi}{10^{19}} \right)^{0.5}$$

where ϕ = neutron fluence, E > 1.0 MeV, and
$\Delta NDTT$ = transition temperature shift.

This relationship should be evaluated again once results are available from surveillance materials irradiated to a higher fluence.

The measured shift for the weld material was 20% lower than that for the base metal material even though the copper content of the weld was significantly higher (0.30% Cu for the weld versus 0.14% Cu for the plate). The greater irradiation resistance of the weld is a result of the low nickel content (0.06%). Based on on empirical evaluation of weld metal irradiation sensitivity [9], low nickel weldments (eg, less than 0.2% Ni) exhibited significantly smaller NDTT shifts

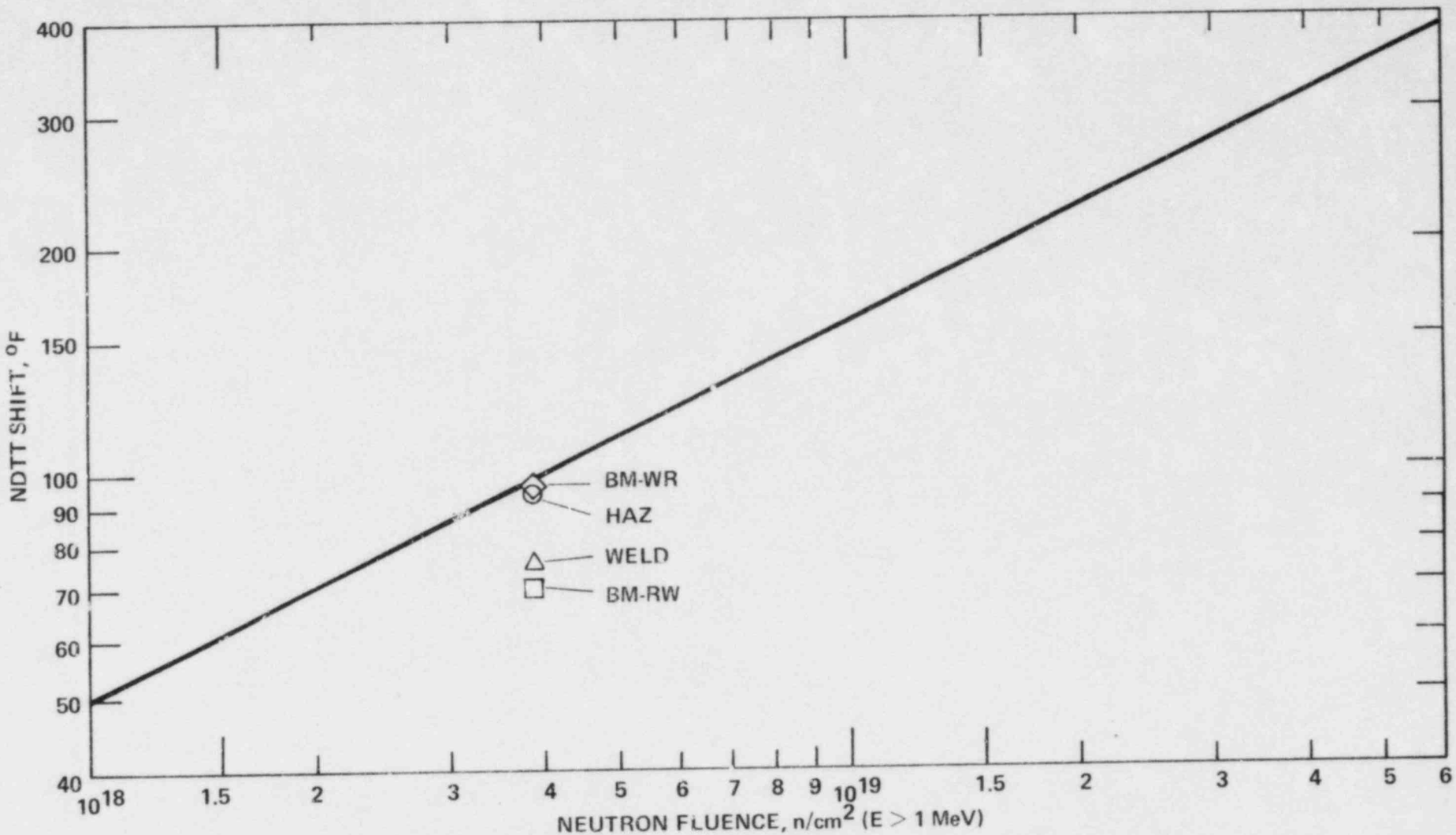

Figure VI-1 PREDICTED NDTT SHIFT FOR THE MILLSTONE UNIT 2 REACTOR VESSEL BELTLINE

than high nickel weldments. For the higher copper (inner) section of the Millstone Unit 2 surveillance weld, the predicted shift based on the empirical weld model is 74°F versus the 76°F measured shift. Similarily, for the lower copper (outer) section of the weld, the predicted shift is 48°F versus the 37°F measured shift. (Note that the measured shift for the outer section is based on only four Charpy test specimens.) Therefore, the low weld metal shift determined from the W-97 surveillance capsule evaluation is consistent with experimental results. Furthermore, it is reasonable to expect that the base metal, rather than the weld metal, will continue to be the most limiting (highest shift) material in the reactor vessel beltline.

The current pressure/temperature operating limits (Amendment 24, June 24, 1977) given in Figure 3.4-2b of the Technical Specifications [7] are based on an initial RT_{NDT} of 5°F and a shift of 135°F after 10 EFPY (equivalent to the original design fluence of 5.3×10^{18} n/cm^2). Given the revised shift prediction method and vessel fluence projection, the estimated base metal shift after 10EFPY is 150°F based on surface fluence (9.27×10^{18} n/cm^2) and 108°F based on the one-quarter thickness (1/4 t) fluence (4.83×10^{18} n/cm^2). Conversely, the design base 135°F shift is predicted to occur at a fluence of 7.5×10^{18} n/cm^2, which corresponds to 8.1 EFPY at the vessel inside surface and 15.6 EFPY at the vessel 1/4 t.

Projected values of NDTT shift and adjusted RT_{NDT} are given in Table VI-2. Based on the revised shift prediction method and vessel fluence, the predicted shift (vessel inside surface) after 32 EFPY is 268°F versus the original estimate [7] of 225°F. Similarily, the 1/4 t shift is projected to be 194°F.

The predicted decrease in upper shelf energy at end-of-life based on the method given in Regulatory Guide 1.99[8] is 38% at the one-quarter thickness location in the vessel. Using this conservative prediction, the upper shelf energy of the plates will remain above 65 ft-lb during the design life of the vessel. The upper shelf energy of the weld will remain above 80 ft-lb throughout vessel life. These projected values of upper shelf energy are well in excess of the 50 ft-lb value currently considered to provide a reasonable margin for continued safe operation.

Recommended changes to the surveillance capsule removal schedule are contained in Table VI-3. The schedule is designed based on 10CFR50, Appendix H and a lead factor (capsule to vessel ID) of 36%. (For example, the fourth capsule's exposure after 18 EFPY will be equivalent to that at the vessel inside surface after 24 EFPY). Data from the second capsule will be available in time for updating the pressure/temperature operating limits. The 104° and 284° capsules are designated for standby purposes.

TABLE VI-1

SUMMARY OF TOUGHNESS PROPERTY CHANGES FOR MILLSTONE UNIT 2
SURVEILLANCE MATERIALS (550F IRRADIATION, 3.78×10^{18} n/cm^2)

Material	Index Temperatures (°F)						Upper Shelf Energy	
	Cv 30[a]	ΔCv 30	Cv 50[b]	ΔCv 50	Cv 35[c]	Δ Cv 35	Energy (ft-lb)	Change (%)
Base Metal (WR)	17[d]		55[d]		25[d]		108[d]	
	113	96	168	113	123	98	79	27
Base Metal (RW)	38[d]		59[d]		40[d]		131[d]	
	108	70	102	93	116	76	94	28
Weld Metal	-30[d]		-10[d]		-28[d]		132[d]	
	46	76	78	88	62	90	98	26
Heat-Affected Zone	-30[d]		5[d]		0[d]		129[d]	
	64	94	96	91	85	85	91	29

a - 30 ft-lb Index Temperature

b - 50 ft-lb Index Temperature

c - 35 mils lateral expansion Index Temperature

d - Unirradiated values

TABLE VI-2

PROJECTED NDTT SHIFT AND ADJUSTED

RTNDT FOR CONTROLLING MATERIAL

Vessel Location	10 EFPY			32 EFPY		
	Fluence[a]	NDTT Shift	Adj. RTNDT[b]	Fluence[a]	NDTT Shift	Adj. RTNDT[b]
Inside Surface	$9.27 \times 10^{18} n/cm^2$	150°F	155°F	$2.96 \times 10^{19} n/cm^2$	268°F	273°F
1/4 t	$4.83 \times 10^{18} n/cm^2$	108°F	113°F	$1.54 \times 10^{19} n/cm^2$	194°F	199°F
3/4 t	$9.08 \times 10^{17} n/cm^2$	47°F	52°F	$2.90 \times 10^{18} n/cm^2$	84°F	89°F

a - Projected fluence assuming same power level, coolant inlet temperature and fuel management strategy as for first 3 EFPY of plant operation.

b - Adjusted RT_{NDT} = Initial RT_{NDT} (5°F) plus NDTT shift.

TABLE VI-3

PROPOSED NEW CAPSULE REMOVAL SCHEDULE
FOR MILLSTONE UNIT 2

Removal Sequence	Azimuthal Location	Approximate Removal Time*
1	97°	3 EFPY
2	83° or 263°	7-8 EFPY
3	263° or 83°	12-14 EFPY
4	277°	17-20 EFPY
5	104°	Standby
6	284°	Standby

* Time in effective full power years (EFPY) at 2700 MWt.

VII. REFERENCES

1. "Program for Irradiation Surveillance of Millstone Point Unit 2 Reactor Vessel Materials," Combustion Engineering, Inc., N-NLM-011, October 15, 1970.

2. "Northeast Utilities Service Company, Millstone Nuclear Unit No. 2, Evaluation of Baseline Specimens, Reactor Vessel Materials Irradiation Surveillance Program," 18767-TR-MCD-009, October 1976.

3. SAND Users Manual, AFWL-TR67-41, September 1967.

4. DOT-III Users Manual, ORNL-TM-4280, September 1973.

5. C-E Drawing J-18767-164-001, "Millstone Reactor Assembly," January 3, 1973.

6. C-E Drawing E-18767-165-111-02, "Weld Metal Test Specimens," June 20, 1972.

7. Northeast Nuclear Energy Company, Millstone Nuclear Power Station, Unit No. 2, Waterford, Conn., Safety Technical Specifications, Docket 50-336.

8. Regulatory Guide 1.99, Revision 1, "Effects of Residual Elements on Predicted Radiation Damage to Reactor Vessel Materials," April 1977.

9. J. D. Varsik and S. T. Byrne, "An Empirical Evaluation of the Irradiation Sensitivity of Reactor Pressure Vessel Materials," Effects of Radiation on Structural Materials, ASTM STP 683, 1979.

APPENDIX A

TENSION TESTS - DESCRIPTION AND EQUIPMENT

The tension tests were performed using a Riehle universal screw testing machine with a maximum capacity of 30,000 lb and separate scale ranges between 50 lb and 30,000 lb. The machine, shown in Figure A-1, is capable of constant cross head rate or constant strain rate operation. The tension testing was covered by the certificate of calibration which is included at the end of the Appendix A.

Elevated temperature tests were performed in a 2-1/2" ID x 18" long high temperature tension testing furnace with a temperature limit of 1800F. A Riehle high temperature, dual range extensometer was used for monitoring specimen elongation.

The tension specimen is depicted in Figure A-2. Figures A-3 through A-5 are isometric drawings showing the orientation and location of the tension specimens in the base metal, weld metal and heat-affected-zone, respectively.

Tension testing was conducted in accordance with ASTM Method E 8-77, "Tension Tests of Metallic Materials" and/or Recommended Practice E 21-70, "Short-Time Elevated Temperature Tension Tests of Materials," except as modified by Section 6.1 of Recommended Practice E 184-62, "Effects of High-Energy Radiation on the Mechanical Properties of Metallic Materials." Implementation of the ASTM Test Methods to the testing of irradiated tension specimens is described in C-E Laboratory Procedure 00000-MCM-041, Revision 0, "Procedure for Tension Testing of Irradiated Metallic Materials," August 16, 1978.

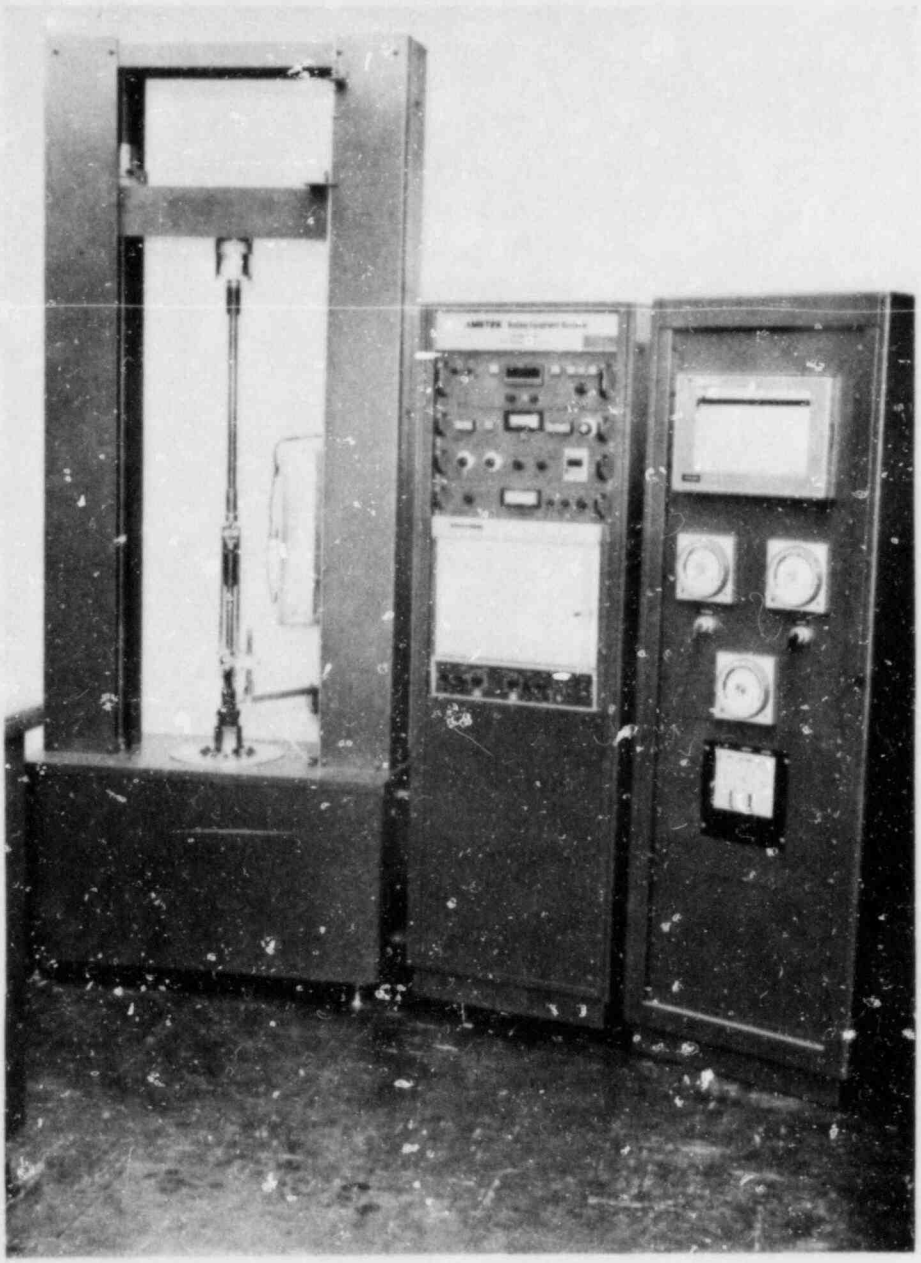

FIGURE A-1 TENSILE TEST SYSTEM WITH CONTROL CONSOLE AND ELEVATED TEMPERATURE TESTING EQUIPMENT

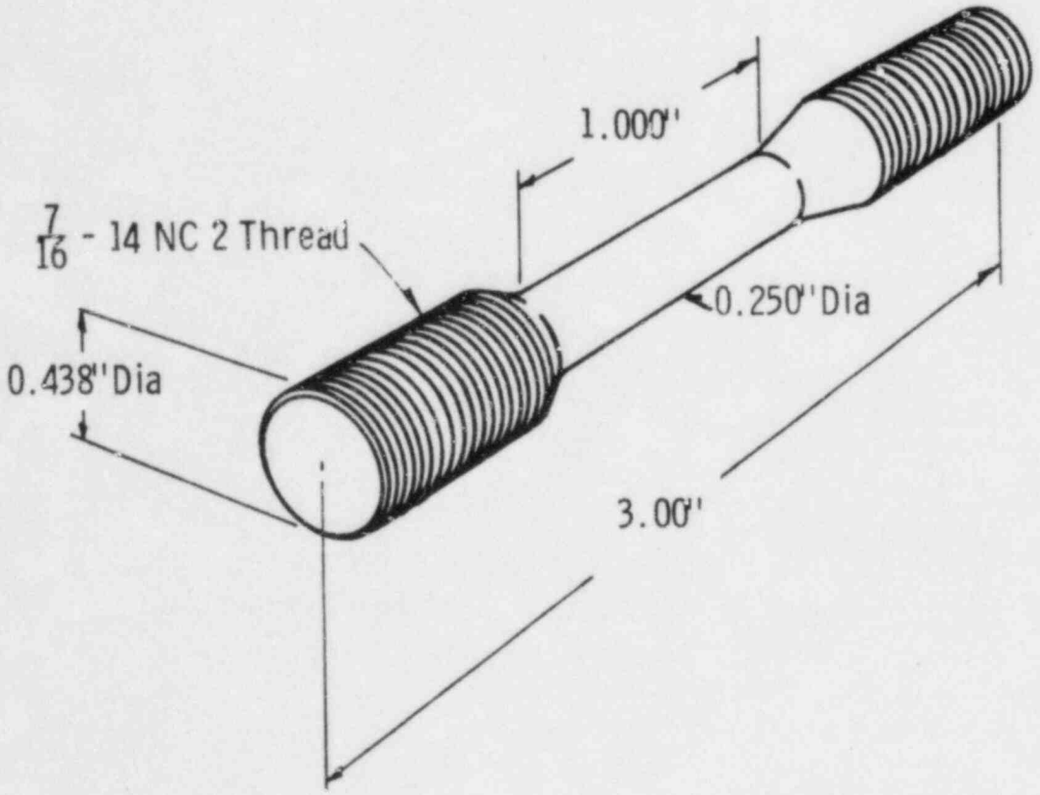

FIGURE A-2 TYPICAL TENSILE SPECIMEN

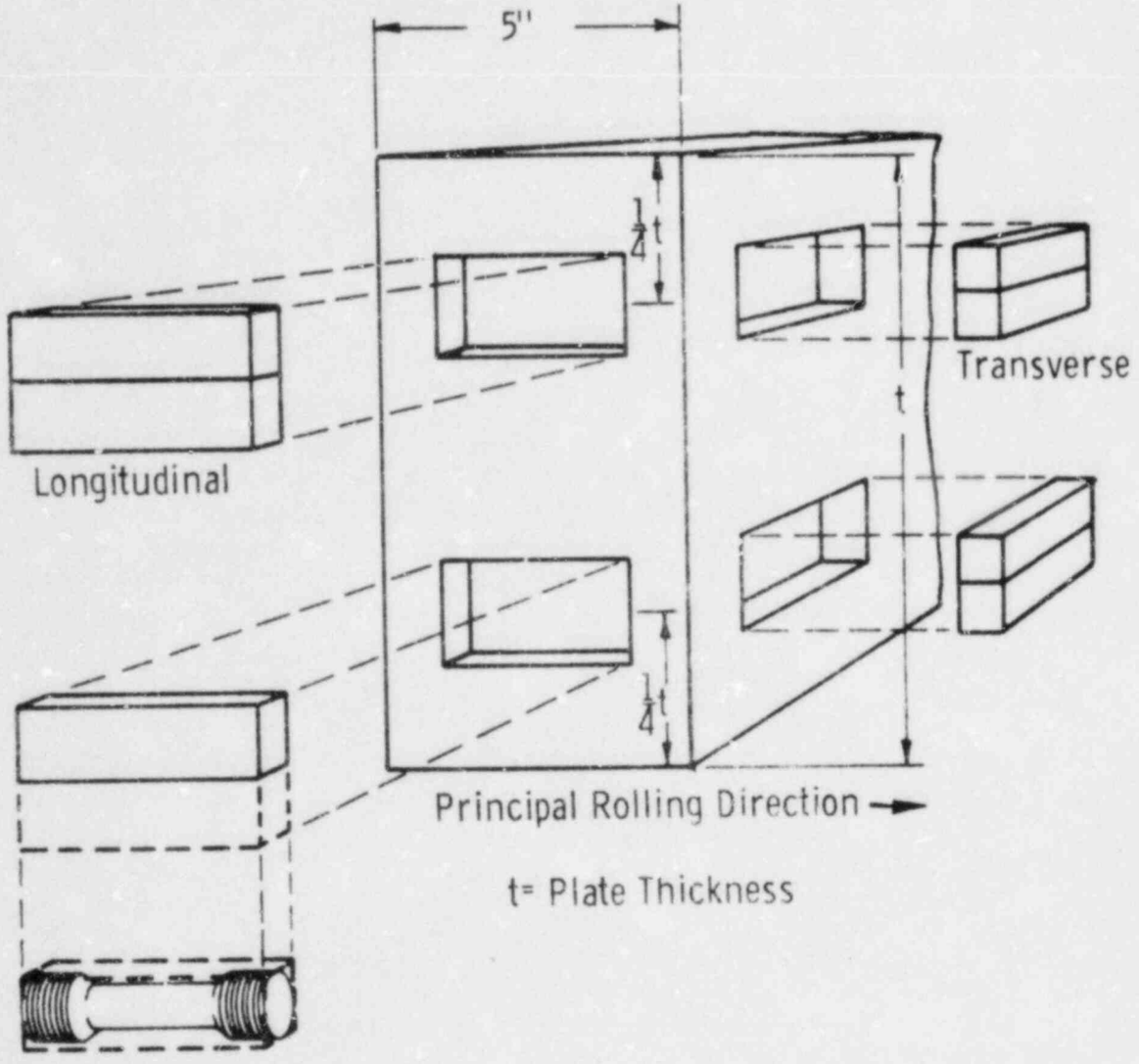

FIGURE A-3 LOCATION OF TENSILE SPECIMENS WITHIN BASE METAL TEST MATERIAL

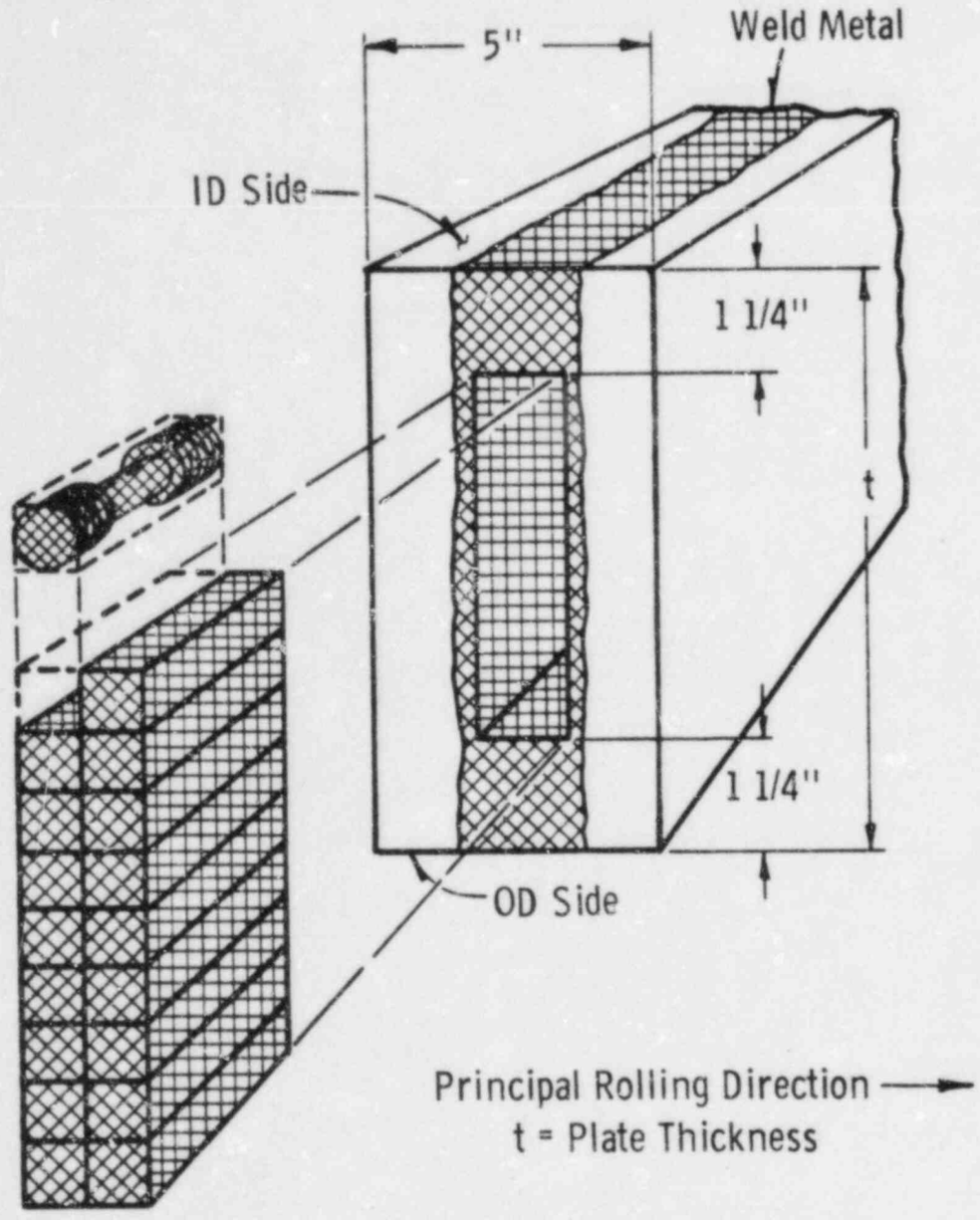

FIGURE A-4 LOCATION OF TENSILE SPECIMENS WITHIN WELD METAL TEST MATERIAL

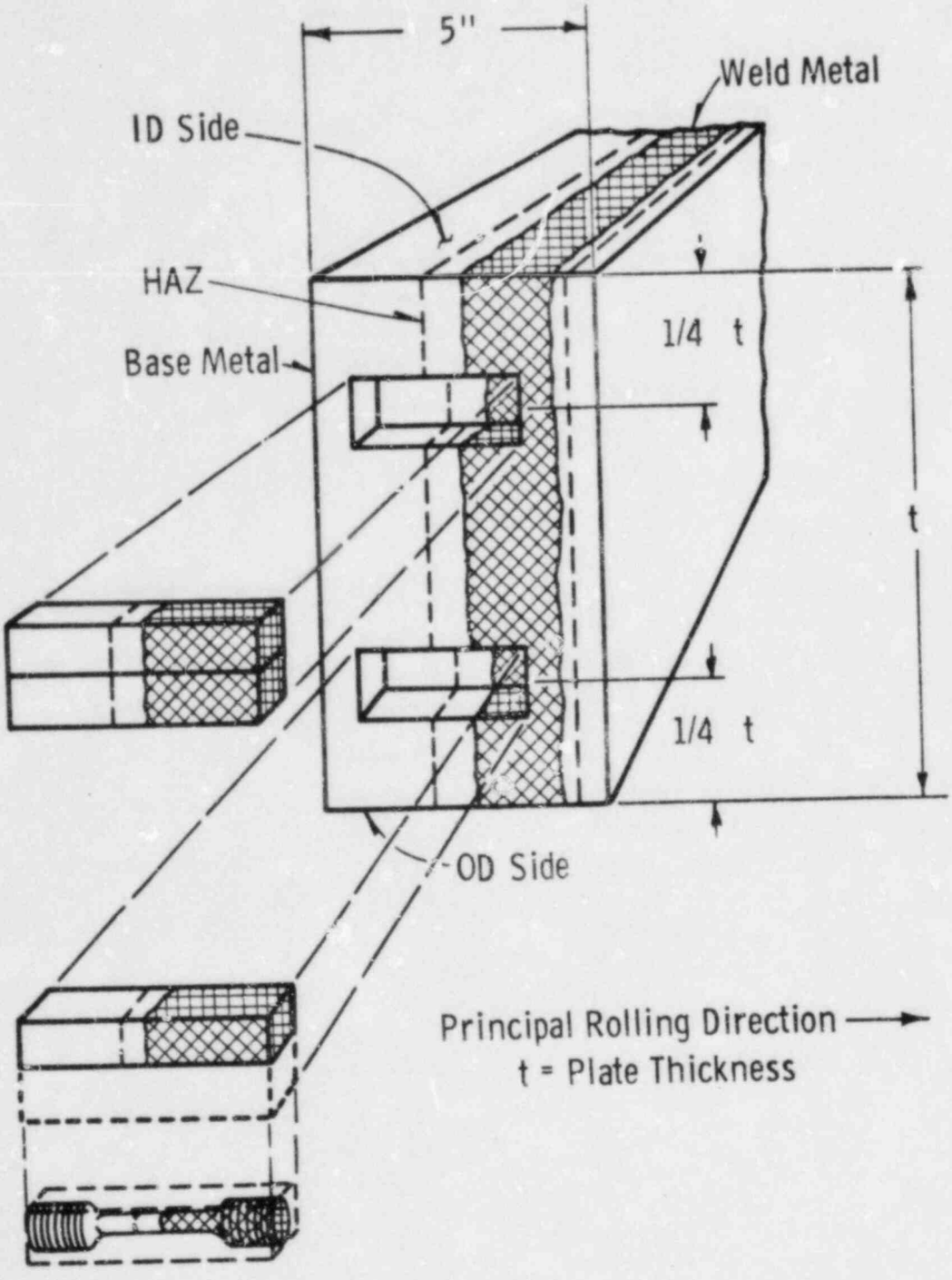

FIGURE A-5 LOCATION OF TENSILE SPECIMENS WITHIN HEAT-AFFECTED-ZONE TEST MATERIAL

Acco Industries Inc.
Measurement Systems Division
929 Connecticut Avenue, Box 9021, Bridgeport, Connecticut 06602
Telephone 203 335 2511

Certificate of Calibration

Riehle® Testing Machines

Calibration Date January 12,1981 Machine Description Riehle DS-30

Customer Combustion Engineering
Building #5
Prospect Hill Road
Windsor, CT

Attn: D. Vielleux

Serial No. RA-44372

Measurement Systems Division of Acco Industries Inc. certifies that the machine described above has been calibrated to ASTM designation E4 using calibrated weights and/or proving rings calibrated to National Bureau of Standards specification.

TENSION

Machine Range 3,000

Machine reading	% Error
600	+.114
1200	+.287
1800	+.251
2400	+.195
3000	+.156

Machine Range 6,000

Machine reading	% Error
1200	+.292
2400	+.244
3600	+.228
4800	+.196
6000	+.157

Machine Range 15,000

Machine reading	% Error
3000	+.117
6000	+.177
8000	+.066
12000	+.123
15000	+.074

Machine Range 30,000

Machine reading	% Error
6000	+.184
12000	+.092
18000	+.021
24000	+.031
30000	+.025

Machine Range

Machine reading	% Error

Machine Range

Machine reading	% Error

Calibrating apparatus used

Capacity	Serial no.	Cal. date	Lab. no.
2,000	579	3-8-79	SJT.232.09/209275
10,000	4354	11-29-79	SJT.01/101631
60,000	239	6-16-80	SJT.01/101738

R. C. Lyon
Calibration Engineer

Andrew R. Lee
Standards Manager

Acco Industries Inc.
Measurement Systems Division
929 Connecticut Avenue, Box 9021, Bridgeport, Connecticut 06602
Telephone 203 335-2511

Certificate of Calibration
Riehle® Testing Machines

Calibration Date January 13,1981

Instrument Description Riehle Extensometer, Riehle Recorder

Customer Combustion Engineering
Prospect Hill Road
Windsor, CT

Serial No. DN-120007
R-67338

Measurement Systems Division of Acco Industries Inc. verifies that the attached graph is certification of calibration of the instrument described above. This instrument was calibrated to ASTM designation E83.

Recorder Extensometer Calibrator
Equipment used in calibration EM 528864

P.C. Lepak
Calibration Engineer

Andrew R. Lee
Standards Manager

APPENDIX B

CHARPY IMPACT TESTS - DESCRIPTION AND EQUIPMENT

The standard impact tests and instrumented tests were performed on a calibrated instrumented impact testing system, shown in Figure B-1. C-E's instrumented impact test equipment provides for signal retention and the subsequent data analysis. The output signal from the instrumented tup is recorded by an oscilloscope. A permanent visual record was made of the load signal, as it was displayed on the oscilloscope screen, with a polaroid camera.

The system consists of the following elements:

a. A Model SI-1 BLH Sonntag Universal Impact Machine with a specifically machined pendulum tup, instrumented with four resistance strain gages in full bridge circuit. This tup "load cell" is calibrated statically and dynamically to provide a given pounds/volt sensitivity for known settings of the balance and gain on the dynamic response system. The instrumented machine meets all impact test machine requirements of ASTM and is certified by AMMRC, the U.S. Army Materials and Mechanics Research Center (Watertown Arsenal). A copy of the certification papers is included in this Appendix.

b. A Model 500 Dynatup dynamic response system which supplies regulated and constant dc excitation to strain gages on the pendulum tup, provides balancing, variable load sensitivity and calibration functions, and amplifies load-time signal to a $\pm$10 volt, $\pm$100 milliampere level while preserving kHz frequency response and 0.05 percent accuracy while simultaneously recording the area beneath the load-time trace.

c. A photoelectric triggering device and velocometer composed of a high intensity light directed through a grid mounted on the pendulum of the impact tester, and passed to a photosensor through fiber optics. A special circuit ensures accurate, reliable and fail safe triggering of the oscilloscope recorder plus an accurate display of the average velocity of the pendulum during impact.

d. A 5103N Dual Beam Tektronix Storage Oscilloscope with a No. 5A18N dual-trace amplifier plug-in unit and a No. 5B12N dual time base plug-in unit. Also included is a C-58 camera with mounting adapter. This device gives a display of each test trace for visual analysis of the load-time impluse recorded by the instrument.

The standard Charpy specimen is described in Figure B-2. Figures B-3 through B-5 are isometric drawings showing the orientation and location of the Charpy impact specimens in the base metal, weld metal and heat-affected-zone, respectively.

All Charpy impact tests were conducted in accordance with ASTM Method E 23-72, "Notched Bar Impact Testing of Metallic Materials." Implementation of ASTM E23 for the testing of irradiated Charpy specimens is described in C-E Laboratory Procedure 00000-MCM-040, Revision 0, "Procedure for Instrumented Charpy Impact Testing of Irradiated Metallic Materials," July 31, 1978.

The constant temperature necessary for conducting the Charpy impact tests was obtained from a series of circulating liquid baths capable of maintaining stable temperature throughout the range of -150°F to +250°F. Any selected temperature in this range was maintained to an accuracy of 2°F. For tests above 250°F, specimens were heated in a controlled circulation furnace where temperature was maintained to an accuracy of 5°F. The temperature baths were composed of the following equipment:

Two Neslab Constant Temperature Circulating Baths - Model TEZ 10, with Model CT 150 Thermoregulators and Labline 11 inch diameter thermocups. Designated Baths 1 and 4.

Medium: Ethylene Glycol - room temperature to 250°F.

One Neslab Constant Temperature Circulating Bath - Model TEZ 10 with a Model CT 59 Thermoregulator and a Labline 11 inch diameter thermo cup. Designated Bath 2.

Medium: Isopropanol - room temperature to -10°F. Neslab Portable Bath Cooler, Model PCB-2 connected.

One Low Temperature Stirred Bath, one 11 inch diameter thermo cup, one Honeywell Controller and Solenoid control valves to Flexi-Cool cooling system. Designated Bath 5.

Medium: Isopropanol - room temperature to -150°F.
Coolant: Freon

One Grieve Industrial oven, controlled air circulation. Designated Bath 3.

Medium: Air, 100°F to 800°F.

All baths - Copper Constantan Thermocouple
Honeywell Six Point Temperature Chart Recorder
Digitec Thermocouple Thermometer - Model 590 TF
Standard Mercury Column Thermometer
Bimetallic - spring Thermometer

The temperature instruments were calibrated in accordance with the ASME Boiler and Pressure Vessel Code, Section III, Paragraph 2360. Copies of the applicable calibration certificates are provided at the end of this appendix.

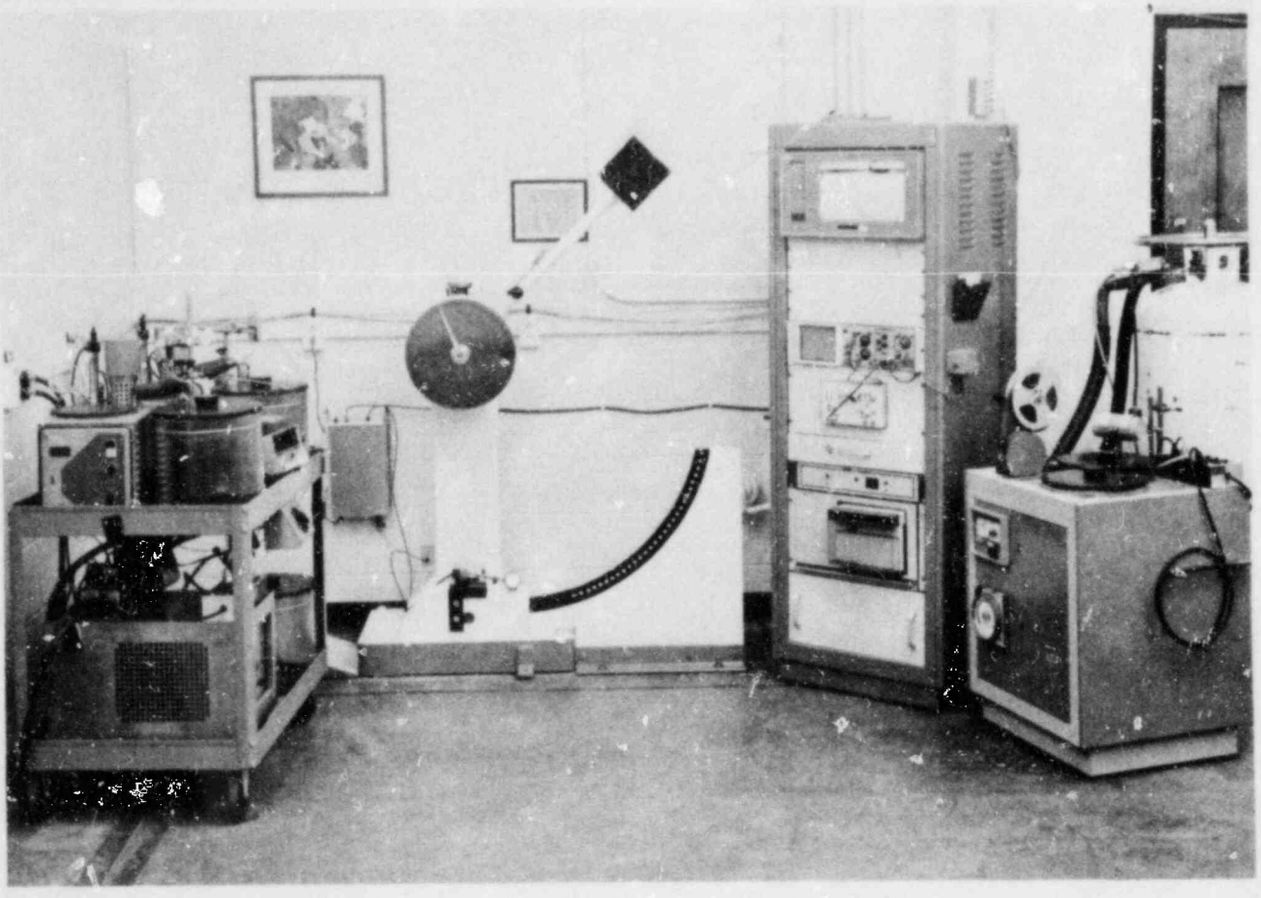

FIGURE B-1 CHARPY IMPACT TEST SYSTEM, ASSOCIATED CONSTANT TEMPERATURE BATHS AND INSTRUMENTED CHARPY IMPACT DATA PROCESSING EQUIPMENT

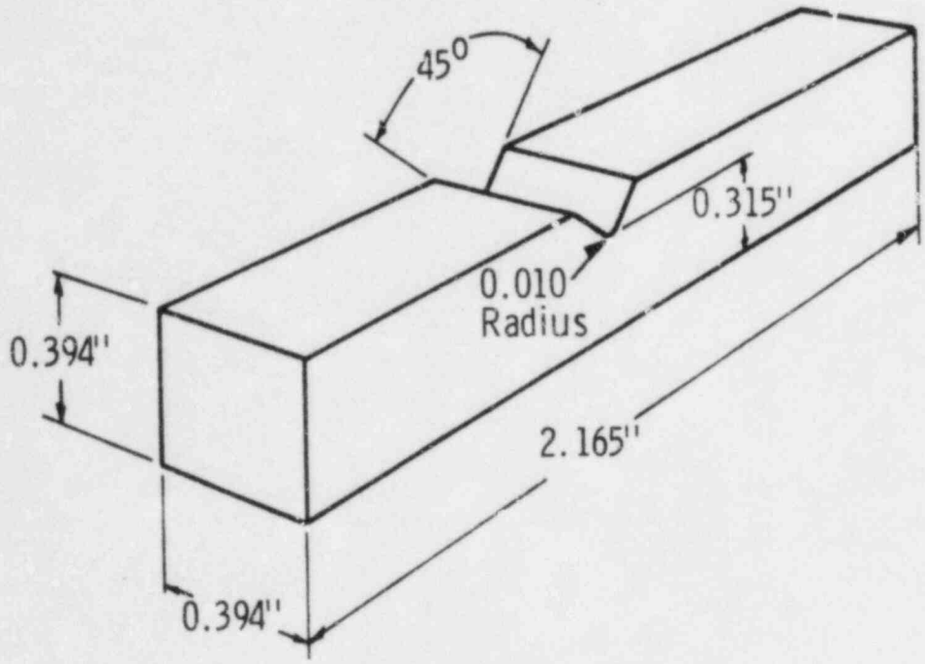

FIGURE B-2 TYPICAL CHARPY V-NOTCH IMPACT SPECIMEN

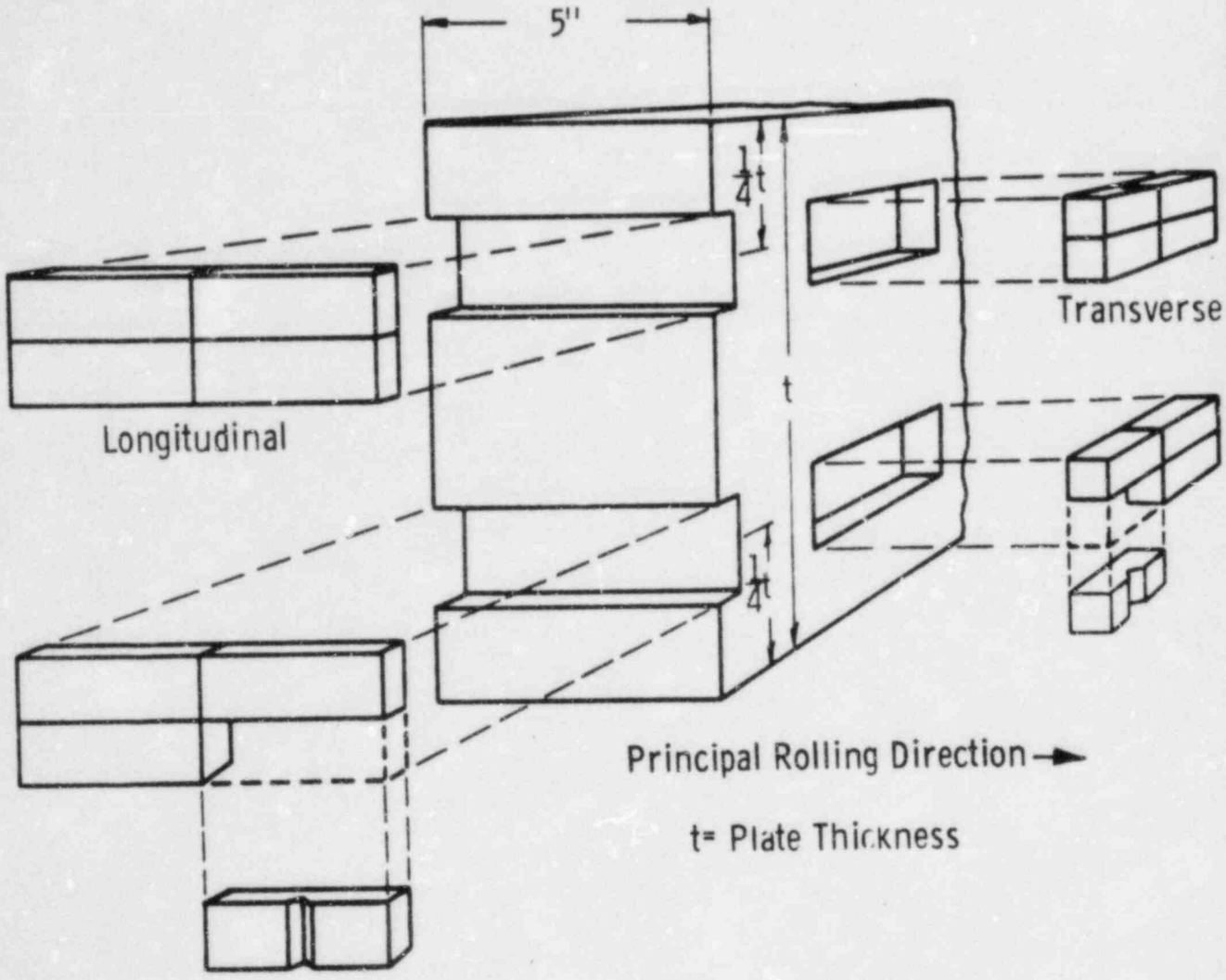

FIGURE B-3 LOCATION OF CHARPY IMPACT SPECIMENS WITHIN BASE METAL TEST MATERIAL

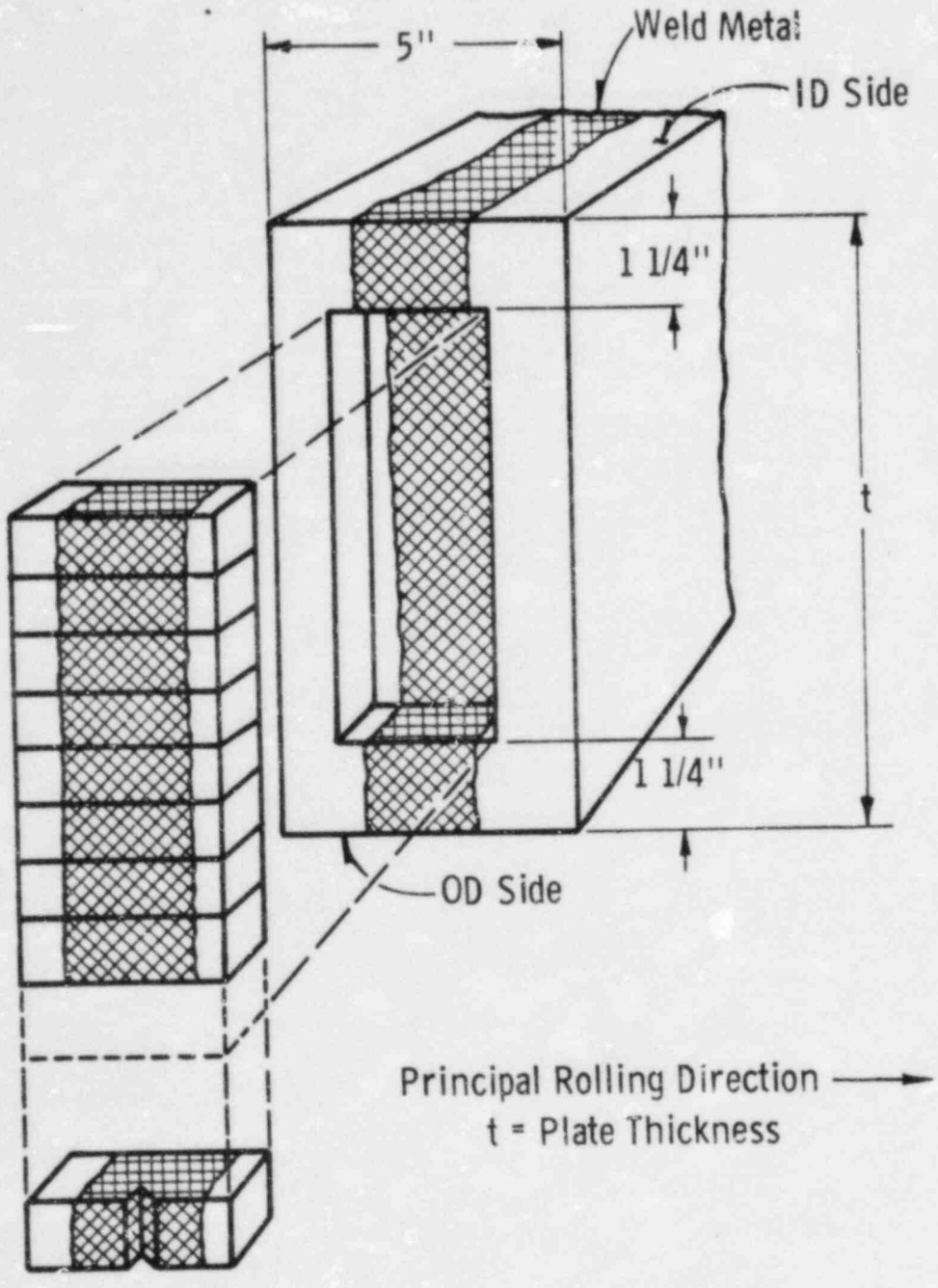

FIGURE B-4 LOCATION OF CHARPY IMPACT SPECIMENS WITH
WELD METAL TEST MATERIAL

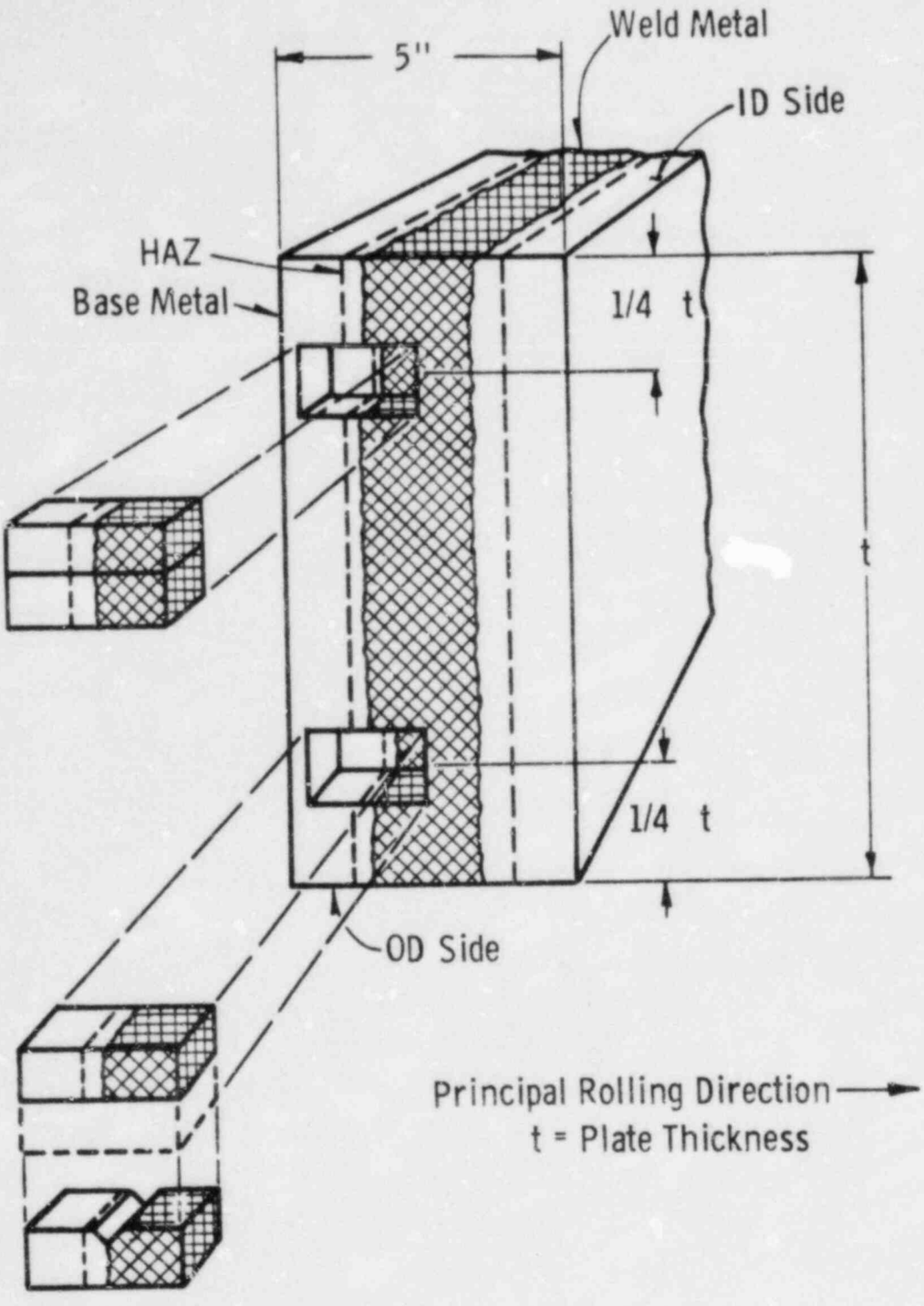

FIGURE B-5 LOCATION OF CHARPY IMPACT SPECIMENS WITHIN HEAT-AFFECTED-ZONE TEST MATERIAL

DEPARTMENT OF THE ARMY
ARMY MATERIALS AND MECHANICS RESEARCH CENTER
WATERTOWN, MASSACHUSETTS 02172

DRXMR-MQ

8 January 1981

Combustion Engineering, Inc.
ATTN: Mr. Ray Hurlburt
Dept. 9454-501
1000 Prospect Hill Road
Windsor, CT 06095

Dear Mr. Hurlburt:

A set of Charpy impact test specimens broken on the 240 ft-lb capacity Satec machine, Serial No. 1366 has been received for evaluation along with the completed questionnaire.

The results of the tests indicate the machine to be producing acceptable energy values at both energy levels (see inclosed table).

This machine satisfies the proof-test requirements of ASTM Standard E-23.

If this machine is moved or undergoes any major repairs or adjustments, this certification becomes invalid and the machine must be rechecked. Removal of the pendulum, replacement of anvils or adjusting the height of drop are examples of such major repairs or adjustments. It should be noted that if a specimen requires over 80% of the machine capacity to fracture, the machine should be checked to assure that the pendulum is straight, the anvils or striker have not been damaged and that all bolts are still tight. This certification is valid for one year from the date of the test.

Sincerely yours,

Paul W. Rolston

PAUL W. ROLSTON
Chief
Quality Engineering Branch

1 Incl
Table

XMR Form 1FL-3

ARMY MATERIALS AND MECHANICS RESEARCH CENTER

Watertown, Massachusetts 02172

Date of Test: 12/10/80

TABLE

COMPARISON TESTS ON CHARPY IMPACT MACHINES

Facility Combustion Engineering, Inc.

Make of Machine Satec Serial No. 1366

	AMMRC (ft-lb)	Combustion Eng. (ft-lb)	Variation Actual		Allowed
High Energy	68.7	69.6	+1.3	%	±5.0%
Medium Energy				%	±5.0%
Low Energy	14.2	14.9	+0.7	ft-lb	±1.0 ft-lb

XMR Form 105
Rev 1 Mar 79

COMBUSTION ENGINEERING, INC.
Nuclear Laboratories
INSTRUMENT CALIBRATION REQUIREMENT SHEET

DATE: 1/22/81

EQUIPMENT Digital Thermocouple Thermometer
E[illegible]-96

AREA 235-5

INSTRUMENT		READABILITY		CALIBRATION		CHECKED
FUNCTION	TYPE	RANGE	MIN READABILITY	ACCURACY	FREQUENCY	BY
Thermometer	Digital	-313°F to +752°F	1°F	±1°F	3 months	

PREPARED BY Raymond J. Hurlburt

APPROVED BY _____

APPROVED BY Al Ragl

APPENDIX C

INSTRUMENTED CHARPY V-NOTCH DATA ANALYSIS

All baseline and irradiated Charpy impact tests in this program were performed on an instrumented test system. Instrumented impact testing provides more quantitative data from a Charpy specimen which enable a more detailed analysis of the surveillance material toughness behavior.

Photographs of the oscilloscope traces of load and energy versus time were taken for each test of the base plate (transverse and longitudinal orientation), weld, and heat-affected-zone. From each trace, the general yield load (PGY), maximum load (PM), and fracture load (PF) were determined, as shown in Tables C-1 through C-4. For each material, the loads were plotted against the corresponding test temperature to generate the irradiated load/temperature diagrams. The post-irradiation load/temperature results are shown in Figures C-1 to C-4.

Three index temperatures are of interest. T_B, the brittle transition temperature, corresponds to the onset of ductile fracture; below T_B the fracture is completely brittle. T_N, the ductility transition temperature, corresponds to the mid-transition region where the fracture has become predominantly ductile. T_D, the ductility temperature, corresponds to the onset of the upper shelf energy where fracture is completely ductile.

The radiation-induced toughness property changes of the surveillance materials are summarized in Table C-5. Standard Charpy impact data are included with the instrumented data since each method represents a unique material property. The standard Charpy test provides a bulk measurement of the energy to initiate and propagate a crack through to failure of the material. In contrast, analysis of the instrumented data enables characterization of the components of the dynamic load behavior prior to material failure. The shift in the brittle transition temperature, T_B, and the ductility transition temperature, T_N, are comparable to the shift in the 30

ft-lb Charpy index temperature, Cv_{30}. The radiation induced changes in the instrumented data therefore tend to corroborate the changes determined from the standard Charpy impact data.

The third parameter obtainable from the instrumented data is T_D, the ductility temperature, which is given in Table C-5. T_D corresponds closely with the onset of the upper shelf energy (minimum temperature for the material to exhibit 100% shear fracture). The agreement is seen to hold for both the unirradiated and irradiated data.

The instrumented Charpy analysis substantiates the results from the standard impact tests. In particular, this approach provides a more quantitative means of measuring radiation induced property changes by analysis of the entire load record rather than using the single (bulk) measurement of impact energy. As more experience is gained with this technique, it offers the potential of providing a more quantitative measurement of toughness property changes than is possible with current impact testing.

TABLE C-1

INSTRUMENTED CHARPY IMPACT

TEST, MILLSTONE UNIT 2 IRRADIATED

BASE METAL (TRANSVERSE)

Specimen Identification	Test Temperature (°F)	Yield Load, PGY (lb)	Maximum Load, PM (lb)	Fast Fracture Load, PF (lb)
252	0	3400	3800	--
21M	60	3200	3600	--
21E	100	3000	3800	--
23U	100	--	No Record --	
21K	160	2800	3800	--
23M	160	2900	3900	3800
23T	200	2900	3800	3600
25J	240	3000	3900	--
23A	240	2700	3900	--
251	280	2700	3800	--
23K	280	2600	3700	--
25C	320	2700	3800	--

TABLE C-2

INSTRUMENTED CHARPY IMPACT

TEST, MILLSTONE UNIT 2 IRRADIATED

BASE METAL (LONGITUDINAL)

Specimen Identification	Test Temperature (°F)	Yield Load, PGY (lb)	Maximum Load, PM (lb)	Fast Fracture Load, PF (lb)
114	40	3000	3200	--
16B	80	2800	3600	--
11Y	120	2700	3500	--
14P	120	2900	3900	--
135	160	2800	3800	--
147	160	-- No Record --		
122	160	2800	4000	3900
14M	200	-- No Record --		
137	240	-- No Record --		
11B	280	2800	4000	--
14U	280	2600	3900	--
14D	350	-- No Record --		

TABLE C-3

INSTRUMENTED CHARPY IMPACT

TEST, MILLSTONE UNIT 2 IRRADIATED

WELD METAL

Specimen Identification	Test Temperature (°F)	Yield Load, PGY (lb)	Maximum Load, PM (lb)	Fast Fracture Load, PF (lb)
33B	0	3500	4000	--
33J	40	3400	3900	--
31D	40	--	4400	--
33C	60	3300	4000	--
36M	80	3300	4300	3400
31L	80	3300	4300	4000
352	120	3100	4100	3900
317	120	3100	4100	3400
31C	160	3000	4100	--
34A	160	3000	4000	--
34D	200	2900	3900	--
36U	240	2800	3900	--

TABLE C-4

INSTRUMENTED CHARPY IMPACT

TEST, MILLSTONE UNIT 2 IRRADIATED

HEAT-AFFECTED ZONE

Specimen Identification	Test Temperature (°F)	Yield Load, PGY (lb)	Maximum Load, PM (lb)	Fast Fracture Load, PF (lb)
455	0	3500	3900	--
43U	40	3400	3900	--
45A	40	3400	3800	--
45M	60	3400	4000	--
42D	80	3300	3900	--
451	100	3300	4300	4200
44D	100	3300	4300	4100
435	120	-- No Record	--	
464	160	3000	4300	3100
44M	200	3000	4100	--
447	200	2900	4200	--
432	240	3000	4200	--

TABLE C-5

TOUGHNESS PROPERTY CHANGES BASED ON

INSTRUMENTED CHARPY IMPACT TEST

Material	T_B (°F)	ΔT_B (°F)	T_N (°F)	ΔT_N (°F)	ΔCv_{30} (°F)	ΔCv_{50}	T_D (°F)	Min. Temperature For 100% Shear Fracture (°F)
Base Metal (WR)								
unirrad	-76	--	60	--	--	--	160	160
irrad	-40	36	130	70	96	113	200	240
Base Metal (RW)								
unirrad.	-60	--	66	--	--	--	132	160
irrad	30	90	160	94	70	93	225	240
Weld Metal								
unirrad.	-84	--	-16	--	--	--	56	80
irrad.	-40	44	47	63	76	88	150	160
Heat-Affected Zone								
unirrad.	-150	--	-10	--	--	--	70	80
irrad.	-45	105	85	95	94	91	135	200

Figure C-1 INSTRUMENTED CHARPY LOAD - TEMPERATURE DIAGRAM, BASE METAL (TRANSVERSE)

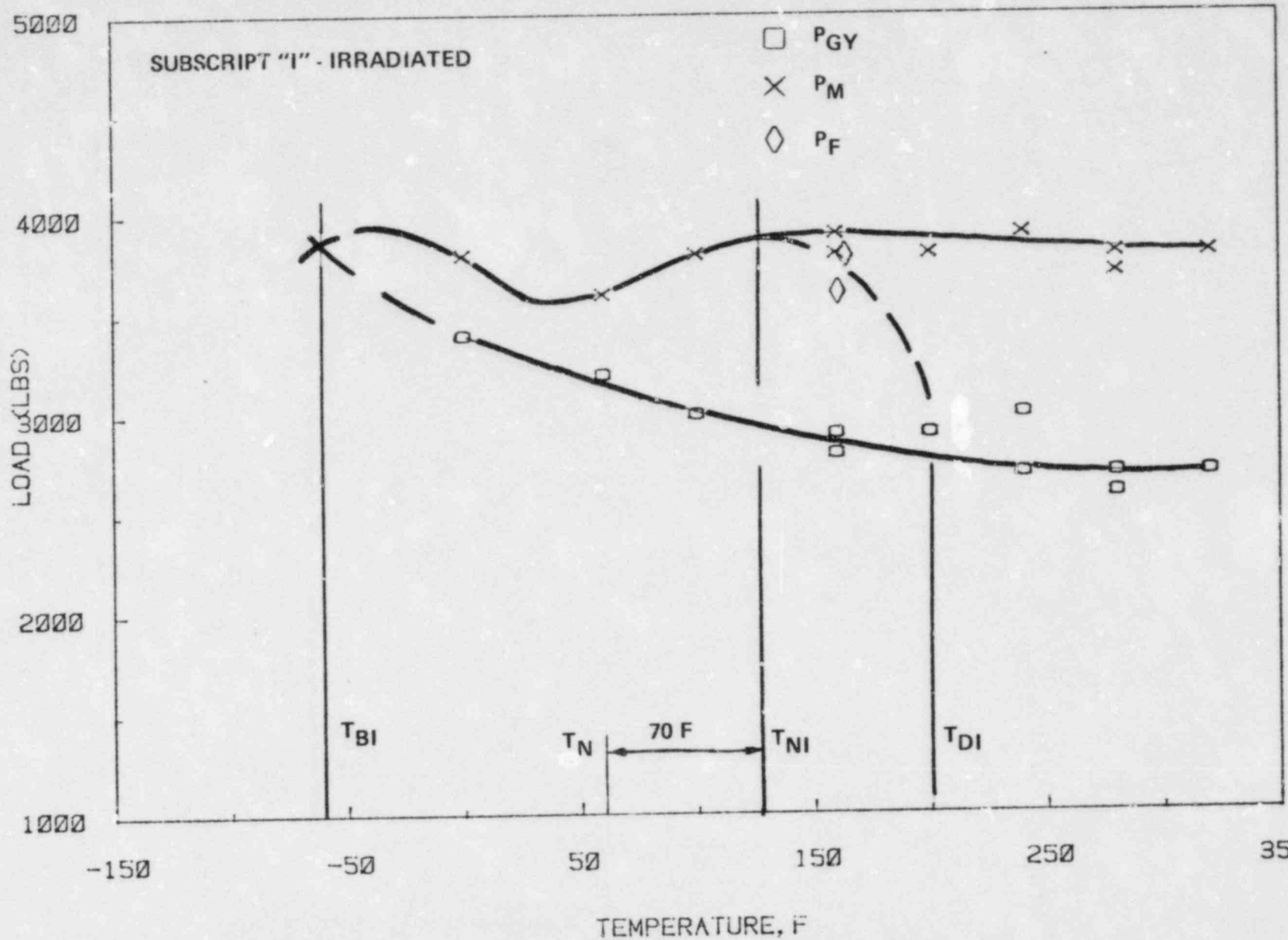

Figure C-2 INSTRUMENTED CHARPY LOAD - TEMPERATURE DIAGRAM, BASE METAL (LONGITUDINAL)

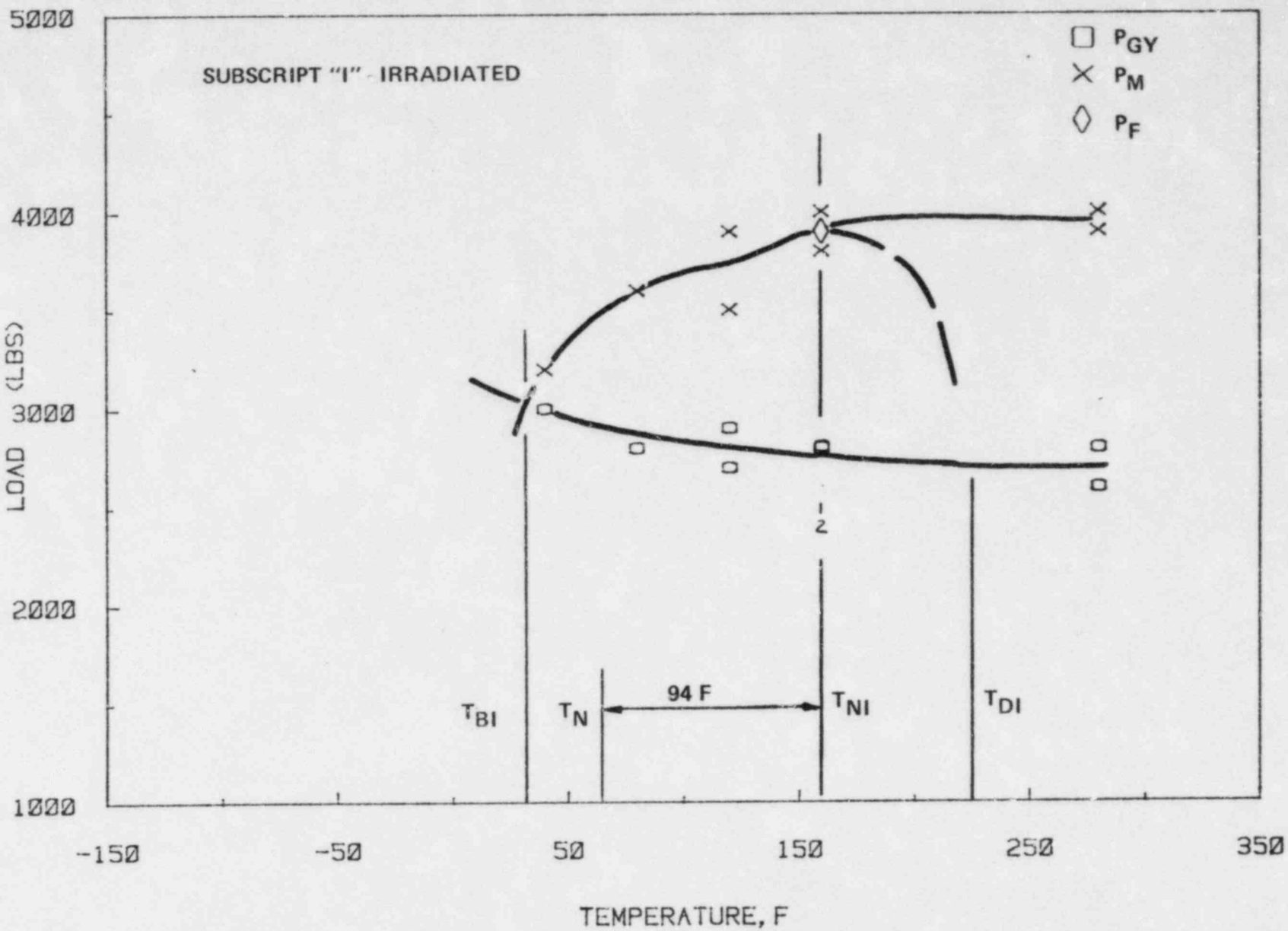

Figure C-3 INSTRUMENTED CHARPY LOAD - TEMPERATURE DIAGRAM, WELD METAL

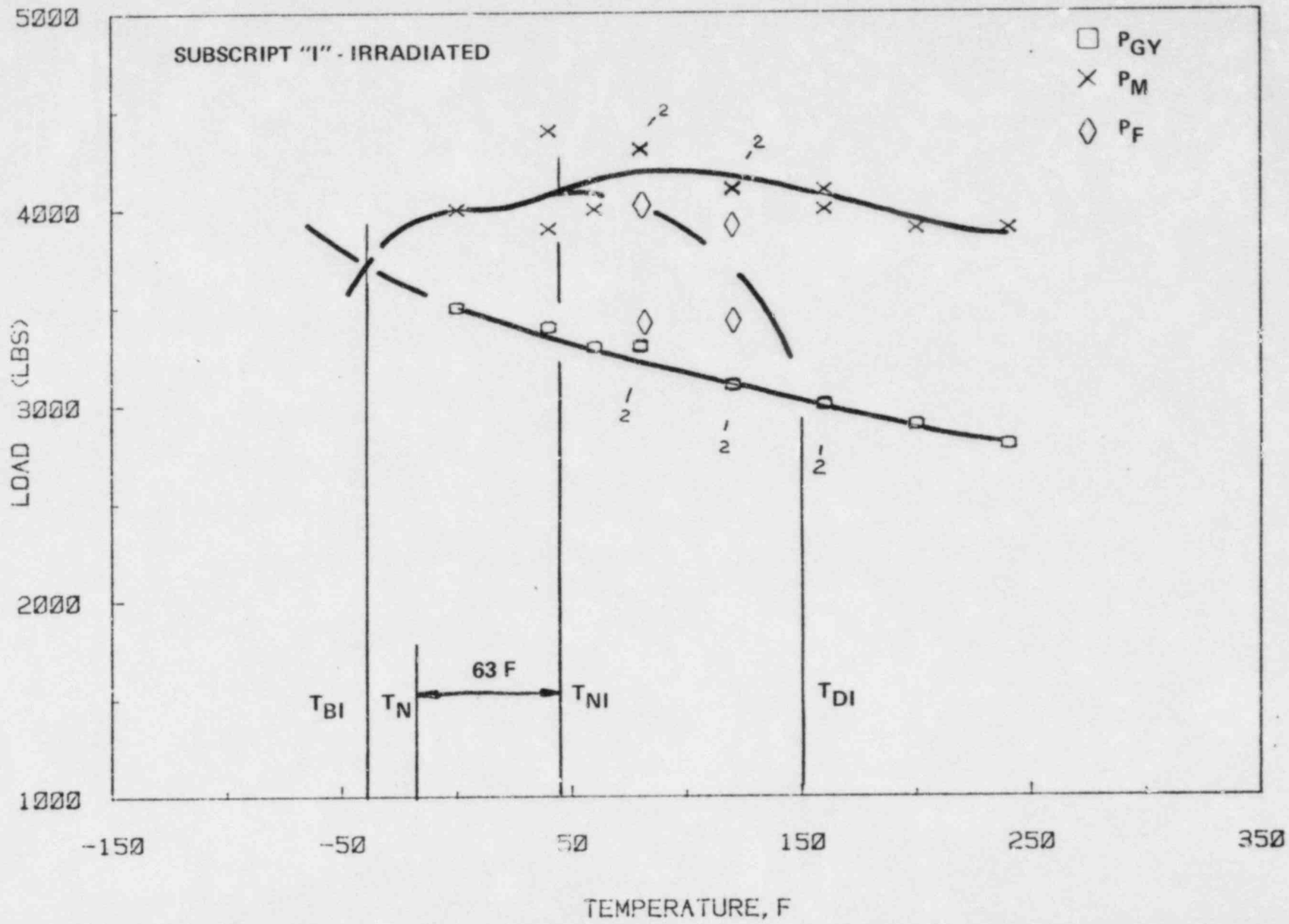

Figure C-4 INSTRUMENTED CHARPY LOAD - TEMPERATURE DIAGRAM, HEAT-AFFECTED ZONE